203

TRANSIENT MOISTURE TRANSFER THROUGH AN OPENING IN A VERTICAL PARTITION

by

SAYED AMIR FARTAJ

B.S., Kansas State University, 1980

A MASTER'S THESIS

Submitted in partial fulfillment of the requirements for the degree

MASTER OF SCIENCE

Department of Mechanical Engineering

KANSAS STATE UNIVERSITY
Manhattan, Kansas

1983

Approved by:

B. Terry Beck

Major Professor

TABLE OF CONTENTS

Chapter Page

LIST OF FIGURES

Figure		Page

LIST OF TABLES

THIS BOOK CONTAINS NUMEROUS PAGES WITH THE ORIGINAL PRINTING BEING SKEWED DIFFERENTLY FROM THE TOP OF THE PAGE TO THE BOTTOM.

THIS IS AS RECEIVED FROM THE CUSTOMER.

CHAPTER I

INTRODUCTION

1.1 Scope of Investigation

This research project specifically addresses the problem of transient moisture infiltration through openings into environmentally controlled air spaces where the magnitude of the latent load is significant. The motivation for this project is evident from a variety of practical applications. One common problem is that encountered in public buildings such as supermarkets, where heavy pedestrian traffic causes a periodic opening and closing of doorways, with an accompanying time dependent interchange of air. A similar problem encountered in cold storage rooms is that of transient air interchange through the access doorways. Still another application involves the periodic opening of windows in environmentally controlled air spaces, which causes the transient movement of air and moisture into and out of the conditioned air space.

The central focus in the present study was to determine experimentally the effect of various physical and geometrical parameters upon the transient rate of moisture transfer through openings in a vertical partition. These parameters were temperature and humidity differences, opening geometry and bulk flow of air that was passed through the opening. The direct measurement of the transient rate of moisture transfer through the opening was rather difficult. Thus, an indirect approach was used to determine the effect of the parameters upon the transient moisture transfer through the opening. Using a mass balance of all water vapor crossing the boundary of the chamber the transient humidity response in the hot chamber was obtained. Therefore by measuring the transient humidity in the hot chamber the effect of the parameters on transient rate of moisture transfer through the opening could be indirectly determined. Experiments were conducted on rectangular openings ranging in size from 6" x 12" (15 cm by 30 cm) to 18" x 12" (45 cm by 30 cm) with temperature differences ranging from 9°C to 24°C (16°F to 43°F), humidity ratios ranging from 2.2 gr H_2O/Kg dry air to 11.9 gr H_2O/Kg dry air, dewpoint temperatures ranging from 3°C to 24°C (37°F to 75°F), and bulk flow rates from zero to 59 Kg/hr (0 to 130 lbm/hr). The conditions on one side of the opening were kept at high temperature and high humidity, while the other side was kept at low temperature and low humidity. To correlate the experimental data, an attempt was made to investigate the extent to which a simple model is applicable to represent the transient rate of moisture transfer through such openings in a partition separating hot and cold air spaces.

Data taken for both free as well as combined forced and free convection through the opening are presented graphically on a normalized set of coordinates, based on the simple theory proposed by Steele [1]. These data verify that the simple model correlated experimental results not only under steady-state conditions, but also applies to transient moisture transfer, given that the transfer process is sufficiently slow so that it may be considered to be quasi-steady.

1.2 Review of the Literature

1.2.1 Mechanisms of Moisture Migration. There are three major physical mechanisms associated with transient moisture migration into an environmentally controlled air space which can lead to significant latent loads. These are: (1) movement as a bulk component of the air (by convection), (2) by diffusion and (3) by hygroscopic action [2]. With convection an entire volume is moved from one region to another, carrying along with it moisture as a bulk component of the air. In order for moisture to transfer by this mechanism, there must be an interchange of air (infiltration) at an opening(s) between the conditioned air space and the surroundings. Movement by diffusion is a mechanism by which moisture is transferred due to the presence of a concentration or partial pressure gradient of water vapor in the air. Hygroscopic action is a mechanism by which moisture migrates through permeable media. This mechanism requires physical interaction between the air and a solid material (absorption and/or adsorption).

As the size of the opening and/or temperature difference across the opening increases, the moisture transfer through the opening by diffusion becomes less significant, compared with convection. Hence, in the present study of transient moisture transfer through a large opening on the order of 1 ft x 1 ft square, only convection is presumed to be a significant mechanism [1]. A survey of the literature concerned with moisture transfer by convection (both free convection as well as combined forced and free convection) is presented in the following section.

1.2.2 Movement as a Bulk Component of the Air. With the exception of the theoretical and experimental investigation by Steele [1], the problem of moisture transfer through an opening has been given very little attention. This is particularly true for the case of transient moisture transfer. There have been very limited experimental measurements of actual moisture transfer and little theoretical analysis has been concerned with this problem. By comparison, the problem of convective heat transfer through openings has been investigated much more thoroughly both experimentally and theoretically.

Nearly all of the theories for convection through large openings are modifications of Emswiler's simple theory [3], and are based on a simplified application of Bernoulli's model for determining the effect of the velocity distribution across the opening. Emswiler [3] was apparently the first to realize the influence of the neutral pressure line (the level where zero pressure difference exists) in convection through large openings. He obtained an expression for the rate of air flow through multiple openings in a wall. The driving force for the air flow was assumed to be the density difference across the opening. He did not investigate heat or mass transfer through single openings.

Brown and Solvason [4] were the first to experimentally investigate the thermally driven free convection phenomenon through a single large rectangular opening between two air spaces at different temperatures. Their measurements of heat transfer through the opening were made with a large-scale wall heat flow measuring apparatus [5], which consisted of two large chambers. One of these chambers was eight by eight feet square and fourteen feet deep (2.4 x 2.4 x 4.3 m) and was maintained at the desired temperature, ranging from -20°F to 55°F (-29°C to 13°C). The hot chamber was insulated to prevent heat losses. The experimental tests were conducted on single rectangular openings of 3 in by 3 in (7.5 cm by 7.5 cm), 6 in by 6 in (15 cm by 15 cm), 9 in by 9 in (23 cm by 23 cm), 12 in by 12 in (30 cm by 30 cm) and 6 in by 12 in (15 cm by 30 cm). The ratios of thickness to height of the opening were 0.19, 0.25, 0.38 and

0.75. Air temperature differences across the opening ranged from 15° F to 90° F (-9°C to 32°C).

Brown and Solvason [4] developed theoretical relationships for the steady-state heat transfer coefficient and the coefficient of convective water vapor mass transfer, based on an extension of the work of Emswiler [3]. Heat transfer was correlated in terms of a Nusselt number, which was expressed as a function of a Grashoff number, and the Prandtl number. Mass transfer was correlated in terms of a Sherwood number expressed as a function of the Grashoff number and Prandtl number.

Brown and Solvason [4] also experimentally investigated the effect of a horizontal velocity, parallel to the wall and opening. Their experimental results indicated that it could reduce the convective heat transfer. The Grashof number ranged from 10^6 to 10^8, depending on the opening thickness to height ratio, air temperature and humidity difference. In their theoretical analysis, it was assumed that no heat transfer took place by conduction and that no water vapor transfer took place by diffusion.

Brown and Solvason [4] also extended their earlier investigation, to include free convection through openings in a horizontal partition [6]. Experimental tests were conducted with single openings of 6 in by 6 in (15 cm by 15 cm), 9 in by 9 in (23 cm by 23 cm) and 12 in by 12 in (30 cm by 30 cm) with the thickness of the partition from one to eight inches (2.5 cm to 20 cm). The temperature differences across the openings in a horizontal wall were in the same range as that for the vertical partition.

Wilson, Brown and Solvason [7] have presented a summary of results in the form of empirical relationships and charts, with which it is possible to calculate the heat and moisture transfer through openings in both vertical and horizontal partitions. They did not experimentally nor theoretically investigate the effect of bulk flow upon the heat and mass transfer.

Shaw [8] investigated, both experimentally and theoretically, free convection and combined forced and free convection for steady-state heat transfer through a large rectangular opening in a vertical partition. He extended the earlier theoretical developments by Brown and Solvason in free convection by introducing the coefficient of discharge. The value for this coefficient was determined by dividing the actual (measured) volumetric exchange by the theoretical calculated value. The theoretical volumetric discharge was expressed in terms of opening area and temperature differential. The coefficient of discharge was found to be solely dependent on the temperature difference across the opening. The values for this coefficient, which was referred to as the coefficient of the temperature, C_T were presented graphically as a function of the temperature difference across the opening and ranged from 0.6 - 1.0.

In his study of combined free and forced convection through an opening, Shaw [8] developed an equation for the heat transfer coefficient in terms of the Nusselt number, which was shown to be proportional to the Prandtl number and the Shaw number. An equation for the mass transfer coefficient was also developed in terms of the Sherwood number which was proportional to the Schmitt number and the Shaw number. He expressed the proportionality as an overall discharge coefficient, which was found to be the product of a temperature coefficient C_T, and a velocity coefficient C_V, to account for the effect of forced air flow. This coefficient was a function of both the temperature difference and the bulk air velocity through the opening. Therefore it was not possible to determine C_V independently by experimental means. However, an overall coefficient was obtained by dividing the actual inflow volume by the theoretical inflow volume. The values for this coefficient were presented graphically for various temperature differences, with the bulk velocity as the independent variable.

In Shaw's experiments, two rooms were separated by a door with a height of 6.73 ft (2.05 m). The thickness to height ratio was 0.05, the door widths ranged from 0.10 to 0.33 to 2.95 ft (0.10 to 0.90 m), and the temperature difference across the opening ranged from 32°F to 54°F (0°C to 12°C). The free air velocity or turbulence varied between about 0.10 and 20-30 ft/min (0.10 and 0.15 m/s).

The most recent paper concerning steady-state exchange of water vapor through openings is that of Steele [1]. The main emphasis in this study was to experimentally determine the parameters affecting moisture migration through an opening. The influencing parameters considered, included the humidity and temperature difference, the geometry of the opening, and the bulk flow of air through the opening.

The basis for Steele's [1] theory to correlate the data was the concept of hydrostatic pressure difference, as the driving force for water vapor migration. He related the pressure difference to temperature difference across the opening, using the ideal gas law. Using Bernoulli's steady flow model, the velocity of air flow was determined as a function of the opening height above and below the neutral pressure line (N.P.L.). This model assumes that all of the available pressure potential energy is converted into kinetic energy. From this velocity profile the rate of mass flow above and below the was then determined. He also looked at the situation of combined natural convection and forced convection, in which a bulk flow of air was forced through the opening. This bulk flow, which caused the neutral pressure line to shift, was determined by the difference between the mass flow rates above and below the neutral pressure line. The reverse flow of moisture was determined by the difference between the simple bulk flow (bulk flow in absence of counter flows) and the net transfer of moisture across the opening.

Steele [1] conducted experimental tests on rectangular openings of 6 in by 6 in (15 cm by 15 cm), 12 in by 12 in (30 cm by 30 cm), 12 in by 6 in (30 cm by 15 cm), 6 in by 12 in (15 cm by 30 cm). The tested openings were in a vertical partition which separated a chamber of 182 cm by 364 cm (6 ft by 12 ft) into two 91 cm by 182 cm (6 ft by 6 ft) subchambers. The chamber was covered with 2 in Styrofoam to prevent heat loss. The insulation adjacent to the opening was tapered outward at a 45° angle to approximate a "zero length" opening. The air temperature difference between the hot side of the opening and the cold side ranged from 0° F to 67° F (0°C to 37°C). The bulk flow ranged from zero to 57 lbm/hr (0 to 26 Kg/hr), and the air humidity difference across the opening ranged from about 4×10^{-3} to 9×10^{-3}.

The results obtained from the experiments approximated a straight line relationship between normalized bulk flow and normalized reverse flow, and were in good agreement with the results obtained earlier by Shaw [8]. The comparison between Steele's actual moisture transfer data and the data of Brown and Solvason [4] cannot be made in depth. This is because all of the data of Brown and Solvason are for no bulk flow of air through the opening. However, if their data is compared for no bulk flow of air alone, there is a significant difference between the calculated data of Brown and Solvason and those measured by Steele [1] and Jones, et. al. [14].

1.2.3 Transient Moisture Migration. There have been very few experimental or theoretical investigations of transient moisture migration through large or small openings. A very limited experimental and theoretical investigation was done by Queer and Mclaughlin [9]. They experimentally investigated the problem of transient moisture transport into a sealed low humidity room, through very small holes, under isothermal conditions. The main emphasis was on moisture transfer by diffusion. Diffusion was presumed to be significant for small openings in contrast with large openings. They did not consider convection, since no net air exchange (there was no velocity distribution across the holes) and/or temperature difference existed between the room and the surroundings.

Queer and Mclaughlin [9] developed a differential equation model to estimate the time required for the establishment of humidity equilibrium. Using the model, they also estimated the net air flow necessary to suppress net water vapor transfer into the controlled environment. No experimental verifications were given for their predictions. Use of their prediction of moisture migration for a large opening where a temperature difference exists, is questionable due to the presence of significant convection.

Schmidt [10] briefly looked into the transient exchange of matter through an opening in a container. He visually studied the transient mixing of carbon dioxide and air in a container. The container was filled with carbon dioxide and it had a vertical window, which could be opened to initiate the matter exchange. Based on his observations of CO_2 replacement by air, he could measure the time required for state of uniform density to be established. He did not consider a net or sustained flow of moisture nor the effect of bulk flow on matter exchange.

In an effort to expand on the observations of Schmidt [10], Gögüs [11] looked into a more detailed experimental and theoretical investigation of the so-called window ventilation problem.

1.2.4 Summary and Conclusions. For the problem of moisture infiltration through large openings, of the three basic mechanisms [2], only the convection mechanism appears to be significant. The only investigation that was specifically concerned with actual moisture infiltration through openings in a partition was that of Steele [1]. Most other investigations were involved both experimentally and analytically with convective heat and mass transfer through the openings. Most existing analyses are based on a modification of the simple theory of Emswiler [3].

The effect of a bulk flow on moisture infiltration has been given limited attention theoretically by Shaw [8], while Steele [1] has experimentally measured the effect of a net bulk flow on moisture transfer through openings. Shaw [8] introduced a general discharge coefficient, to adjust the forced and free convection of air velocities through the opening.

As was discussed in previous sections, there has been relatively little attention given to the problem of transient moisture transfer, but there has been a limited investigation done by Queer and Mclaughlin [9] and Schmidt [10] and Gögüs [11].

CHAPTER II

DEVELOPMENT OF A SIMPLE MODEL FOR TRANSIENT MOISTURE RESPONSE

The purpose of this chapter is to obtain a prediction of the transient rate of moisture transfer through an opening in a partition which separates a hot chamber from a cold chamber. This will be accomplished by adopting Steele's [1] simple model for steady-state moisture transfer. The modified Steele's [1] simple theory will then be used in an attempt to correlate the transient rate of moisture transfer through an opening for various conditions of humidity, temperature, geometry and bulk flow of air through the opening. The simple model is dependent on the air interchange occurring at the rectangular opening in a vertical partition (Figure 2.1).

It is rather difficult to measure the transient moisture transfer directly, but the amount of moisture transfer through the opening can be indirectly estimated by using a mass balance of all water crossing the boundaries of the hot chamber as shown in Figure 2.2. Alternatively the effect of the humidity in the hot chamber upon the transient moisture response can be observed easily. Thus, by measuring the transient humidity in the hot chamber the effect of variables described earlier on the transient rate of moisture transfer can be indirectly indicated. The net moisture transfer through the opening can be expressed as:

$$\dot{m}_{H_2O,net} = \frac{\dot{m}_H \omega_H}{1 + \omega_H} - \frac{\dot{m}_c \omega_c}{1 + \omega_c} \qquad (2.1)$$

Steele [1] developed an expression for the mass flow rates of moist air $\dot{m}_c$, $\dot{m}_H$, through the opening. His simple model development is summarized in the following section.

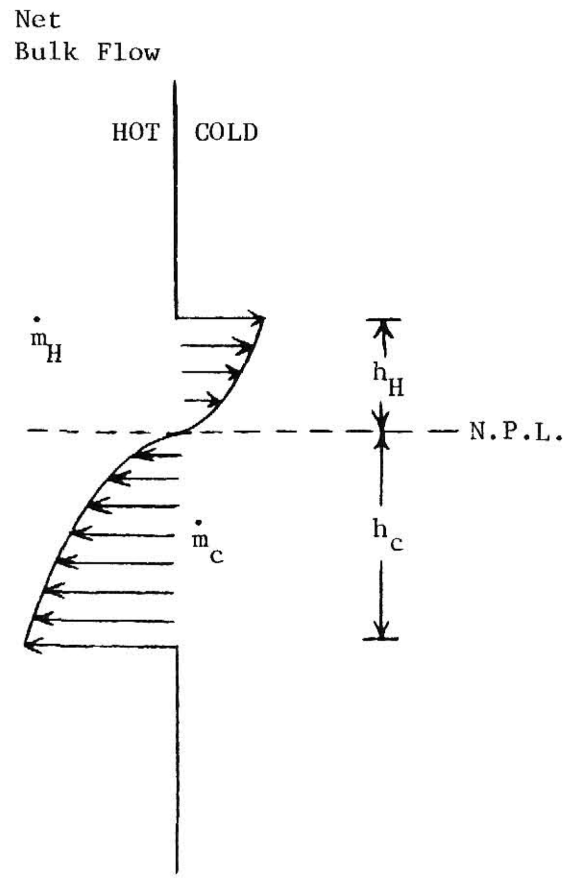

Figure 2.1 Velocity profile across opening

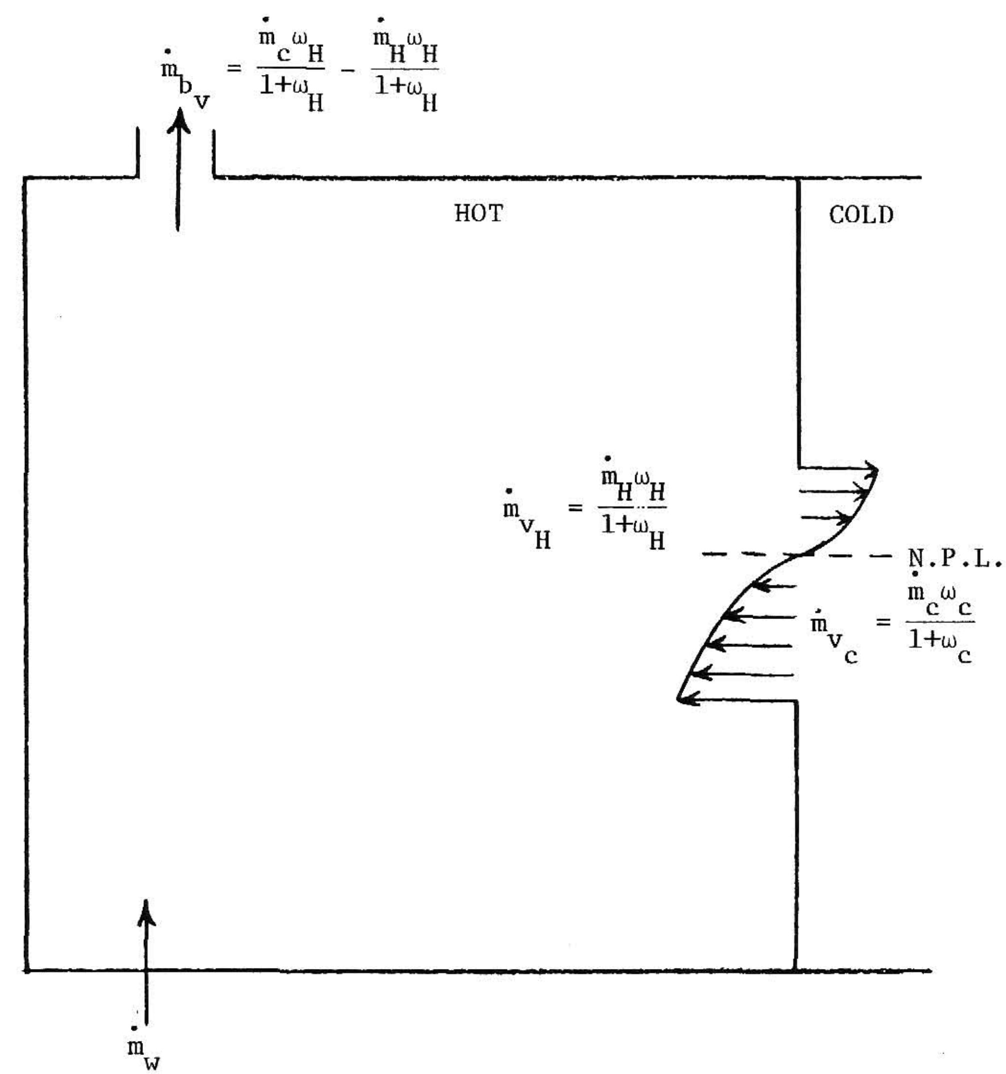

Figure 2.2 Mass balance of water (liquid, vapor) in hot chamber

2.1 Development of A Simple Model for Steady-State Moisture Transfer

The development of a simple model was based on several assumptions, as stated below:

(1) The air was treated as an ideal gas.

(2) Air density, temperature and specific humidity are all uniform in the chamber.

(3) The effect of free air turbulence on moisture transfer is neglected.

(4) Water vapor transfer by diffusion is negligible.

(5) Temperature, density, specific humidity and net bulk flow rate through the opening are all known.

(6) The specific humidity in the cold chamber, ω_c, is kept constant.

The density differences across the opening produce a hydrostatic pressure difference, which is the driving force for water vapor migration through the opening. In Figure 2.1, the neutral pressure line is referred to as the reference level where the pressure difference across the partition is zero. The pressure at this level is considered to be atmospheric pressure. The air density in the hot subchamber is less than that in the cold subchamber, so that the hydrostatic pressures on each side of the vertical opening with respect to height, h, above or below the neutral zone can be expressed by

$$P_c = P_{atm} + \rho_c gh \tag{2.2}$$

$$P_H = P_{atm} + \rho_H gh \tag{2.3}$$

The pressure difference is then given by

$$P_c - P_H = (\rho_c - \rho_H)\ gh \tag{2.4}$$

where g, is the acceleration due to gravity. From the ideal gas law the air densities in each subchamber are inversely proportional to the absolute temperatures in the subchambers, thus

$$\rho_H = \frac{P_{atm}}{R_a T_H} \qquad \rho_c = \frac{P_{atm}}{R_a T_c} \tag{2.5}$$

The density of water vapor was neglected in the above equations because it is small compared with the density of dry air (see Appendix D). By substituting equation (2.5) into (2.4), the magnitude of the pressure difference across the opening can be expressed in terms of the absolute air temperatures, and the distance h, from the neutral zone. Thus,

$$\Delta P(h) = \frac{P_{atm}}{R_a} gh \left(\frac{1}{T_c} - \frac{1}{T_H}\right) \tag{2.6}$$

Using Bernoulli's steady flow model and assuming that all the potential energy associated with the pressure difference at the opening is converted to the kinetic energy, the air velocity v, associated with the pressure difference across the opening can be expressed as

$$V = \sqrt{\frac{2\Delta P}{\rho}} \tag{2.7}$$

where ρ refers to either the density in the hot or the cold chamber. By substituting equation (2.6) into (2.7), the velocity of air flow across the opening will be a function of the height h, above or below the neutral pressure line as given below

$$V(h) = \sqrt{2ghT_c\left(\frac{1}{T_c} - \frac{1}{T_H}\right)} \tag{2.8}$$

The above parabolic velocity profile is shown in Figure 2.1.

In determining the mass flow rates above and below the N.P.L., Steele [1] integrated the mass flux between the N.P.L. and the height of opening with uniform width and assuming constant density for the range of h. Thus, for either hot or cold fluid

$$\dot{m} = W\rho \int_{o}^{h} V(h)\ dh \tag{2.9}$$

Now, by substituting the expression for V(h) into equation (2.9) and integrating, the mass flow rates above and below the N.P.L., the flow rate, $\dot{m}_c$, above the N.P.L. becomes

$$\dot{m}_c = \frac{2}{3} W\rho_c \sqrt{2gT_c \left(\frac{1}{T_c} - \frac{1}{T_H}\right) h_c^3} \tag{2.10}$$

and the flow rate below the N.P.L. is in like manner given by

$$\dot{m}_H = \frac{2}{3} W\rho_H \sqrt{2gT_H \left(\frac{1}{T_c} - \frac{1}{T_H}\right) h_H^3} \tag{2.11}$$

If a net bulk flow of air is made to pass through the opening, the N.P.L. will shift vertically. This net bulk flow is the difference between $\dot{m}_c$ and $\dot{m}_H$.

$$\dot{m}_b = \dot{m}_c - \dot{m}_H \tag{2.12}$$

There is only a small error for the range of air properties in this study if $\bar{\rho}$ and $\bar{T}$ are used in the above equations in place of the actual densities (ρ_c, ρ_H) and temperatures (T_c, T_H). Thus the net bulk flow can be expressed as:

$$\dot{m}_b = \frac{2}{3} W\bar{\rho} \sqrt{2g\bar{T} \left(\frac{1}{T_c} - \frac{1}{T_H}\right) \left(h_c^3 - h_H^3\right)} \tag{2.13}$$

where $\bar{\rho}$ and $\bar{T}$ are the average air density and average air temperature for the two subchambers, respectively. For simplicity, and consistent with Steel's analysis, a simple arithmetic average was used. This suggests that if no net mass flow of air is transferred through the opening, the mass flow rates above and below the N.P.L. will be equal. Hence, the neutral pressure line lies on the horizontal centerline of the opening (Figure 2.1).

It is assumed that the location of the N.P.L. in the presence of net bulk flow through the opening is unknown. Hence, the values of h_c and h_H in equations 2.10 and 2.11 will not be available to determine the mass flow rates of air through the opening. In providing a solution to this problem, Steele introduced a normalization factor, $\dot{m}'$, defined as the mass flow rate of air when the N.P.L. is shifted vertically all the way up to the top the opening. Thus

$$\dot{m}' = \frac{2}{3} W\bar{\rho} \sqrt{2g\bar{T} \left(\frac{1}{T_c} - \frac{1}{T_H}\right) H^3} \tag{2.14}$$

Introducing the normalization factor, $\dot{m}'$, into equations the normalized $\dot{m}_c$ and $\dot{m}_b$ may be expressed as

$$\frac{\dot{m}_c}{\dot{m}'} = \sqrt{\frac{h_c^3}{H^3}} \tag{2.15a}$$

$$\frac{\dot{m}_b}{\dot{m}'} = \frac{\dot{m}_c - \dot{m}_H}{m'} = \sqrt{\frac{h_c^3}{H^3}} - \sqrt{\frac{h_H^3}{H^3}} \tag{2.15b}$$

After substituting and rearranging equations (2.15a) and (2.15b) and knowing that $h_c+h_H = H$, Steele [1] obtained an expression for the

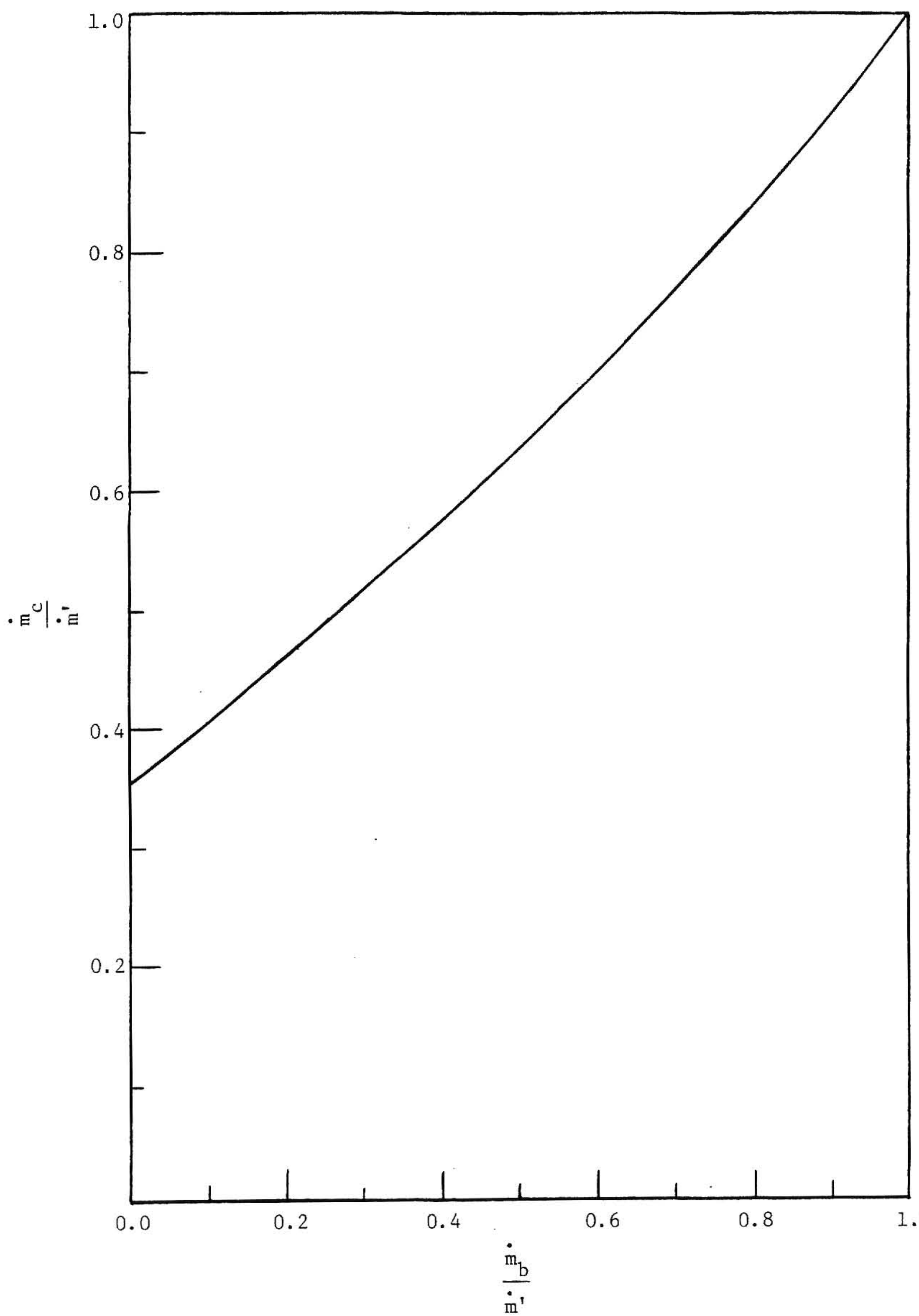

Figure 2.3 Normalized forward flow vs. normalized bulk flow

normalized bulk flow as a function of the normalized mass flow rates above (or below) the N.P.L. Thus,

$$\frac{\dot{m}_b}{\dot{m}'} = \frac{\dot{m}_c}{\dot{m}'} - \left[1 - \left(\frac{\dot{m}_c}{\dot{m}'}\right)^{2/3}\right]^{3/2} \qquad (2.16)$$

and

$$\frac{\dot{m}_b}{\dot{m}'} = \left[1 - \left(\frac{\dot{m}_H}{\dot{m}'}\right)^{2/3}\right]^{3/2} - \frac{\dot{m}_H}{\dot{m}'} \qquad (2.17)$$

These equations apparently cannot be solved explicitly for either $\dot{m}_c$ or $\dot{m}_H$ in terms of $\dot{m}_b$. Graphical representations of the solutions are provided in Figure 2.3 for $\dot{m}_c$, and in Figure E.1 for $\dot{m}_H$. For a given bulk flow the net moisture transfer through the opening can now be determined from equations 2.16 and 2.17 in conjunction with equation 2.1.

2.2 General Formulation of A Model for Transient Moisture Response

A simple transient mathematical model can be obtained for correlating the transient rate of moisture transfer through an opening for various conditions of humidity, temperature, geometry and bulk flow of air. The development of the simple transient model is based on additional assumptions of what was stated in the previous section. The additional assumptions are stated below:

(7) Air density, temperature, and humidity in the chamber are all uniform at each instant of time.

(8) Water addition to the chamber is continuous.

(9) The process of transient moisture transfer through the opening is quasi-steady.

In Figure 2.2, a mass balance diagram is depicted which shows the mass flow rates of water crossing the boundaries of the hot subchamber. The net rate at which water vapor enters the chamber at time t, $\dot{m}_v$, is equal to the net at which water vapor is stored in the chamber at time t; thus,

$$\frac{dM_v}{dt} = \dot{m}_v \tag{2.18}$$

From the definition of specific humidity of an air-water vapor mixture

$$\frac{dM_v}{dt} = \frac{d}{dt}\left(M_a \omega_H\right) \tag{2.19}$$

Since the change in mass of dry air in respect to time is very small (typically 1% error), for the purpose of this study it will be assumed to be approximately constant.

Thus,

$$\frac{dM_v}{dt} = M_a \frac{d\omega_H}{dt} \tag{2.20}$$

From the mass balance diagram (Figure 2.2) the net mass flow rate, $\dot{m}_v$, can be expressed as

$$\dot{m}_v = \dot{m}_w + \dot{m}_{H_2O,net} - \dot{m}_{bv} \tag{2.21}$$

Using the definition of specific humidity and substituting equations 2.1 and 2.12 into equation 2.21, yields

$$\dot{m}_v = \dot{m}_w + \frac{\dot{m}_c \omega_c}{1 + \omega_c} - \frac{\dot{m}_H \omega_H}{1 + \omega_H} - \frac{\dot{m}_c \omega_H}{1 + \omega_H} + \frac{\dot{m}_H \omega_H}{1 + \omega_H} \tag{2.22}$$

Since the values of ω_H and ω_c are very small compared to 1; ω_c and ω_H in above demonimators can be neglected. This assumption indicates that the mass flow rate of moist air and the mass flow rate of dry air are approximately equal. Thus

$$\dot{m}_v = \dot{m}_w - \dot{m}_c\,(\omega_H - \omega_c) \tag{2.23}$$

Substituting equation 2.23 and 2.20 into equation 2.18 yields

$$M_a \frac{d\omega_H}{dt} = \dot{m}_w - \dot{m}_c\,(\omega_H - \omega_c) \tag{2.24}$$

Now, let

$$\tau = \frac{M_a}{\dot{m}_c} \tag{2.25}$$

where τ is a characteristic time. The above differential equation for the specific humidity in the hot chamber as a function of time now becomes,

$$\frac{d\omega_H}{dt} + \frac{1}{\tau}\,\omega_H - \frac{1}{\tau}\,\omega_c - \frac{\dot{m}_w}{M_a} = 0 \tag{2.26}$$

In the above equation the terms M_a, ω_c and τ can be calculated for a given set of test conditions. Since the mass flow of water is also known the above differential equation can be solved for $\omega_H(t)$ using an appropriate initial condition. Two different cases of moisture response will now be considered. The first is the case of moisture addition during which water vapor is added to the hot chamber (see Figure 2.2). The second is the case of moisture decay during which a net flow of water vapor is transferred from hot to cold chamber when the flow of water to the hot chamber is shut off. The solutions for the above transients can be obtained from the above differential equation using the appropriate initial conditions. Each case is summarized below.

Case I. Moisture Addition with (and without) bulk flow

Assuming constant rate of moisture addition and bulk flow, the initial condition in this case is $\omega_{H,i} = \omega_i = \omega_c$ with the net bulk flow of air being made to pass into and out of the opening. The general solution to equation 2.26 for this case is

$$\omega_H(t) = C_1 e^{-\frac{t}{\tau}} + \omega_c + \frac{\dot{m}_w}{\dot{m}_c} \tag{2.27}$$

where C_1 is a constant of integration. Using the above condition, the constant C_1 is found to be

$$C_1 = \frac{\dot{m}_w}{\dot{m}_c} \tag{2.28}$$

substituting C_1 back into equation 2.27 yields

$$\omega_H(t) = \left(1 - e^{-\frac{t}{\tau}}\right) \frac{\dot{m}_w}{\dot{m}_c} + \omega_c \tag{2.29}$$

The final steady-state condition in this case is $\omega_{H,f} = \omega_f$, where ω_f is the specific humidity in the hot chamber when steady-state conditions within the chamber are reached. From equation 2.29, the final specific humidity is found to be

$$\omega_f = \frac{\dot{m}_w}{\dot{m}_c} + \omega_c \tag{2.30}$$

By substituting equation 2.30 into equation 2.29 so as to eliminate $\dot{m}_w$ the result is

$$\omega_H(t) = \left(1 - e^{-\frac{t}{\tau}}\right)(\omega_f - \omega_c) + \omega_c \tag{2.31}$$

Rearranging equation (2.31), the humidity response becomes

$$\theta(t) = \frac{\omega_H(t) - \omega_c}{\omega_f - \omega_c} = 1 - e^{-\frac{t}{\tau}} \tag{2.32}$$

where θ is a normalized specific humidity ratio. The above solution incorporates the effects of temperature difference, humidity difference, geometry and bulk flow of air on the transient moisture response. This solution suggests that as the height of opening, temperature difference and net bulk flow rate through the opening increases, the response of moisture buildup in the chamber gets faster.

In absence of bulk flow through the opening, the solution is expressed in the same fashion as that of equation 2.32. Note that the value of τ is going to be different for cases with and without bulk flow. With no bulk flow the response is expected to be slower than that with bulk flow.

Case II. Moisture Decay with (and without) Bulk Flow

In this case, after the moisture is added to the hot chamber and steady-state conditions are established, the flow of water into the chamber is initially shut off so that $\dot{m}_w$ will no longer be in the mass balance diagram, thus $\omega_{H,i} = \omega_i$. The differential equation 2.26 becomes

$$\frac{d\omega_H}{dt} + \frac{1}{\tau}\omega_H - \frac{1}{\tau}\omega_c = 0 \tag{2.33}$$

and the solution to this differential equation is:

$$\omega_H(t) = C_1\, e^{-\frac{t}{\tau}} + \omega_c \tag{2.34}$$

Using the initial condition, the constant C_1 is found to be

$$C_1 = \omega_i - \omega_c \tag{2.35}$$

Substituting C_1 back into equation 2.34,

$$\omega_H(t) = (\omega_i - \omega_c)\ e^{-\frac{t}{\tau}} + \omega_c \tag{2.36}$$

The normalized specific humidity ratio can be written as

$$\theta(t) = \frac{\omega_H(t) - \omega_c}{\omega_i - \omega_c} = e^{-\frac{t}{\tau}} \tag{2.37}$$

The absence of bulk flow of air has also no effect upon the expression of the differential equation 2.37 but does effect the magnitude of the time constant τ. Similar to the solution that was obtained earlier, this solution also indicates the effects of humidity difference, temperature difference, geometry and bulk flow of air on the transient moisture response.

CHAPTER III

EXPERIMENTAL APPARATUS

In order to measure the transient humidity response within the hot chamber, a special-purpose test chamber was required, as shown in Figure 3.1 and 3.3. This chamber was a modification of the chamber that was used by Steele [1] for measurement of steady-state moisture transfer through the opening. Due to the specific needs of the transient measurements several modifications were necessary. These modifications included the regulation of water flow into the chamber and the instrumentation which was used to measure the temperature and humidity in the chamber. Previously the water input was by gravity-feed from a jug reservoir. However, frequent clogging in its supply line resulted in inconsistent flow of water into the chamber. Therefore to maintain a constant flow of water a positive displacement pump was installed. In the earlier steady-state measurements, time was not a significant factor in determining the average temperature and average humidity. But, to obtain meaningful averages during transient tests humidity and temperature measurements at specific locations in the chamber were needed at nearly the same time. It was not possible to measure the spatial distributions of temperature and humidity during a test; therefore, the apparatus was modified so that the average temperature and average humidity could be measured directly at each instant of time. A detailed description of the modifications follows:

3.1 The Test Chamber

The chamber [1] was 12 ft (3.65 m) long, 6 ft (1.8 m) wide and 6 ft (1.8 m) high. The chamber was made of ½-in plywood and standard 2 x 4-inch studs spaced 4 ft apart. It was 20 inches above the floor, making

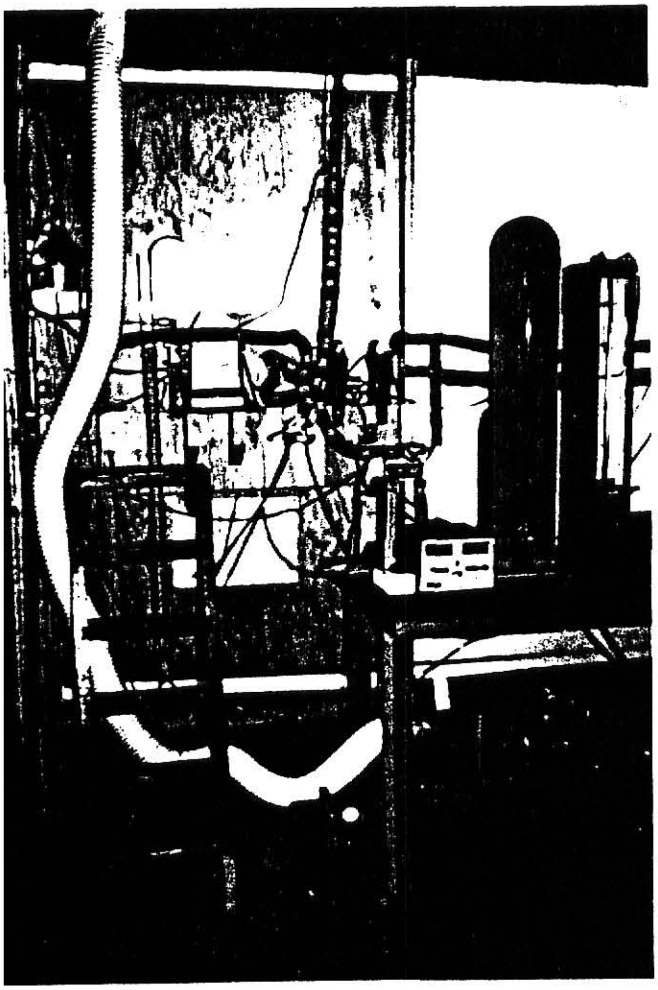

Figure 3.1 Photograph of the left hand side of chamber

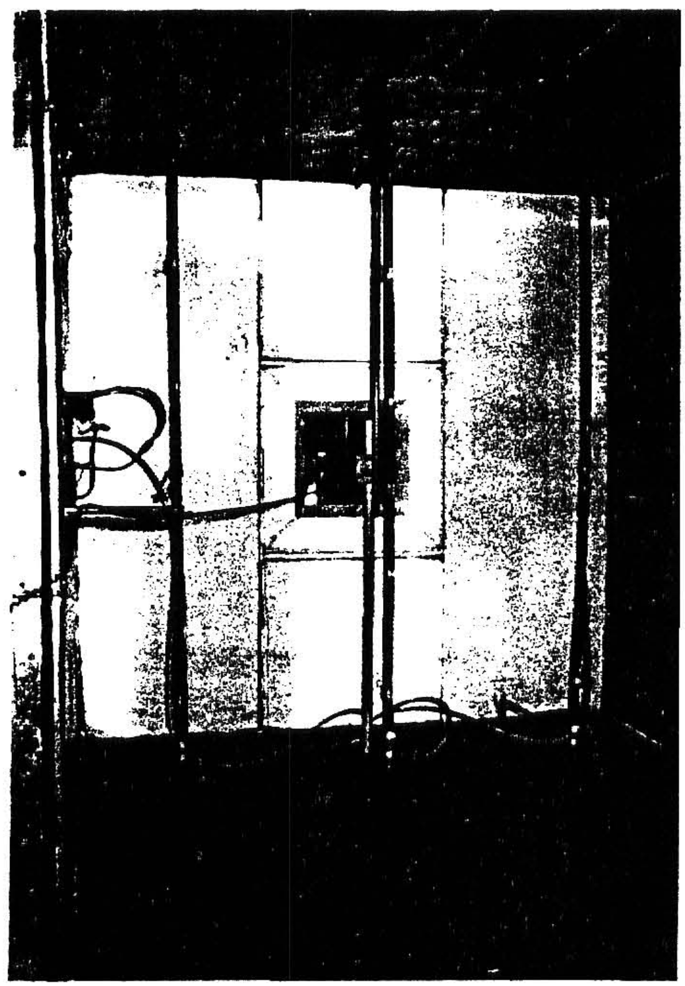

Figure 3.2 Photograph of the opening and sample columns in the chamber

access to the bottom of the test chamber. Also, both ends of the test unit were removable to provide additional access to all equipment inside the chamber. The entire chamber was lined with 24 gauge galvanized steel sheets. They were folded over and soldered at the seams to prevent absorption of moisture (hygroscopic action) by the wood frame of the chamber, and to ensure a vapor-tight seal for preventing any leakage of moisture through the seams. As an added precaution, all major joints in the hot chamber were also caulked with silicone sealant. There was a vertical partition of 24 gauge galvanized sheet that divided the chamber into two 6 ft x 6 ft x 6 ft (1.8 m x 1.8 m x 1.8 m) cubical subchambers. This partition had a cutout of 24 gauge galvanized sheet steel 2 ft by 2 ft square on which to place an opening. The opening of desired size was secured in place using silicone rubber sealant.

As shown in Figure 3.4, the left subchamber was maintained hot and humid while the right subchamber was maintained at room conditions since it was open to the room for most tests. Only in the investigation of the effect of free air turbulence on the transient moisture response was the cold chamber closed to the room. There was a baffel that was positioned 2 ft away from the vertical partition in the hot chamber to minimize the free air turbulence or any nonuniform movement effects on the air interchange across the opening. The baffel was 6 ft high with two columns of offset 4 inch wide strips of sheet metal. During the turbulent tests a large blower, with a 16 inch diameter rotor, supplied air to the cold chamber. The flow rate of air could be controlled by using a vane-type damper on the blower inlet. On the cold end of the chamber, there were two 16 inch diameter ports, one at the top and one at the bottom. The supply air was delivered to the cold chamber through the

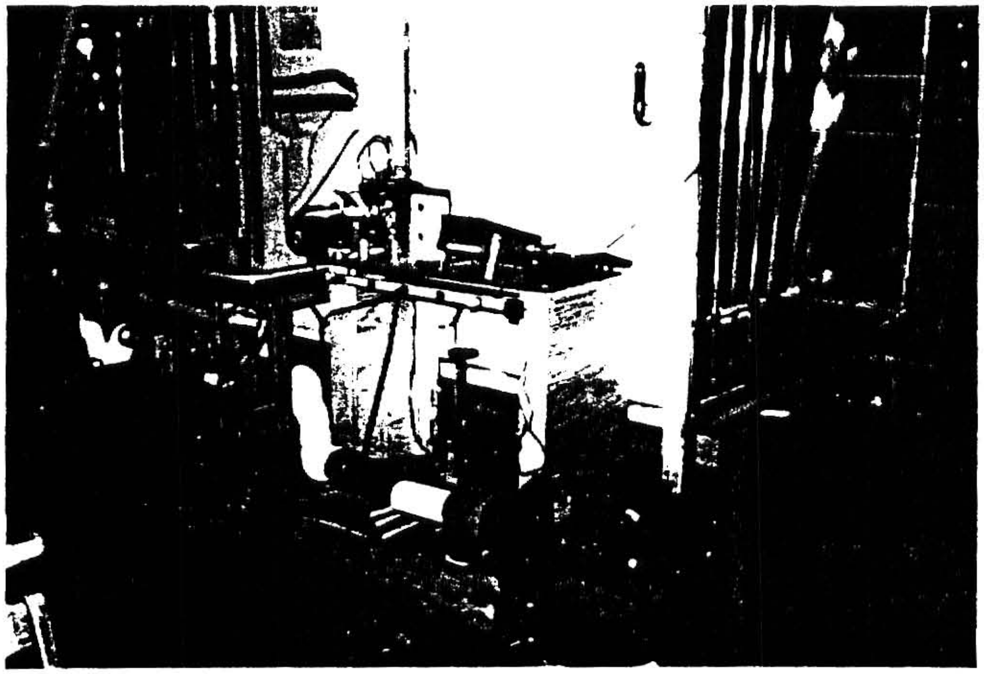

Figure 3.3 Photograph of the right hand side of the chamber

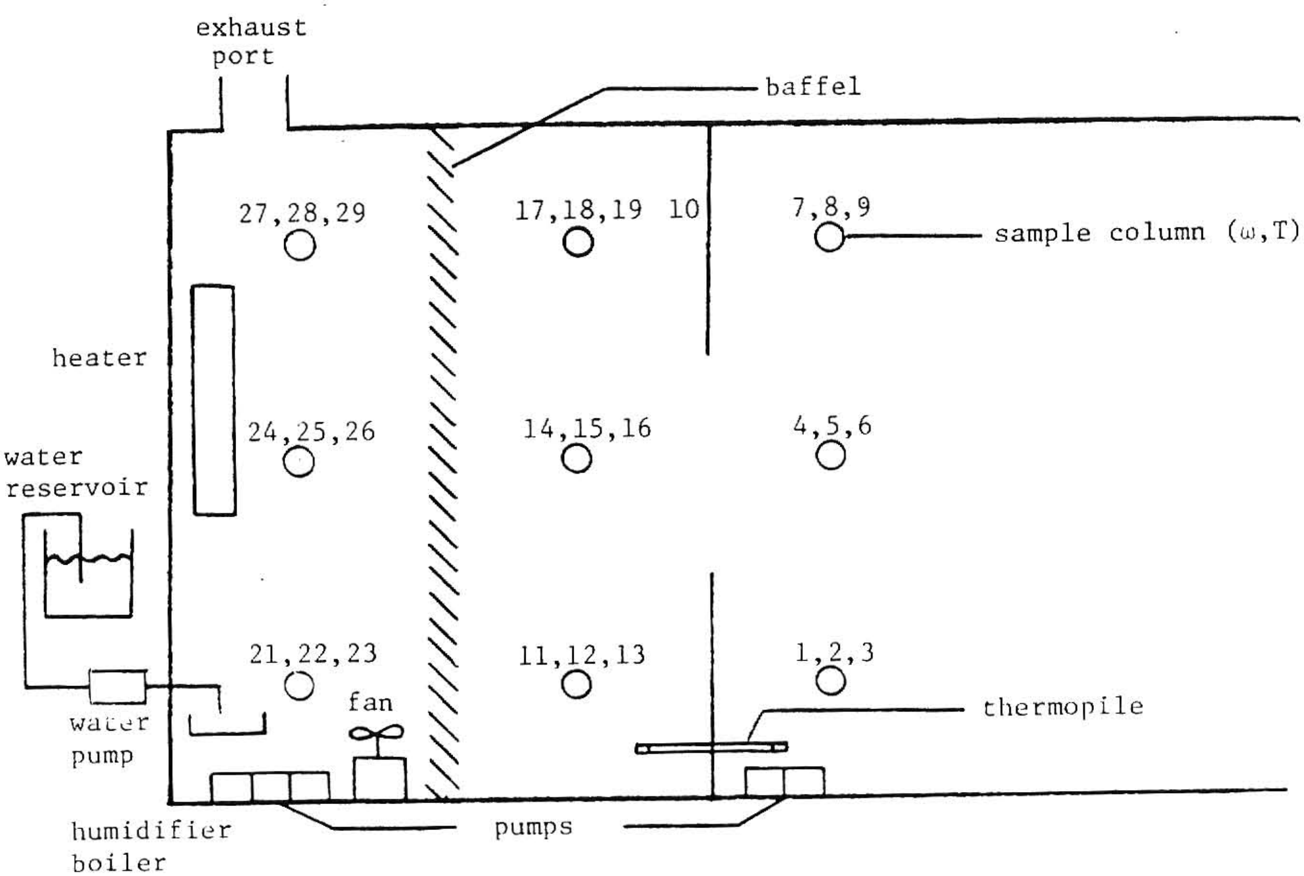

Figure 3.4 Chamber arrangement

bottom port (delivery port) by an insulated plastic duct, and discharged through the top port (exhaust port), therefore circulating the air inside the cold chamber continuously. The flow of air through the top port was controlled by an adjustable damper. Thus the free air turbulence could be adjusted to the desired range by using the two dampers. To limit the heat loss conducted through walls, floor and roof as well as through the vertical partition, two inch thick polystyrene foam was used to cover the exterior of the chamber, as well as the cold side of the vertical partition surrounding the opening. The insulation for the opening was tapered at a 45° angle outward into the cold chamber, as shown in Figure 3.2. This approximated a zero length (or orifice type) opening, and was consistent with the type of opening configuration used by Steel [1].

Initially, several leak tests were run to measure how well the chamber was sealed. For example at a pressure of about 0.1" H_2O in the hot chamber, the leak is expected to be no greater than about 3.5 grams per hour of water vapor from the hot chamber.

3.2 Humidity Control System

The humidity in the hot chamber was maintained by pumping water from a gallon jug reservoir on to a thermostatically controlled boiler in the chamber. The surface temperature of the boiler was set high enough (375°F, 190°C) that it could vaporize the flow of water as it dripped into the boiler. An adjustable positive displacement pump was used to force the water into the hot chamber. The pump, with range of 0-1200 ml/hr, discharged a fixed volume of about 3 ml of water at time intervals of 8 secs at its maximum capacity of flow rate. This represented for all practical purposes a continuous flow rate, as far as the hot chamber was concerned. Thus the desired humidity level in the hot subchamber could be established.

In order to measure average humidity in each chamber, air samples were pumped out through nine sample columns as shown in Figure 3.4. The reason behind the manner of each sample column construction was to pull the intake air samples at different heights, at the same time, so that it could represent the average humidity at that location. Each sample column was made from 5/8 in. O.D. steel conduit and had twelve intake holes of 3/8 in. diameter, as shown in Figure 3.5. The combined sample from each hole was withdrawn through a central exit hole three feet from the floor. This was provided by connecting a sample line to a two foot copper tube (¼ in. O.D.) inside the sample column through the central exit hole. The copper tube was extended one foot above and below the central hole to withdraw air samples from inside the column evenly. Six of the other holes were drilled as three pairs, 1 ft, 3 ft, and 5 ft from the floor. One inch below each of these pairs another pair of holes were drilled, these six holes being at 90° angles from the first set. Three of nine sample columns were placed in the cold chamber, 2 ft apart from each other and 2 ft from the partition. The other six sample columns were placed 2 ft apart in the hot chamber, three on each side of a baffel section, as shown in Figure 3.4.

The air samples that were taken to measure the humidity of either side of the chamber were pumped through the sample lines (3/8 inch O.D. polyethylene tubing) using modified aquarium pumps. In order to minimize the time lag involved in carrying the air sample through the sample lines, a large flow rate of sample was required for fast response (see Appendix A). Due to existence of more resistance (solenoid valves) in

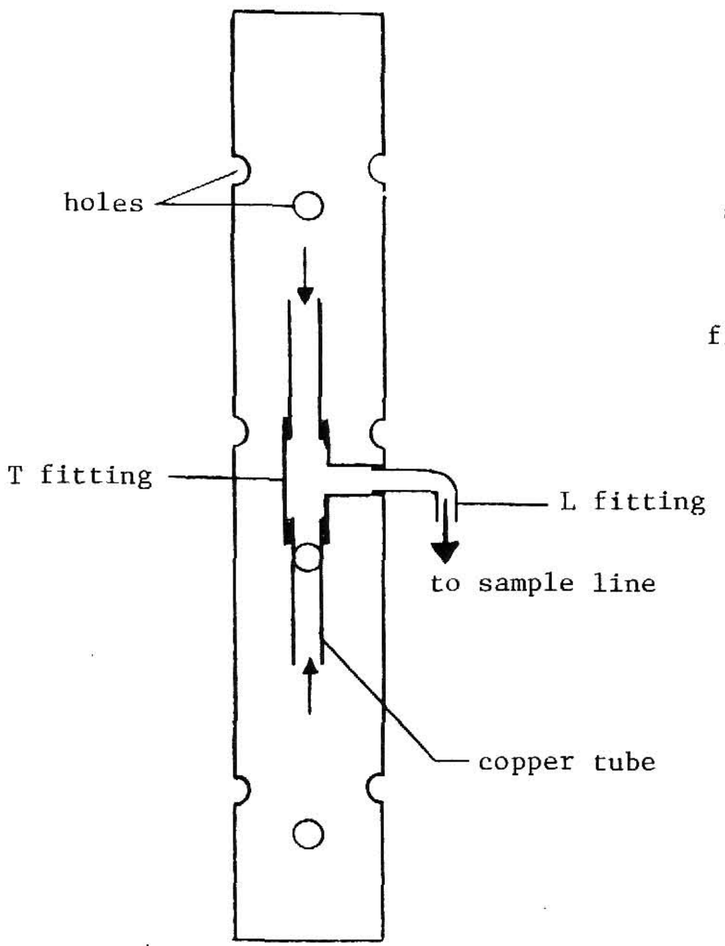

Figure 3.5 Sample column

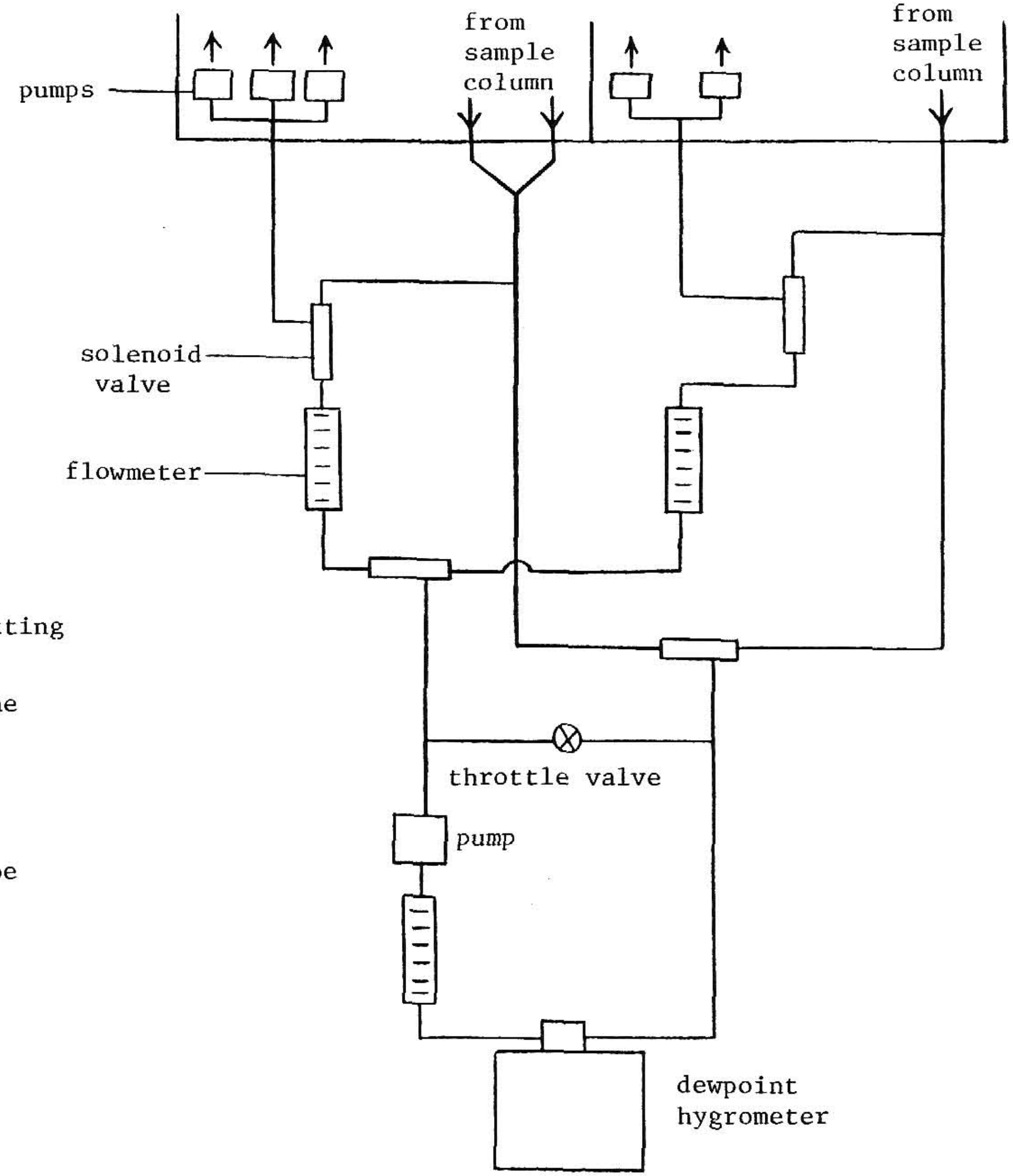

Figure 3.6 Sample line circuit

the hot chamber circuit, three pumps (12 ft^3/min) were used in parallel for collecting air samples from the hot chamber compared to two pumps (8 ft^3/min) for taking air samples from the cold chamber. The sample lines were merged together to represent the average air sample of that section in the chamber. Outside the chamber the sample lines of the two sections in the hot chamber were also combined to represent the average air sample of the subchamber. This modification of sample lines provided the ability to measure the humidity of each separate section in the hot chamber individually.

3.3 Humidity Measurement

In Figure 3.6 the sample line circuit is shown. The combined air sample flow was passed through a dewpoint hygrometer (Cambridge model 990) which measured the dewpoint temperature of the air sample. This hygrometer required a flow of 2-4 scfh for accurate measurement. Thus, a by-pass was provided in the loop to prevent a high flow rate of sample through the hygrometer. A throttle and a pump were used to maintain the volume flow rate of air sample in the loop. Two flowmeters were used to measure the air flow rate of air sample through the sample lines. Selection of the air sample flow from either the hot or cold side of the chamber was made possible by four solenoid valves provided in the loop, which were operated by an on-off switch as shown in Figure 3.6. The air sample collection could be alternated between the cold and hot sides of chamber by switching either all of the valves on or off respectively. To prevent condensation of the sample flow, the sample lines were wrapped with electric heating tape and well insulated. All the air samples were returned to the chamber from which they were withdrawn in order to ensure that the mass fraction of moisture in the chamber would remain unaffected.

3.4 Temperature Control System

The relative temperature within the hot chamber was established by means of a three position (500-1000-1500 W) electrical heater. In order to maintain a constant temperature difference (driving force) across the opening, a thermopile was connected between the hot and cold chambers. The electrical output from the thermopile was connected to an on-off heater-controller which could regulate the power of the electrical heater and thus maintain an approximately constant and adjustable temperature difference between the two subchambers. A small fan was used in the hot subchamber to bring the temperature and humidity into a more uniform state.

3.5 Temperature Measurement

In order to measure the temperature in the subchambers, 27 24-gauge copper-constantan thermocouples were installed. Three thermocouples were mounted to each sample column at heights of 1 ft, 3 ft, 5 ft from the floor, as shown in Figure 3.2. The thermocouples on each set of three sample columns (9 junctions in total) were connected to a common reference junction temperature. The reference junction for these thermocouples was a room temperature water bath, and its temperature was measured using a 24-gauge copper-constantan thermocouple connected to a Digitec digital thermometer model 590 TC type T. The thermocouples on each set were put in series to make a thermopile. The thermopile then provided a measure of average temperature in that section. Furthermore a selector switch and the digital thermometer were used to monitor each individual temperature in the chambers.

3.6 Bulk Flow

There was an exhaust port in the roof of the hot subchamber between the backwall of the chamber and the baffel; thus, a bulk flow of air could be withdrawn from the chamber through the opening. A centrifugal fan and two valves allowed for manual regulation of the desired air flow. The mass flow rate through the exhaust was determined using a 1.049 inch Annubar flowmeter. The dynamic pressure and static pressure associated with the meter were measured by two Meriam water micromanometers model 34FB2. The flowmeter was calibrated prior to installation; complete details of the calibration procedure and calibration curve are presented in Appendix C. The temperature of the exhaust air was also measured by using a 24 gauge copper-constantan thermocouple junction.

3.7 Test Procedure

The actual measurement of transient moisture transfer was made for both moisture addition and moisture decay in the hot chamber. The first step in moisture addition (or decay) was to bring the chamber to the desired steady-state temperature difference. Therefore the electrical heater and on-off heater controller were turned on and a desired setting was chosen. It took as long as two hours for the hot chamber to come to steady-state conditions.

A two-channel Nicolet storage oscilloscope model 201 was used. The first channel being used for storing the readouts of the dewpoint hygrometer at desired time intervals; the second channel was used for measurement of temperature differences across the opening, as well as the temperature in the cold chamber and in both sections of the hot chamber. Due to switching of the on-off controller, the temperature fluctuated some within the hot chamber. The storage scope enabled the average value to be determined as the temperature readout in millivolts. To minimize the effect of background noise on the measurement of temperatures, a 2500 μF capacitor was connected as a low-pass filter across each thermopile output.

3.7.1 Transient Moisture Addition. Prior to adding moisture to the chamber, the boiler, sample line pumps, heating tapes and dewpoint hygrometer were turned on and the dewpoint hygrometer was balanced. At time zero the water pump was turned on and the storage scope triggered simultaneously. The water pump delivered on the average a constant flow of water from a jug reservoir onto the boiler in the hot chamber. The amount of water that was put into the chamber was measured by hand with a 100ml graduate cylinder. The time measurement originated as the water in the one gallon glass jug reservoir passed a reference line. The jug reservoir was then refilled by a known amount of water slightly over the reference level. The time measurement stopped as the water in the reservoir passed the reference line again.

After steady-state conditions of humidity and temperature were well established, data collection began by retrieving the dewpoint temperatures with respect to time, which were stored in the storage scope. The transient electrical output of the dewpoint hygrometer, as well as the output of each thermopile, was recorded on the storage scope in millivolts during each test.

The pressure difference between the chamber and the atmosphere was measured with a (0-24 in H_2O) water manometer and maintained within 0.1" H_2O so as to prevent a significant leakage from the chamber. The atmospheric pressure was determined by means of a mercury-filled barometer with vernier scale movement. The volume flow rate of the air in the sample lines was measured by two variable area flowmeters model 6-1355-B, range 0-50 ft^3/hr. The flow rate in the dewpoint hygrometer was measured by a variable area flowmeter, model R-2-15-C, range from zero to 8 scfm. An anemometer, TSI model 1650, was mounted one foot away from the opening and 3 ft above the floor on a vertical support, so that the approximate range and average velocity of the free air turbulence could be measured.

3.7.2 Transient Moisture Decay. The moisture decay measurement procedure was similar to that for moisture addition measurement. The dewpoint temperature for the cold chamber immediately before and after each test was determined by turning on the solenoid valves, facilitating the passage of the air sample from the cold chamber through the dewpoint hygrometer. After steady-state conditions of humidity and temperature were well established, the water pump was turned off and the storage scope was triggered simultaneously. Hence, data collection for moisture decay began with the recording of the dewpoint temperature decay with respect to time.

In order to investigate the effect of the velocity profile at the opening upon the transient moisture transfer through the opening, a different initial condition was set up. The opening was covered by cardboard and the humidity and temperature control systems were turned on. As soon as the dewpoint temperature reached the desired level, the water pump was turned off. The humidity in the chamber came to equilibrium after several minutes. The cover was then removed upward quickly by hand and storage scope was triggered. In order to further investigate the time required for temperature distribution establishment in the opening, transient temperature measurements were also obtained. A detailed description of this type of test is given in Section IV.

CHAPTER IV

PRESENTATION OF RESULTS

4.1 Experimental Results

The reduction scheme employed is as described in Appendix B for reducing the data to a graphable form. Graphical results presented here indicate the effect of temperature and humidity difference, geometry and bulk flow on transient moisture decay through a zero length rectangular opening. Most of the tests for this study were conducted with an opening of 1 ft by 1 ft (30 cm by 30 cm). In order to show the influence of opening geometry on moisture transfer, three different size openings were tested (see Section 4.1.3). It is important to realize that tests were not conducted so as to form a complete parametric study (since Steele's [1] work already exists); instead, the range of parameters were chosen so as to show the largest influence of parameters on the transient moisture response.

The effect of the above variables on transient moisture decay response are described independently in the following sections. The data are presented on a normalized set of coordinates where normalized specific humidity ratio is plotted as a function of dimensionless time. All of the data presented here have been corrected for the corresponding time lags due to the sample column, sample lines, and hygrometer response (see Appendix A). The uncertainty of measurement as it was described in Appendix B for t/τ is about 4% and for θ is 7%.

4.1.1 Effect of Humidity Difference. It was described in Chapter II and Appendix D, that the humidity difference has a negligible effect on the driving force (density difference). In order to investigate the effect

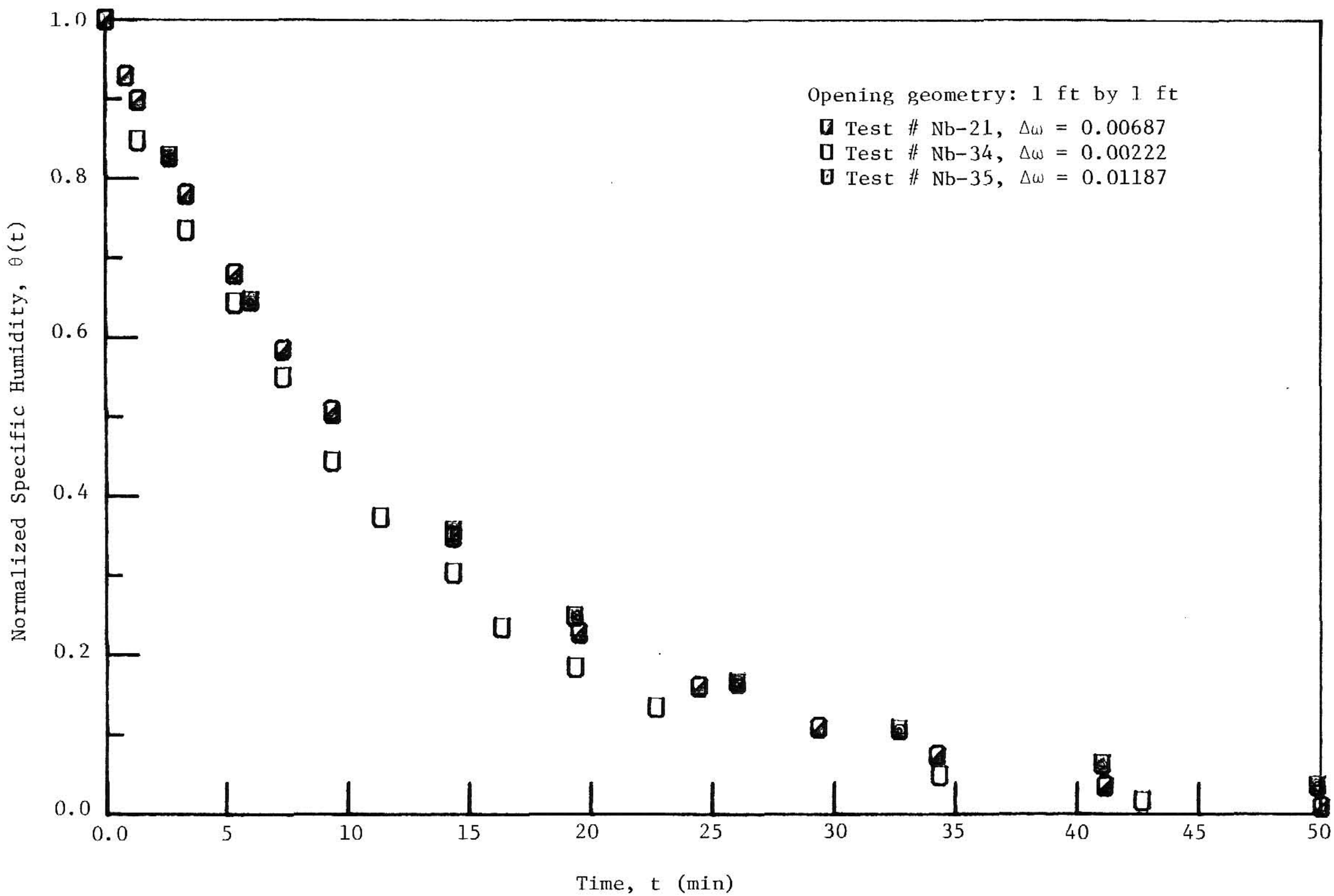

Figure 4.1 Effect of humidity difference

of humidity difference on the transient moisture response through the opening, several tests were conducted under similar conditions, but with different initial humidity differences across the partition. Three different values of about 2.2 gm H_2O/kg dry air, 6.9 gm H_2O/kg dry air, and 15.4 gm H_2O/kg dry air were set up for humidity difference between the hot and cold chambers. In Figure 4.1, on a plot of normalized specific humidity ratio vs. time, it is shown that all the data are superimposed into a single functional relationship which confirms that the data are indeed correlating very well. The fact that the data are coincident with each other, suggests that the humidity difference is not a significant part of driving force. This was expected from the simple theory described in Chapter II.

4.1.2 Effect of Temperature Difference. In order to show the influence of temperature difference on the rate of time dependent moisture transfer, tests were conducted at similar conditions, but at different temperature differences (driving force) across the partition. Three different values of about 9°C, 15°C and 24°C were set up for the temperature difference between the two subchambers. In Figure 4.2, the influence of temperature difference on transient moisture transfer is shown on a plot of normalized specific humidity ratio vs. time. It is clear that there exists a significant difference in response time among the conducted tests. As the temperature difference increases the transient moisture response time decreases which is in agreement with the prediction of the simple theory. In Figure 4.3 all of the data collapse on a normalized set of coordinates into a single functional relationship. This provides evidence for the applicability of the quasi-steady model to correlate the data.

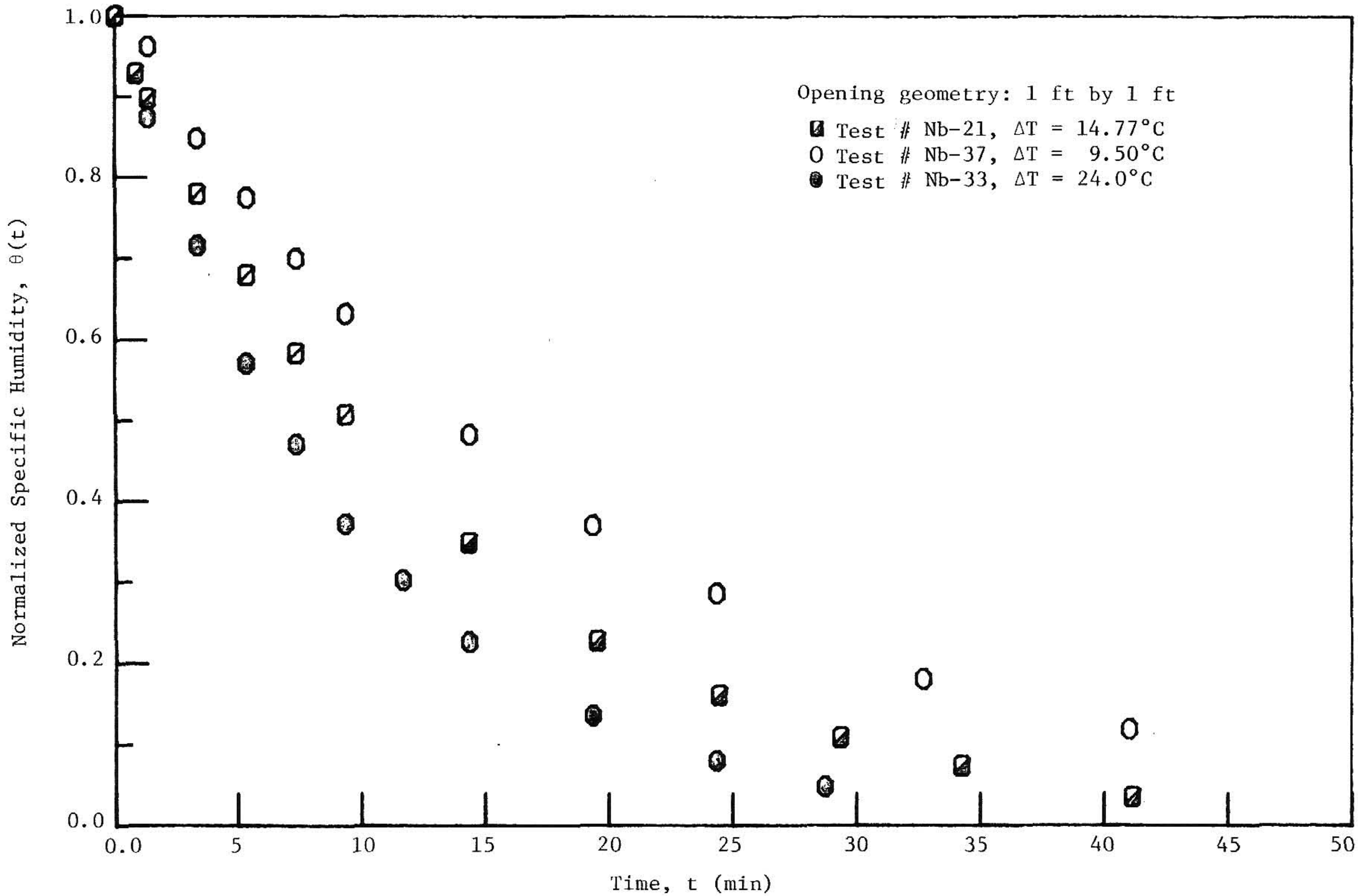

Figure 4.2 Effect of temperature difference

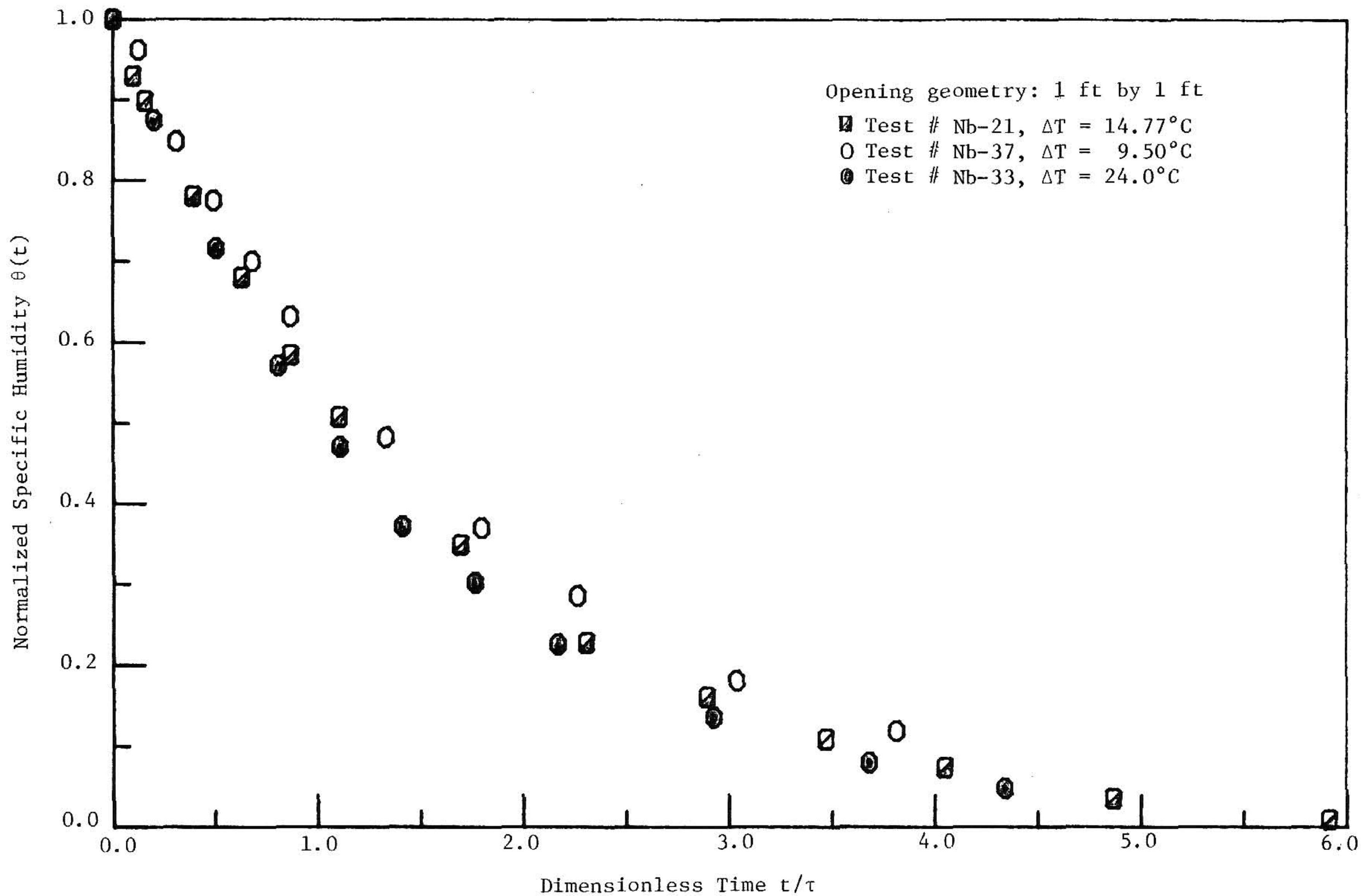

Figure 4.3 Effect of temperature difference with time scaling

4.1.3 Effect of Geometry. In order to demonstrate the influence of opening geometry on the transient moisture transfer through the opening, two additional sizes of rectangular opening, 6 in by 12 in (15 cm by 30 cm) and 18 in by 12 in (45 cm by 30 cm), were tested independently. In Figure 4.4, on a plot of normalized specific humidity ratio vs. time, the influence of opening geometry on the transient moisture transfer is emphasized. It is observed that for the larger openings the response time is faster. This is consistent with the prediction from the theory. In Figure 4.5, all of the data on the normalized graph are nearly coincident, indicating once again that the simple model is correlating the data well.

4.1.4 Effect of Bulk Flow. One series of tests investigated the effect of bulk flow on the transient moisture response. The effect of forcing a net flow of air through the opening is the same as vertically shifting the neutral pressure line and velocity profile. This suggests that more moisture is going to transfer at a given time. In the study of this influential parameter, several tests were conducted under different flow rates of air which were made to pass through the opening. Three flow rates were set up at values of about 0.0 Kg/hr, 22 kg/hr, 59 kg/hr (0 lbm/hr, 49 lbm/hr, 130 lbm/hr).

In Figure 4.6 on a plot of specific humidity ratio vs. time it is apparent that there is a vast difference in response time among the conducted experiments. The result of these experiments are in conjunction with prediction of the simple theory. It is shown in Figure 4.6 that as the bulk flow rate increases the response time for transient moisture transfer decreases (decays faster). In Figure 4.7 the data on the normalized set of coordinates nearly overlap with each other. These

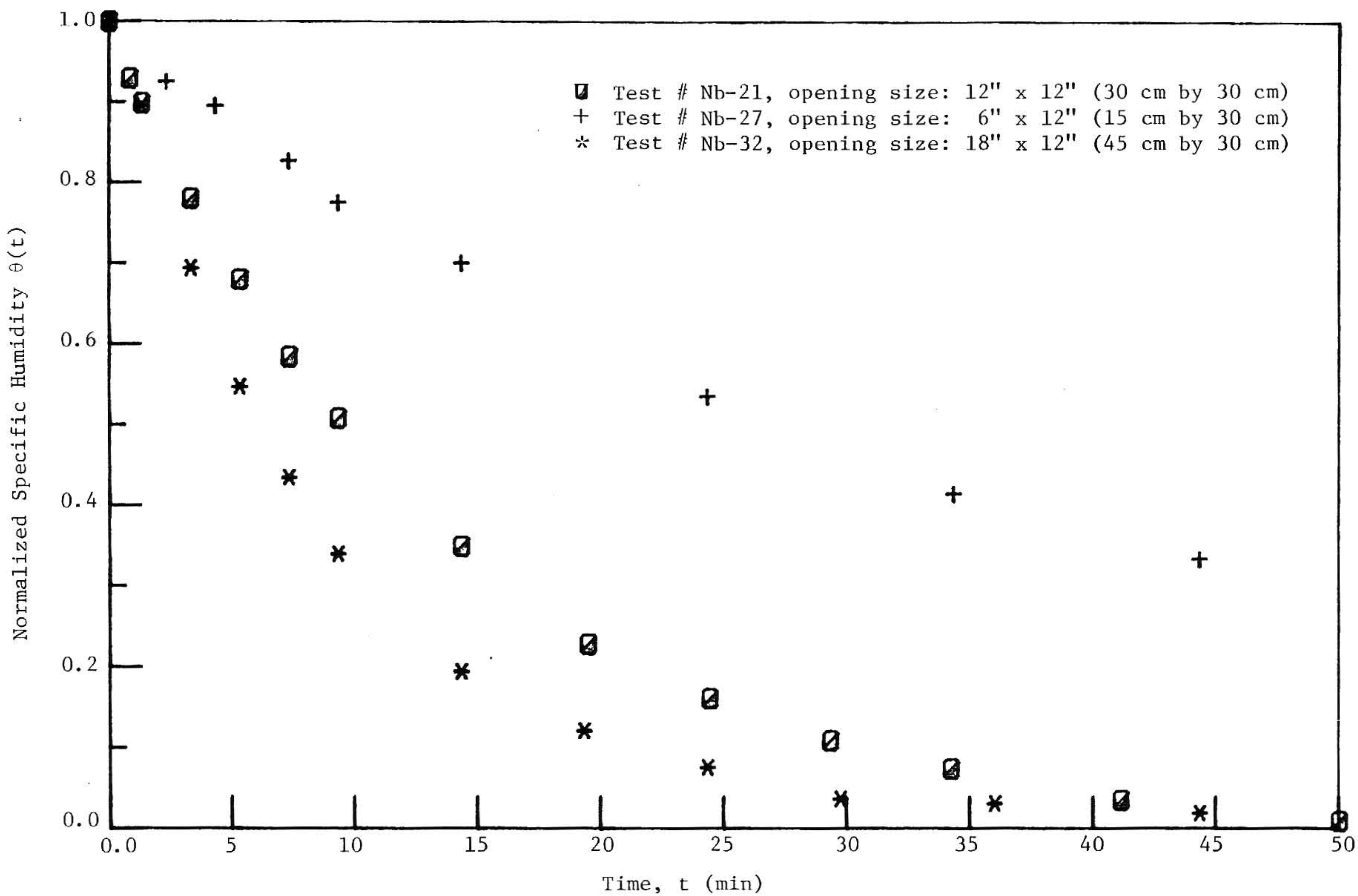

Figure 4.4 Effect of opening geometry

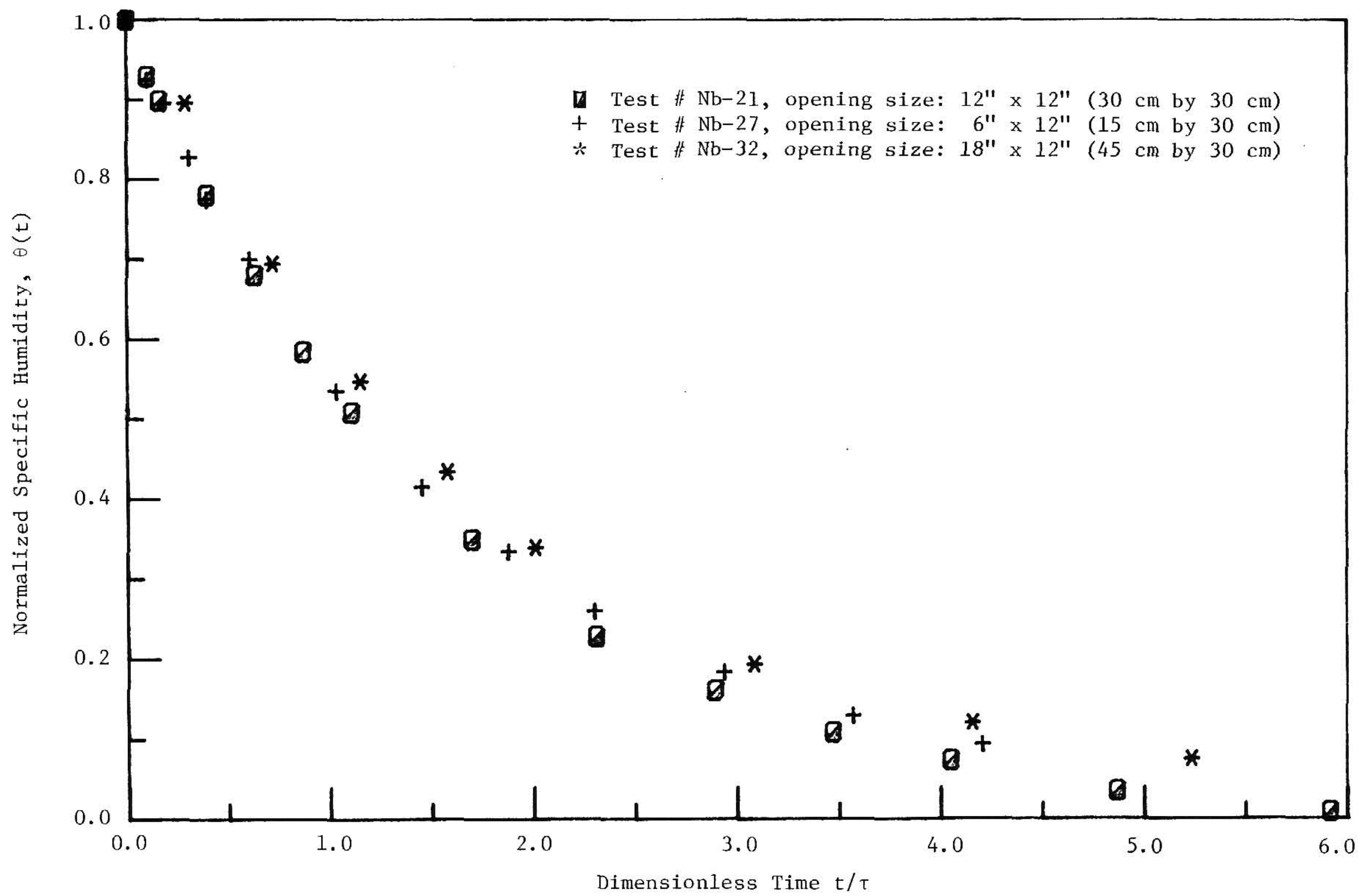

Figure 4.5 Effect of opening geometry with time scaling

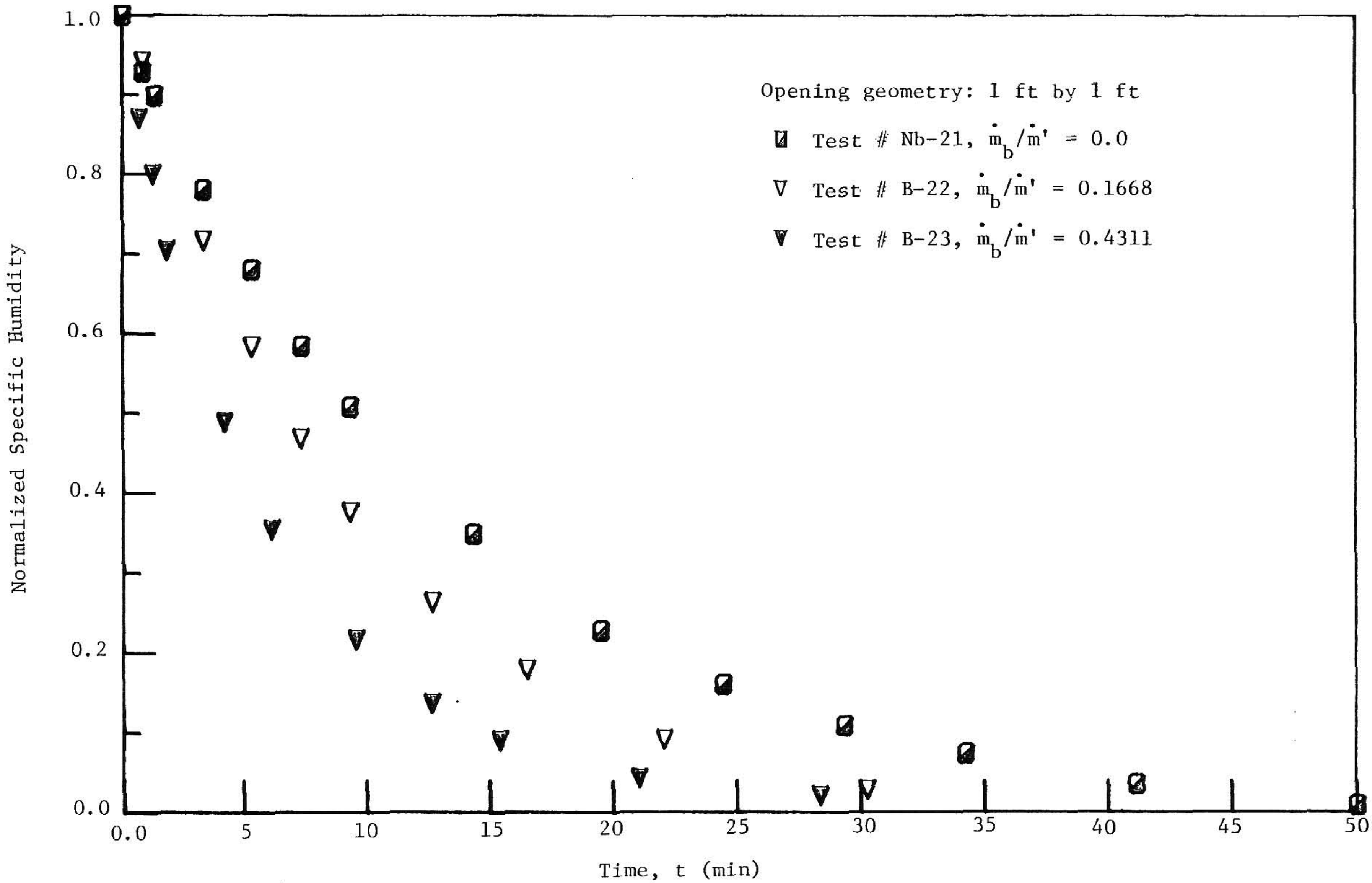

Figure 4.6 Effect of bulk flow

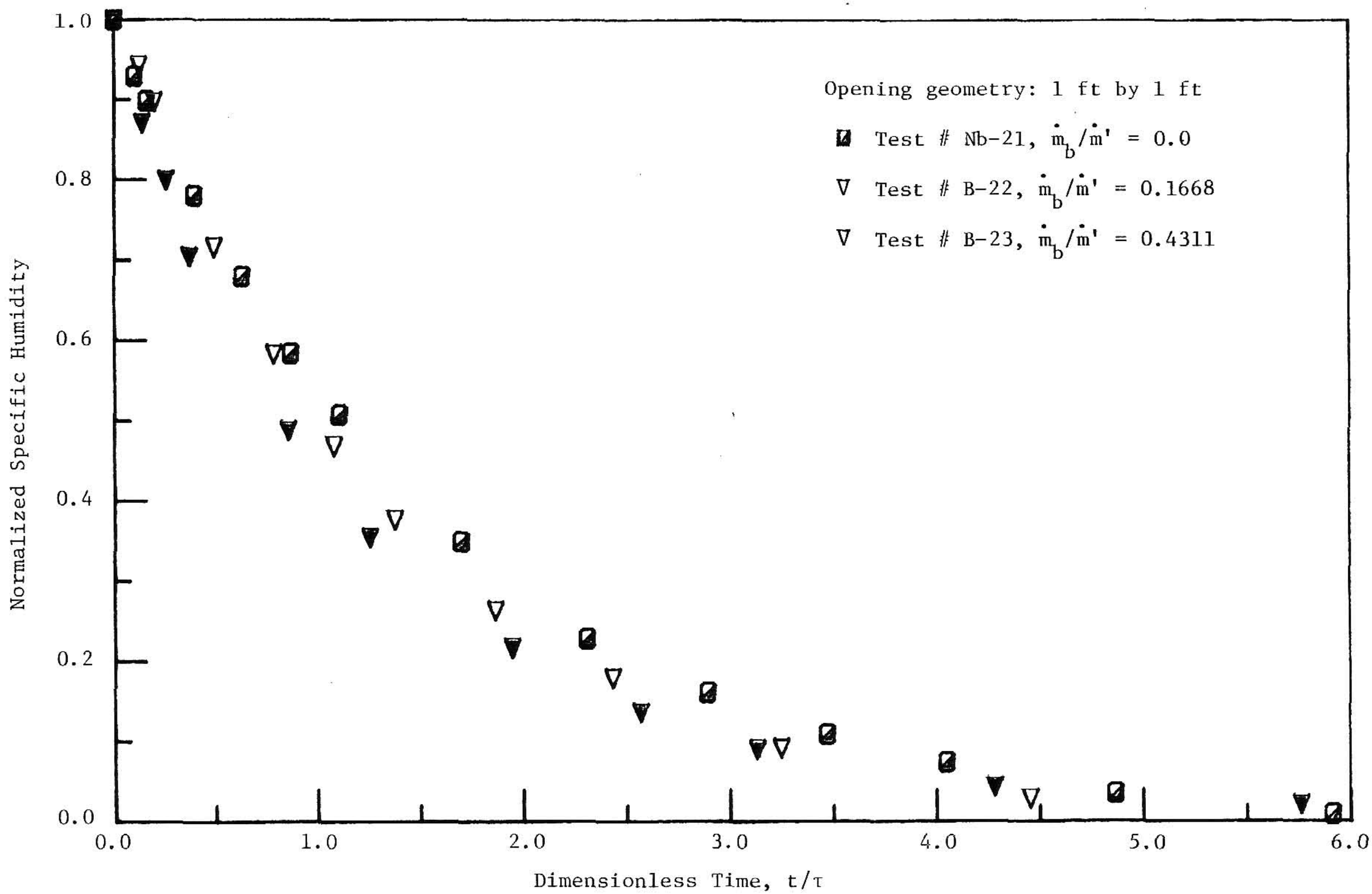

Figure 4.7 Effect of bulk flow with time scaling

data are following a single functional relationship between the normalized specific humidity ratio and the dimensionless time. This indicates that the model is effective in correlating the data.

4.1.5 Summary of Experimental Results. A plot of the data from the variables believed to influence the transient moisture transfer through the opening is shown in Figure 4.8 on a normalized set of coordinates. These data are the exact same data that were presented in previous figures. It is clear that the data are following close to a single functional relationship and are correlating reasonably well using the variables described earlier. This provides considerable additional evidence as to the applicability of the quasi-steady model to correlate the data.

4.2 Predicted Humidity Response

The theoretical correlation between the normalized specific humidity ratio and dimensionless time is also shown in Figure 4.8. In order to bracket the transient moisture decay data a flow coefficient was introduced [8] in equation 8 (Chapter II). This coefficient was determined from steady-state moisture transfer data [1]. The flow coefficients of 0.65 and 0.85 were introduced to put a bound on the data. The detailed theory in bracketing the data is described in Appendix G. In Figure 4.8, it is clear that both the theory and data follow the same trend. The simple theory based on the flow coefficient of 0.65 an 0.85 has bounded the transient moisture decay data reasonably well considering that the uncertainty in measurement of t/τ is 4% and in θ is 7%.

In order to investigate the applicability of the simple model in the case of moisture addition, two moisture addition tests were conducted. One was with and another was without bulk flow. The conditions in the

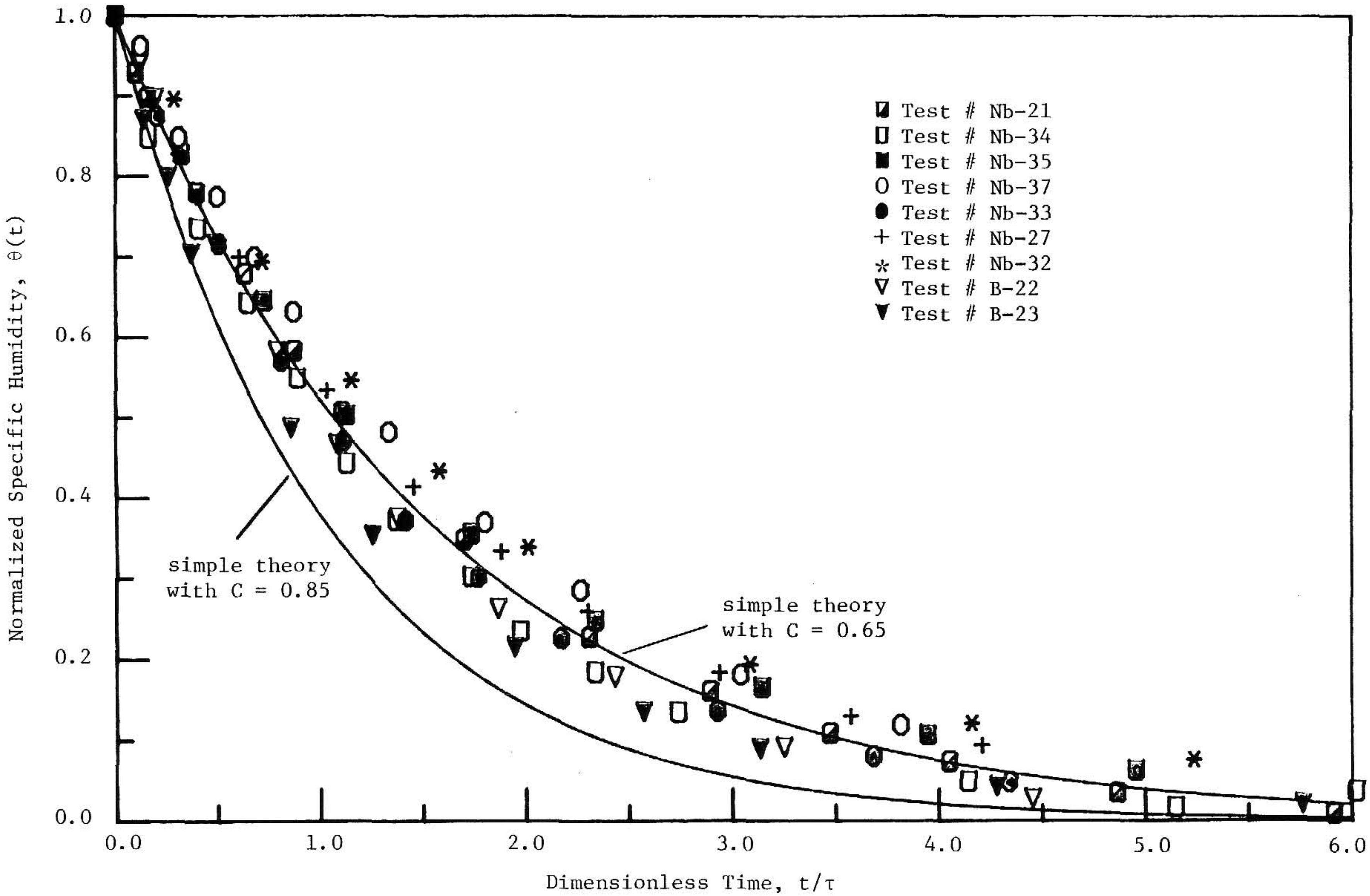

Figure 4.8 Comparison of theory with moisture decay data

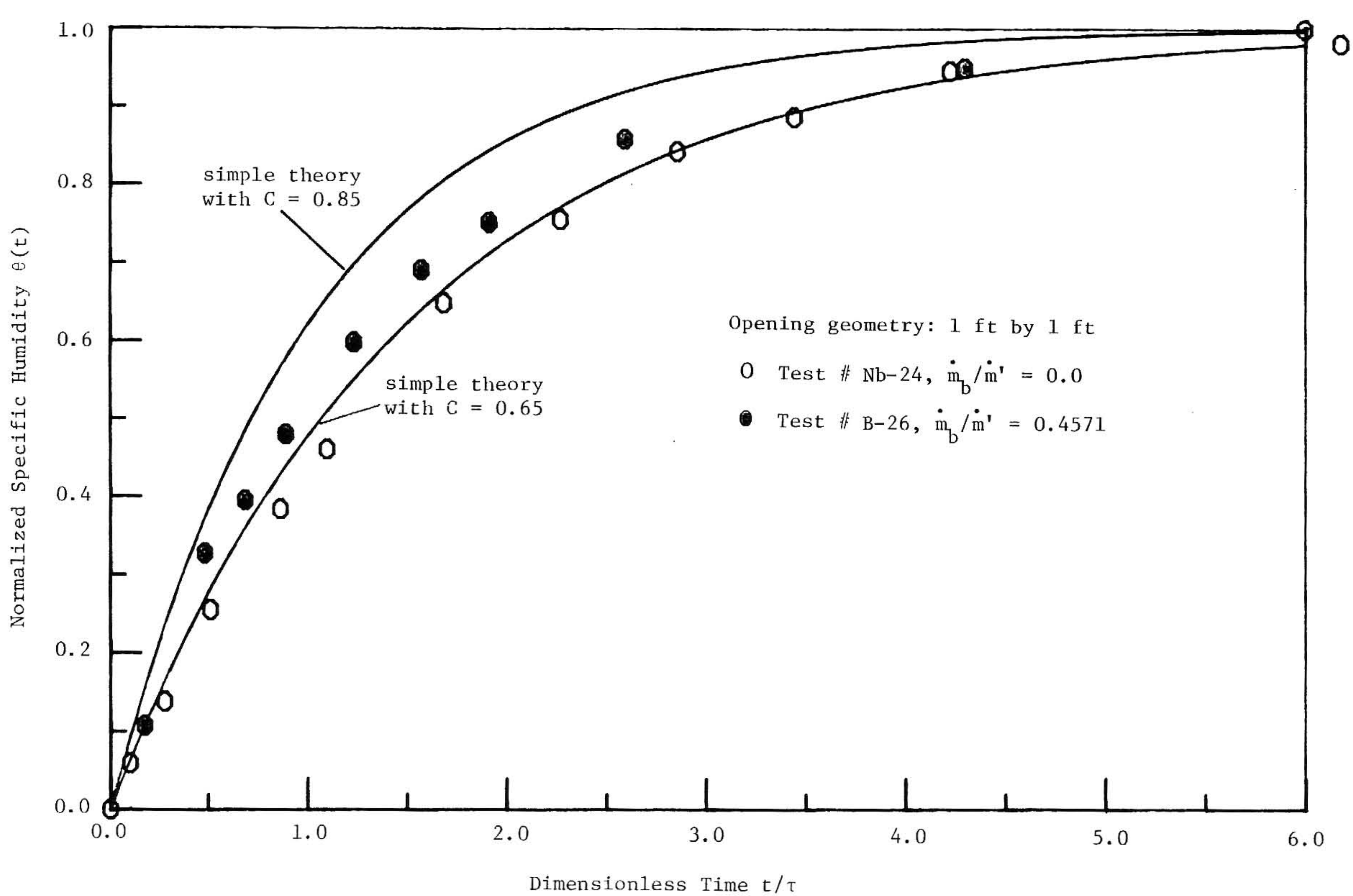

Figure 4.9 Comparison of theory with moisture addition data

test are summarized in Appendix H. The simple theory and data are shown in Figure 4.9 on a normalized set of coordinates. In comparison of the theory and data in case of moisture addition, agreement is similar to that for the moisture decay case. This consistency between the two cases provides additional confidence in using the bounds for most engineering purposes.

4.3 Limitations of Simple Transient Model

The simple transient model, as it was described in Chapter II, was developed on the basis of several assumptions. The validity of three of these assumptions in particular will be investigated below. These assumptions are:

1. The humidity in the hot chamber is uniform.
2. The effect of free air turbulence on moisture transfer is negligible.
3. The velocity profile at the opening is fully established.

It is of interest in this section to study the extent to which these assumptions are valid.

4.3.1 Uniformity of Water Vapor in Hot Subchamber. In Chapter III, the test chamber construction and instrumentation were described in detail. Since the water input to the hot chamber is into only one side of the subchamber (see Figure 3.4) one would expect the humidity to be different in both sides of the hot subchamber. The air samples were taken out from both sides of the baffle in the hot chamber independently, and were merged together at outside of the chamber. In order to determine the uniformity of water vapor in the hot chamber, two tests were conducted. Both tests were kept at similar conditions with the only difference being

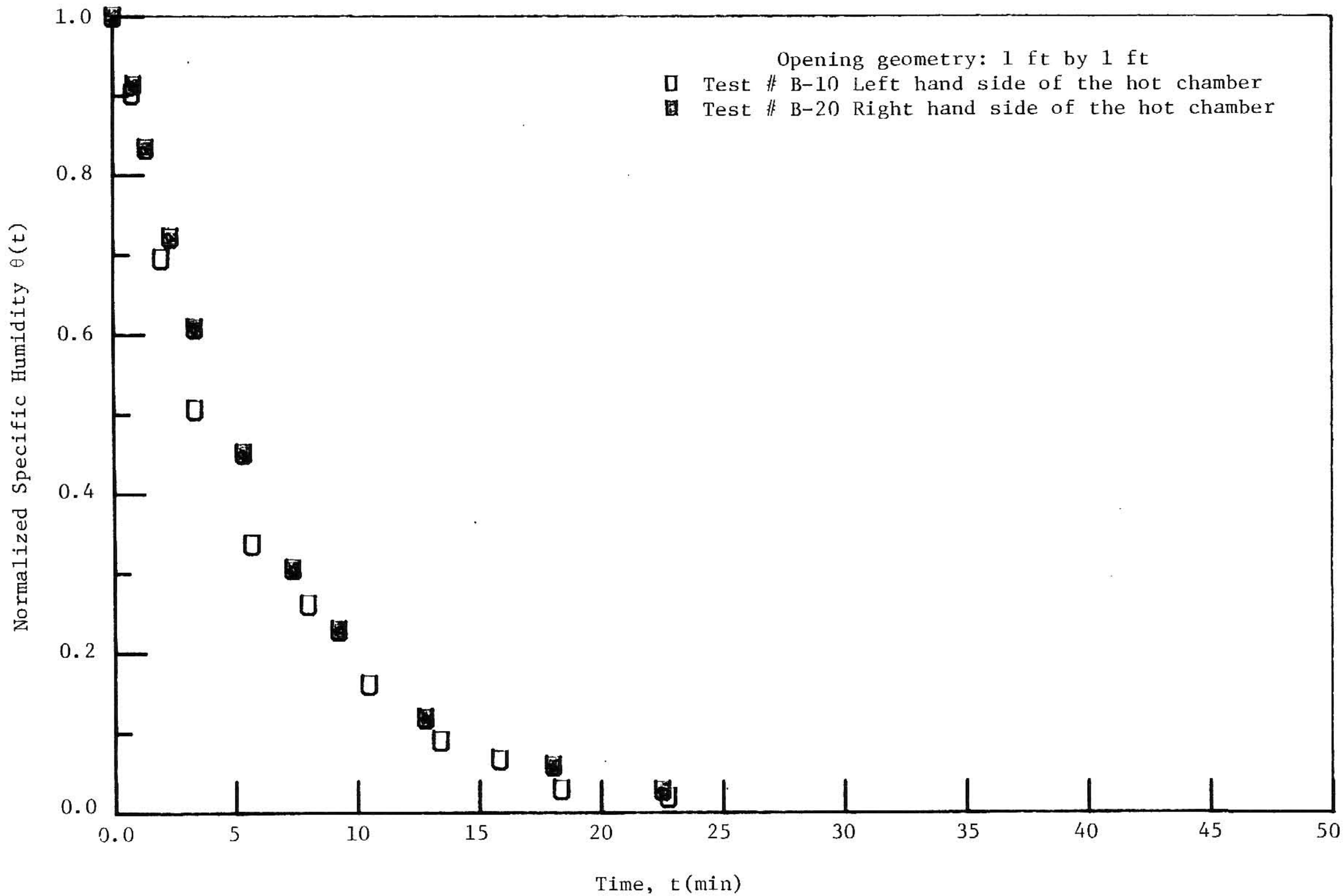

Figure 4.10 Uniformity of water vapor in the hot chamber

that the air samples were collected from different sides of the hot subchamber for each test.

In Figure 4.10, it is observed that the data from both tests nearly coincide with one another. This gives the impression that there exists a uniform water vapor concentration in the hot subchamber.

4.3.2 Effect of Free Air Turbulence. One of the assumptions in developing the simple model was stated as "the effect of free air turbulence on transient moisture transfer is negligible." But from observations that were made of several tests at different turbulence levels, it was concluded that there were indeed some effects on moisture response due to turbulence. As free air turbulence in cold chamber increases, the rate of transient moisture transfer through the opening decreases. This is due to the mixing caused by turbulence at the opening. These results are consistent with Steele's [1] work on steady-state moisture transfer.

In order to show the influence of free air turbulence on the transient moisture transfer three tests were conducted. These tests were run at 4 ft^3/min, 15 ft^3/min, 35 ft^3/min free air turbulences with similar physical and geometrical conditions. The difference in response time is fairly substantial among the conducted tests, as is seen in Figure 4.11. This suggests that with less free air turbulence the transient moisture transfer response is faster. Thus, for comparison of experimental data and theoretical data, it was preferred to run the tests at the lowest free air turbulence possible. This was accomplished by opening the cold chamber to the room so that the differences in the air circulation could not be a significant factor in the experimental results.

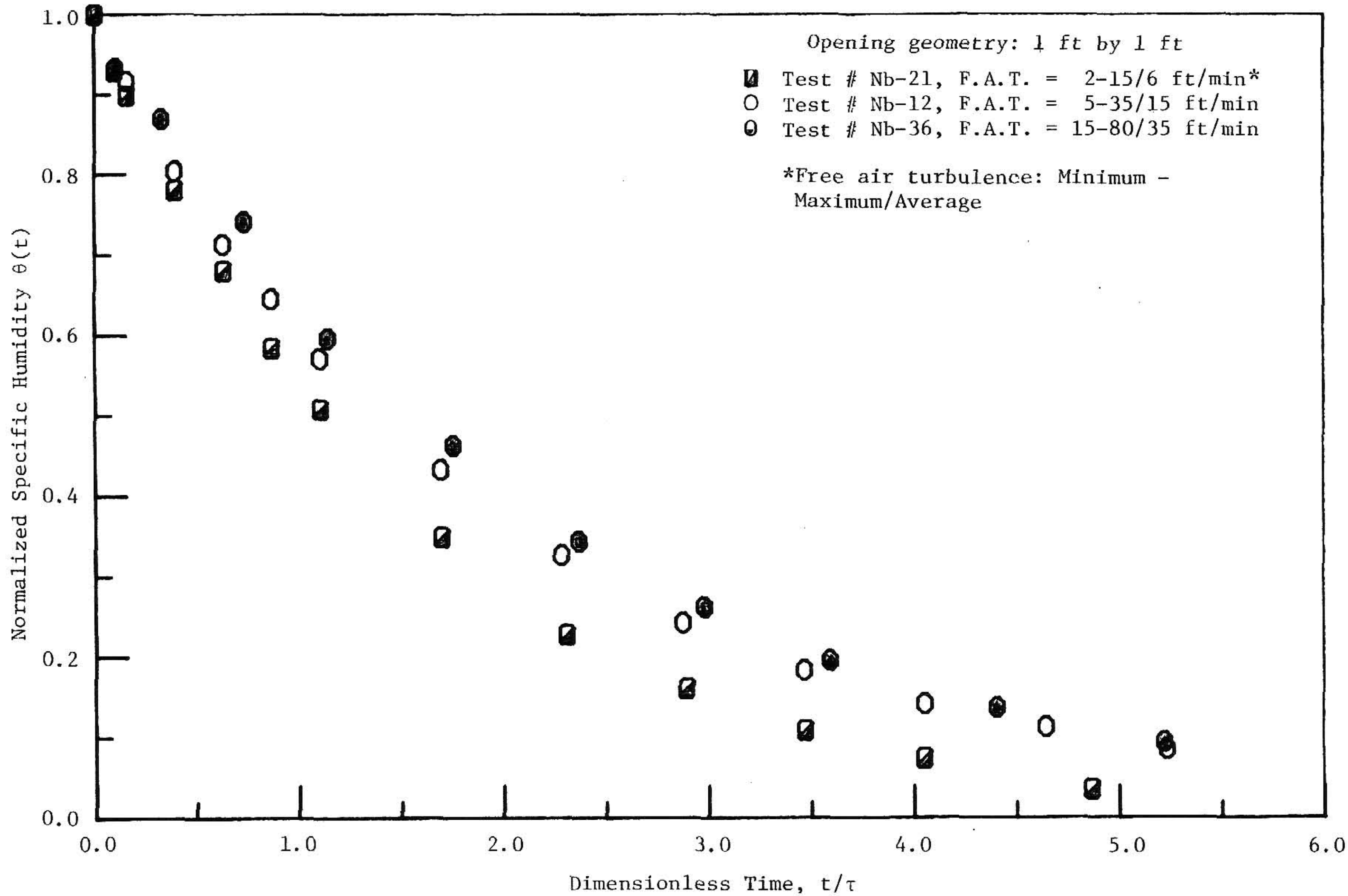

Figure 4.11 Effect of turbulence with time scaling

4.3.3 Method of Initiating Transient. In order to study the applicability of the quasi-steady model under different starting transients, an investigation was directed at the situation where there is an initial transient such as opening a window in environmentally controlled air space. In order to set up a test for this investigation, the opening was covered by cardboard. After the temperature difference and humidity conditions were reasonably well established, the collection of data was begun by uncovering the opening. In Figure 4.12, the data taken in this test is compared with the data that was taken in similar test conditions with an unblocked opening. These two data sets nearly overlap with each other, which suggests that the time that it takes for the velocity profile to be established is very short compared with the time required for humidity to decay within the hot chamber.

4.3.4 Transient Temperature Distribution. The previous section that dealt with the concept of the initial transient at the opening, provided the idea for a study of transient temperature distribution at the time when the opening is uncovered. Since it was difficult to measure the transient velocity distribution at the opening, thus it was a subject of interest to find the time required for temperature profile establishment. Nine thermocouples at distances of 1½ inches from one another were mounted at the opening. After the temperature difference between the hot and cold chamber was well established, the opening was uncovered. A recording potentiometer recorded the temperatures at each location with respect to time. It is shown in Figure 4.13 that after about one minute the steady temperature profile is established. The quasi-steady state model should be applicable provided that the time associated with the

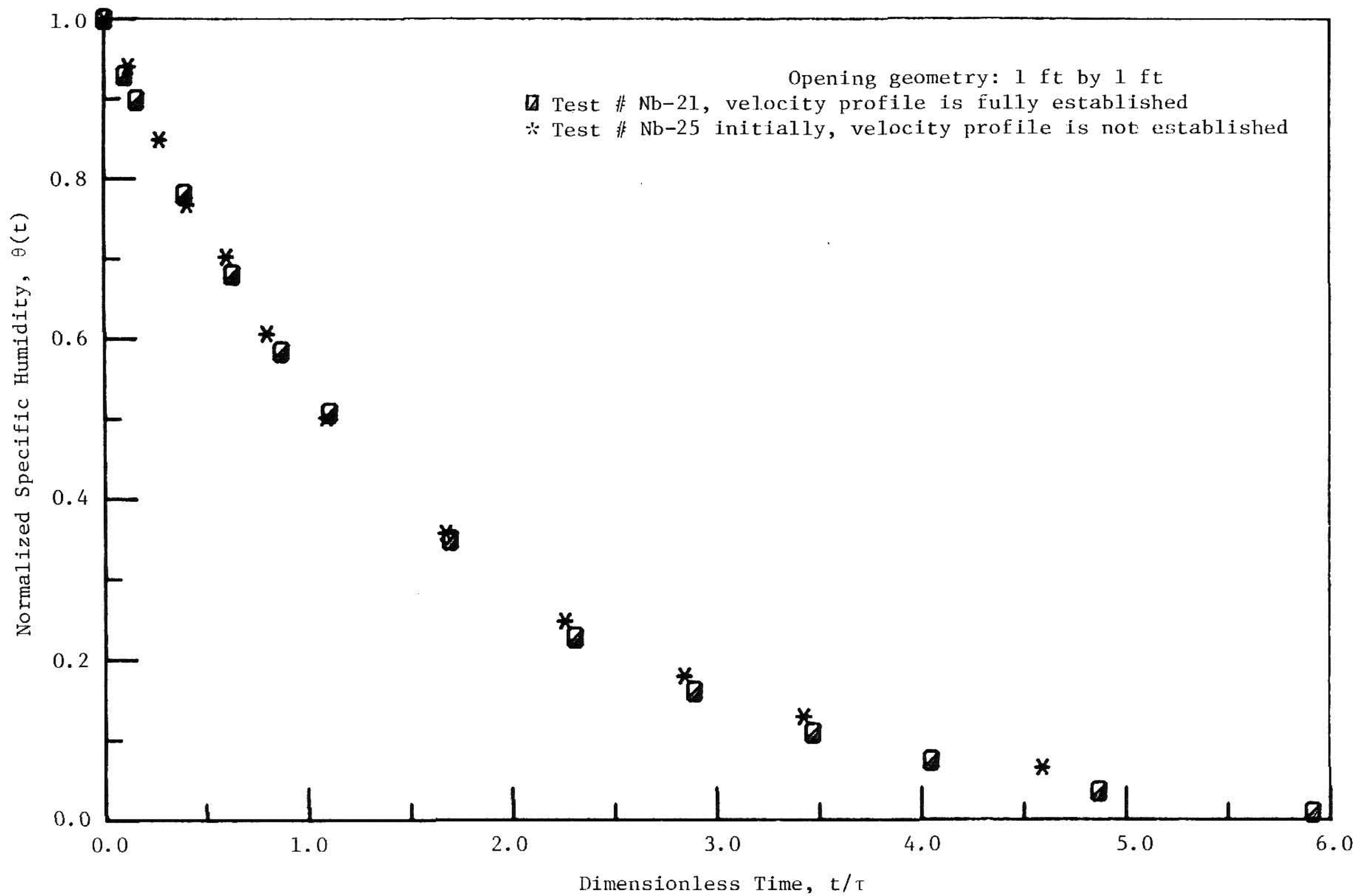

Figure 4.12 Effect of developing velocity profile

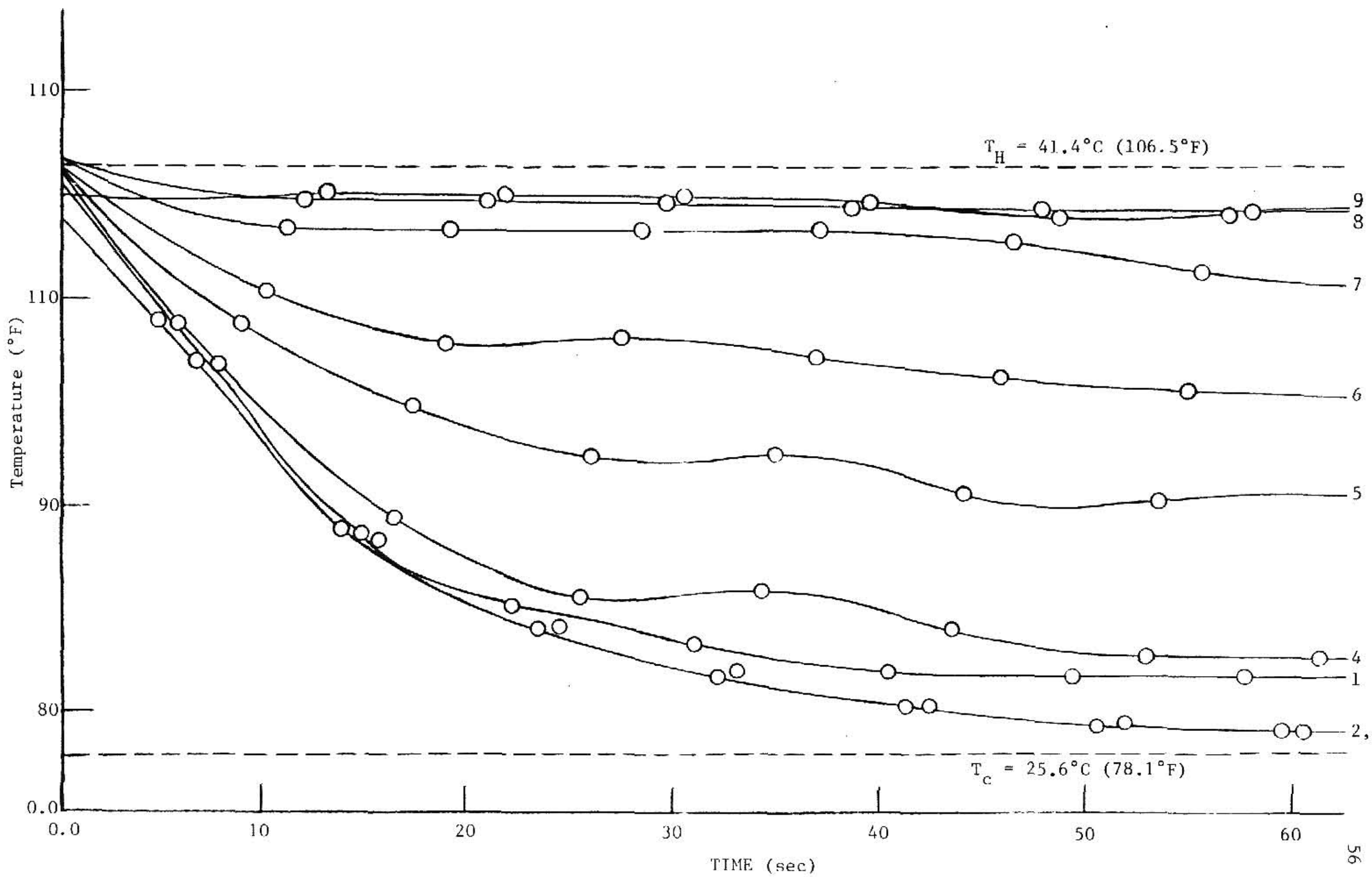

Figure 4.13 Transient temperature distribution at the opening

transient moisture transfer process is significantly larger than the time required for establishment of the velocity profile. Thus, at least for the type of tests in the present investigation, this requires that the transient moisture transfer process take longer than about one minute.

CHAPTER V

GENERAL SUMMARY AND CONCLUSION WITH RECOMMENDATIONS FOR FUTURE RESEARCH

5.1 Summary and Conclusion

This thesis attempted to experimentally investigate the effect of various physical and geometrical parameters upon the transient moisture transfer through an opening in a vertical partition separating hot and cold air spaces. The important parameters included temperature and humidity differences across the opening, opening geometry, bulk flow of air, and volume of the hot chamber. The volume of the hot chamber was fixed in this study; therefore, the effect of volume was not investigated. The direct measurement of the transient rate of moisture transfer through the opening was rather difficult. However, by using a mass balance of all water vapor crossing the boundary of the chamber the transient humidity response in the hot chamber was determined. Thus, by measuring the transient humidity in the hot chamber the effect of the parameters of interest upon the transient rate of moisture transfer through the opening could be indirectly accomplished.

The tests were carried out in a test chamber, described in Chapter III. In an attempt to correlate the experimental data, this thesis investigated the applicability of a simple transient model to correlate the transient rate of moisture transfer through the opening. The simple transient model was dependent on the air interchange occurring at the opening which was based on the density difference (driving force) due to the temperature difference alone. The simple transient model is an extension of the work by Steele [1] on the steady-state moisture transfer through the opening. The experimental data were presented on a normalized set of coordinates, where normalized specific humidity ratio was plotted as a function of dimensionless time. From Figures presented in Chapter IV, it was concluded that the data were following a single functional relationship and indeed were correlating very well within ±10%. This gave a good impression of the applicability of the *quasi-steady* model to correlate the data. In an attempt to bracket these data, as discussed in Appendix G two values of flow coefficient of 0.65 and 0.85 were introduced in the theory. The flow coefficients were determined from the steady-state moisture transfer data of Steele [1]. Considering the uncertainty that was involved in measurements of important parameters, the theory has bracketed the transient data reasonably well.

The theory that was developed in Chapter II was based on several assumptions. The validity of some of these assumptions was investigated in Section 4.3. The uniformity of water vapor concentration in the hot chamber, along with neglecting the time that it takes for establishment of the velocity profile, and neglecting the effect of free air turbulence on moisture transfer, are the assumptions that were investigated. From results that are presented in Chapter IV, it was concluded that there exists an approximate uniform water vapor concentration in the hot chamber. Furthermore, from the investigation that was directed at the situation where there was an initial transient such as opening a window, it was concluded that it takes about one minute for velocity profile to be established. Thus, for the type of tests in the present investigation, the transient moisture transfer process should take longer than one minute. It was also concluded that there is an effect on transient moisture transfer through the opening due to the free air turbulence. As free air turbulence decreased the transient moisture transfer response got faster which is consistent with Steel's steady-state data. This might suggest that some contributing effects due to turbulence exist and is one of the causes for the difference in the theoretical and the actual data.

The above results of this study show that the steady-state moisture transfer data of Steele [1] can correctly predict the transient rate of moisture transfer through a zero length rectangular opening providing the process is sufficiently slow. According to the investigation that was described in subsection 4.3.4, the moisture transfer through the opening must take significantly greater than one minute.

5.2 Recommendation for Future Research

In this study it was concluded that there is some contributing effect due to free air turbulence upon the transient moisture transfer and this is one of the causes for the difference in the theoretical and the actual data. This is consistent with the results that were obtained from Steele's steady-state data. Therefore, a more thorough experimental investigation of free air turbulence and it's effect upon moisture transfer through the opening is recommended. Since the effect of turbulence on moisture transfer in the steady-state is similar to that of the transient, the experimental investigation can be done under steady-state conditions only. From the investigation that was done in this study it was also concluded that the time it takes for velocity profile to be established is negligible compared to the time that it takes for moisture to transfer through the opening. By studying transients for which the time for velocity profile establishment is significant, some insight might be gained as to what extent the simple theory can hold true. An example of this type of transient is a periodic opening.

Therefore an extensive measurement of transient temperature and velocity distribution at the opening and an experimental investigation of moisture transfer through a periodic opening is also recommended.

REFERENCES

1. Steele, J. P., "Water Vapor Transport Through an Opening in a Wall Between Two Air Spaces at Different Temperatures," M.S. Thesis, Department of Mechanical Engineering, Kansas State University, 1981, 97 pages.

2. McDermott, P. F. "Moisture Migration, A Survey of Theory and Existing Knowledge, "Refrigerating Engineering, Vol. 42, August 1941, pp. 103-111.

3. Emswiler, J. E., "The Neutral Zone in *Ventilation*, "*Journal of* American Society of Heating and Ventilating Engineers, Vol. 32, No. 1, January 1926, pp. 1-16.

4. Brown, W. G. and K. R. Solvason, "Natural Convection Through Rectangular Openings in Partitions, Part 1, Vertical Partions, "International Journal of Heat and Mass Transfer," Vol. 5, September 1962, pp. 859-868.

5. Solvason, K. R., "Large-Scale Wall Heat-Flow Measuring Apparatus," ASHRAE Transactions, Vol. 55, 1959, pp. 541-550.

6. Brown, W. G., "Natural Convection Through Rectangular Openings in Partitions, Part 2 - *Horizontal Partitions*," *International* Journal of Heat and Mass Transfer, Vol. 5, September 1962, pp. 869-880.

7. Wilson, A. G., W. G. Brown and K. R. Solvason, "Heat and Moisture Flow Through Openings by Convection," ASHRAE Journal, Vol. 5, No. 9, September 1963, pp. 49-54; also ASHRAE Transactions, Vol. 69, 1963, pp. 351-357.

8. Shaw, B. H., "Heat and Mass Transfer by Natural Convection and Combined Natural Convection and Forced Air Flow Through Large Rectangular Openings in a Vertical Partition," The Institution of Mechanical Engineers, 1972, pp. 31-39; Proceedings of a Symposium arranged by the Thermodynamics and Flud Mechanics Group of IME at the University of Manchester, September 15, 1971.

9. Queer, E. R., E. R. McLaughlin, "What Vapor Transmission Rules Apply when Planning for Dehumidification?" Heating, Piping and Air Conditioning, January 1958, pp. 144-148.

10. Schmidt, E., "Heat Transfer by Natural Convection," Lecture, International Heat Transfer Conference at University of Colorado, 1961.

11. Göguš , Yalcin, "Instationaerer Stoff-und Waermeaus uch to durch Senkrenchte Oeffnunger, Problem der Fensterlueftung (Unstationary exchange of matter and heat through vertical openings - the problem of window ventilations)," *Doctrol Thesis (in German)*, Technische Universitaet Muenchen, 1964.

12. Kline, S. J. and Mclintock, F. A., "Describing Uncertainties in Single-Sample Experiments," Mechanical Engineering 75, January (1953): 3-8.

13. Thomson, W. T., Theory of Vibration with Application, Prentice-Hall, Inc., Englewood Cliffs, N.J., 1972: 79-88.

14. Jones, B. W., B. T. Beck and J. P. Steele, "Latent Loads in Low-Humidity Rooms Due to Moisture," ASHRAE Transactions, Vol. 89, 1983, pp. 35-55.

APPENDIX A

Response of the Humidity Measurement System

As discussed in Chapter III, in order to measure transient moisture response within the hot chamber, air samples were withdrawn through sample column holes, along connecting sample lines, and then passed through a dewpoint hygrometer for dewpoint temperature measurement. The sample columns, sample lines, and hygrometer, introduced a resultant time lag in the measurement of dewpoint temperature as indicated in Figure A.1. The response of each separate subsystem and the individual subsystem time lags are determined below:

A.1 Response of Sample Columns

Due to mixing with sampled air, at each instant of time during a transient moisture transfer test, the humidity inside a typical sample column in the hot chamber was slightly different than that of the hot chamber air. The corresponding lag was due to the mixing that takes place inside the sample column. It was assumed that there was no temperature difference between the inside and the outside of the sample column; thus, free convection occurring at the holes of the column was neglected. The sampled air from the hot chamber was assumed to be forced into the sample column by simple bulk flow. The bulk flow of air was then mixed with the air inside the sample column to represent a new water vapor concentration at each instant of time.

From the conservation of water vapor applied to the air within a typical sample column the net rate at which the water vapor enters the sample column, $\dot{m}_s$, is the same as the rate at which the vapor mass is stored in the sample column; thus

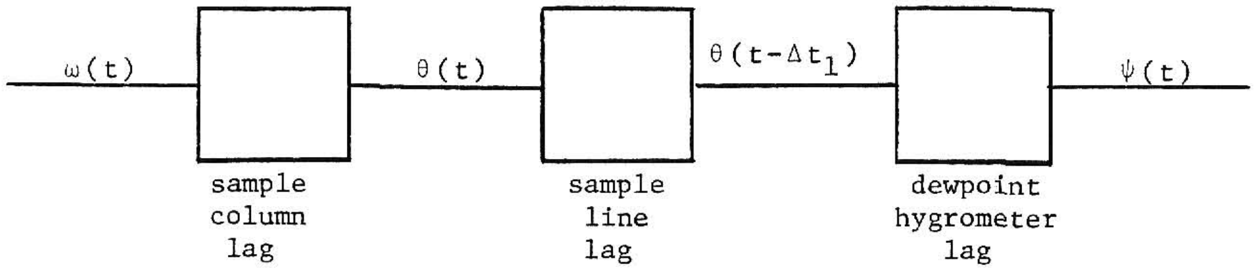

Figure A.1 Schematic of sampling system

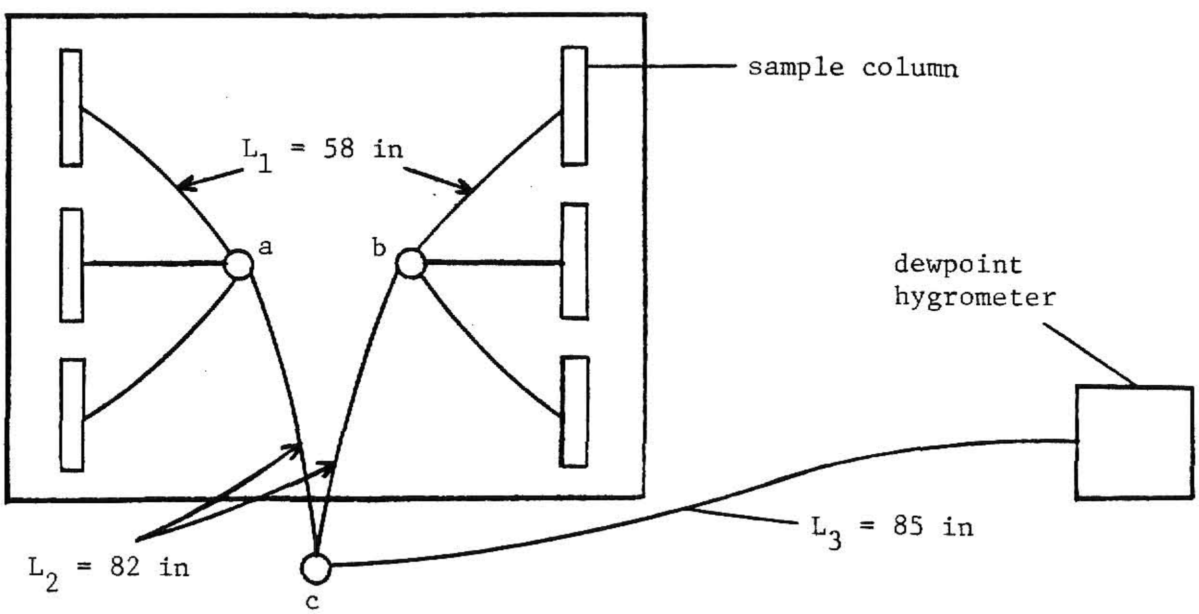

Figure A.2 Sample line configuration

$$\frac{dM_s(t)}{dt} = \dot{m}_s \tag{A.1}$$

The net moisture transfer rate is given by

$$\dot{m}_s = \dot{m}_a \omega_H(t) - \dot{m}_a \omega_s(t) \tag{A.2}$$

Where $\omega_s(t)$ is the instantaneous specific humidity inside the sample column, and $\omega_H(t)$ is the instantaneous specific humidity in the hot chamber. Assuming the mass of dry air in the sample column to be approximately constant, equation A.1 can be written as

$$\frac{M_{as}}{dt} d\omega_s = \dot{m}_a \omega_H(t) - \dot{m}_a \omega_s(t) \tag{A.3}$$

Let τ_s be a characteristic time, defined by

$$\tau_s = \frac{M_{as}}{\dot{m}_a} \tag{A.4}$$

From equation 2.36 the specific humidity response within the hot chamber is given by

$$\omega_H(t) = \omega_c + (\omega_f - \omega_c) e^{-\frac{t}{\tau}} \tag{A.5}$$

Substituting equation A.4 into A.3, and rearranging yields

$$\tau_s \frac{d\omega_s}{dt} + \omega_s = \omega_c + (\omega_f - \omega_c) e^{-\frac{t}{\tau}} \tag{A.6}$$

By introducing a normalized specific humidity, θ, equation A.4 can be written as follows

$$\tau_s \frac{d\theta}{dt} + \theta = e^{-\frac{t}{\tau}} \tag{A.7}$$

where

$$\theta(t) = \frac{\omega_s(t) - \omega_c}{\omega_f - \omega_c}. \tag{A.8}$$

The above differential equation is subject to the initial condition of $\omega_{s,i} = \omega_f$, or $\theta = 1$. Thus,

$$\theta(t) = \frac{\tau}{\tau - \tau_s} e^{-\frac{t}{\tau}} - \frac{\tau_s}{\tau - \tau_s} e^{-\frac{t}{\tau_s}} \tag{A.9}$$

where τ_s is expressed as:

$$\tau_s = \frac{M_{as}}{\dot{m}_a} = \frac{\rho_a \bar{V}}{\rho_a \frac{\dot{V}_s}{n}} = \frac{n\bar{V}}{\dot{V}_s} \tag{A.10}$$

where $\bar{V}$, the volume of the sample column, can be replaced by $\frac{\pi}{4} D_s^2 h_s$ so that

$$\tau_s = \frac{n\pi D_s^2 h_s}{4\dot{V}_s} \tag{A.11}$$

where D_s, is diameter of sample column, n is the number of sample columns in hot chamber, h_s is the height of sample column, and $\dot{V}_s$ is the total volume flow rate though a sample line where all lines combine. The value of t_s for a typical sample column was found from the following:

D_s = 5/8 inches (1.6 cm)

n = 6

h_s = 6 ft (183 cm)

$\dot{V}_s = 10 \frac{ft^3}{hr} \left(440 \frac{cm^3}{hr}\right)$

$$\therefore \tau_s = \frac{6\pi(\frac{5}{8}\text{ in})^2(6\text{ ft})}{4(144\ \frac{in^2}{ft^2})(10\ \frac{ft^3}{hr})} \left(3600\ \frac{sec}{hr}\right) = 27.6 \text{ sec.}$$

A.2 Response of Sample Lines

In transferring moisture from the sample column to the dewpoint hygrometer there exists a transportation time lag due to the finite air velocity in the sample lines. This time lag consists of three parts as indicated in Figure A.2. The first lag occurs during transport from a sample column to a merging point a(or b); the second is from merging point (a) to merging point (c) and the third is from merging point (c) to the dewpoint hygrometer. The time lag due to each part is calculated as follows:

The volume flow rate of air sample in first part is expressed as:

$$\frac{\dot{V}_s}{6} = \frac{\pi D_L^2 L_1}{4\ t_1} \tag{A.12}$$

where L_1 is length of the sample line in the first part, t_1 is the corresponding time lag, and D_L is the inside diameter of a sample line. Solving equation A.9 for t_1 yields

$$t_1 = \frac{6\pi L_1 D_L^2}{4\dot{V}_s} \tag{A.13}$$

The time lags for the second and third part can be found in the same fashion as described earlier. Thus,

$$t_2 = \frac{2\pi L_2 D_L^2}{4\ \dot{V}_s} \tag{A.14}$$

$$t_3 = \frac{\pi L_3 D_L^2}{4\dot{V}_s} \tag{A.15}$$

where L_2 and L_3 are the length of the sample lines in the second and third part respectively. Note that the volume flow rate of the air sample in the second part is $\frac{\dot{V}_s}{2}$ and in the third part is $\dot{V}_s$.

The total time lag is

$$\Delta t_1 = t_1 + t_2 + t_3 \tag{A.16}$$

From the experimental setup and Figure A.2

$n = 6$, $L_1 = 58$ in, $L_2 = 82$ in, $L_3 = 85$ in, $L_3 = 85$ in, $D_L = 0.25$ in, $\dot{V}_s = 10\ ft^3$

Therefore

$$\Delta t_1 = 3.56 \text{ sec} + 1.68 \text{ sec} + 0.86 \text{ sec} = 6.1 \text{ sec}$$

A.3 Response of Dewpoint Hygrometer

In investigating the response of the dewpoint hygrometer to an input of sample air, a storage scope was used to record the response. It appeared that the response had a second order system behavior and the response characteristics were dependent on the sample flow rate. The response behaved like an overdamped second order system for a flow less than about 2 cfh, whereas for the flow between 2-4 cfh, the response behaved like an underdamped second order system. Since the manufacturer of the dewpoint hygrometer recommended a flow of 2-4 cfh for accurate measurements, the sample flow was set at about 3 ft^3/hr.

In determining the damping ratio and natural frequency of the response, a step input was utilized on the dewpoint hygrometer. In order to get an approximate step change in humidity, some modification was done on the sample line loop in Figure 3.6. The solnoid values number 1 and 4 were operated so that number 1 was on and number 4 was off at all times.

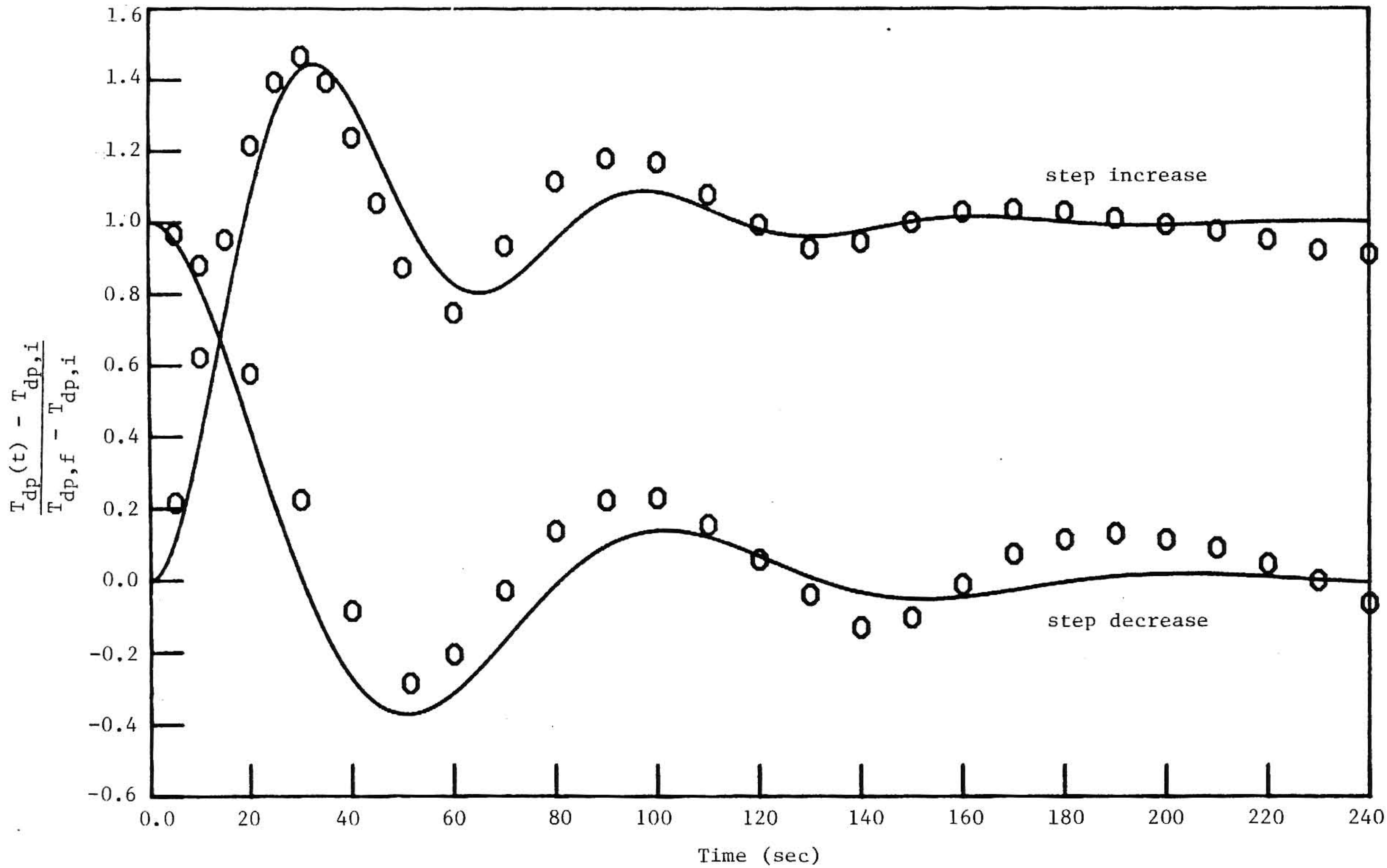

Figure A.3 Hygrometer response

The solenoid valves number 2 and 3 were operated for switching the flow direction. With solenoid valve number 2 on, the air sample was collected from the cold chamber with low humidity, passed through the dewpoint hygrometer and then dumped into the hot chamber (step decrease). When solenoid valve number 3 was on, the air sample was collected from the hot chamber, passed through the dewpoint hygrometer and then dumped into the cold chamber (step increase). The response of the dewpoint hygrometer for both step increase and decrease is shown in Figure A.3. The step increase had a damping ratio of about 0.250 and natural frequency of about 0.1 rad/s whereas the step decrease had a damping ratio of about 0.30 and natural frequency of about 0.065 rad/s.

The differential equation of this system assuming 2nd order behavior [13] for an input of $\theta(t-\Delta t_1)$ (see Figure A.1) can be expressed as

$$\frac{d^2\psi}{dt^2} + 2z\omega_n \frac{d\psi}{dt} + \omega_n^2 \psi = \omega_n^2 \theta(t-\Delta t_1) \tag{A.17}$$

This differential equation is subject to the following two initial conditions:

$$\begin{aligned} \psi &= 1 \text{ at } t = \Delta t_1 \\ \frac{d\psi}{dt} &= 0 \text{ at } t = \Delta t_1 \end{aligned} \tag{A.18}$$

Substituting equation (A.9) into the right hand side of Eqn. (A.17), the input to the dewpoint hygrometer yields

$$\theta(t- t_1) = \frac{\tau}{\tau - \tau_s} e^{-\frac{t-\Delta t_1}{\tau}} - \frac{\tau_s}{\tau - \tau_s} e^{-\frac{t-\Delta t_1}{\tau_s}} \tag{A.19}$$

The solution to Eqn. (A.17) is now obtained by summing the solution to the homogeneous equation and that of the particular solution, yielding the following general expression:

$$\psi(t) = e^{-z\omega_n t}(C_1R + C_2Q) + Y\tau e^{-\frac{t-\Delta t_1}{\tau}} - Z\tau_s e^{-\frac{t-\Delta t_1}{\tau_s}} \tag{A.20}$$

where, C_1 and C_2 are unknown constants, and

$$Y = \frac{\omega_n^2\tau^2}{(\tau-\tau_s)(\omega_n^2\tau^2-2z\omega_n\tau+1)} \tag{A.21}$$

$$Z = \frac{\omega_n^2\tau_s^2}{(\tau-\tau_s)(\omega_n^2\tau_s^2-2z\omega_n\tau_s+1)} \tag{A.22}$$

$$R = \sin\left(\sqrt{1-z^2}\,\omega_n t\right) \tag{A.23}$$

$$Q = \cos\left(\sqrt{1-z^2}\,\omega_n t\right) \tag{A.24}$$

In equation (A.20) the terms $e^{-z\omega_n t}$ and $\exp(-\frac{t-\Delta t_1}{\tau_s})$ die out fast. For example after only about 2 minutes the term $\exp(-z\omega_n t)$ has values of 0.05 and the term $\exp(-\frac{t-\Delta t_1}{\tau_s})$ has values of 0.016; thus, by neglecting these two terms from the general expression, the solution simplifies to:

$$\psi(t) = \frac{\omega_n^2\tau^3}{(\tau-\tau_s)(\omega_n^2\tau^2-2z\omega_n\tau+1)}\, e^{-\frac{t-\Delta t_1}{\tau}} \tag{A.25}$$

A.4 Simplified Time Lag Correction

In Figure A.4 on a normalized set of coordinates the resultant time lags in the measurement of dewpoint temperature due to the sample columns, sample lines and hygrometer response are shown. From Figure

A.4, it appears that after a certain time has elapsed, the response of sample columns, sample lines, and hygrometer have virtually the same shape, but are shifted by a pure time lag from $t = 0$. In order to determine a simple pure time lag correction for the experimental data, the results from the previous sections were simplified. The time constant τ_s in equation (A.6) is very small compared with τ, so that the second term in equation (A.6) dies out fast, resulting in

$$\theta(t) = \frac{\tau}{\tau - \tau_s} e^{-\frac{t}{\tau}} \tag{A.26}$$

The amount of the time lag can be determined from the following condition:

$$\theta(t = \Delta t_s) = 1 \tag{A.27}$$

Applying the above condition to equation A.26 yields

$$1 = \frac{\tau}{\tau - \tau_s} e^{-\frac{\Delta t_s}{\tau}} \cong \frac{\tau}{\tau - \tau_s} (1 - \frac{\Delta t_s}{\tau}) \tag{A.28}$$

since $\frac{\Delta t_s}{\tau} << 1$. Therefore, solving for Δt_s gives

$$\Delta t_s = \tau_s \tag{A.29}$$

Thus, the net effect of the sample column is to produce an approximate time lag equal to the time constant, τ_s.

The dewpoint hygrometer response may also be reduced to an approximate pure time lag using a similar approach to that used in determining the time lag due to the sample columns. The time lag for the hygrometer can be determined from the condition

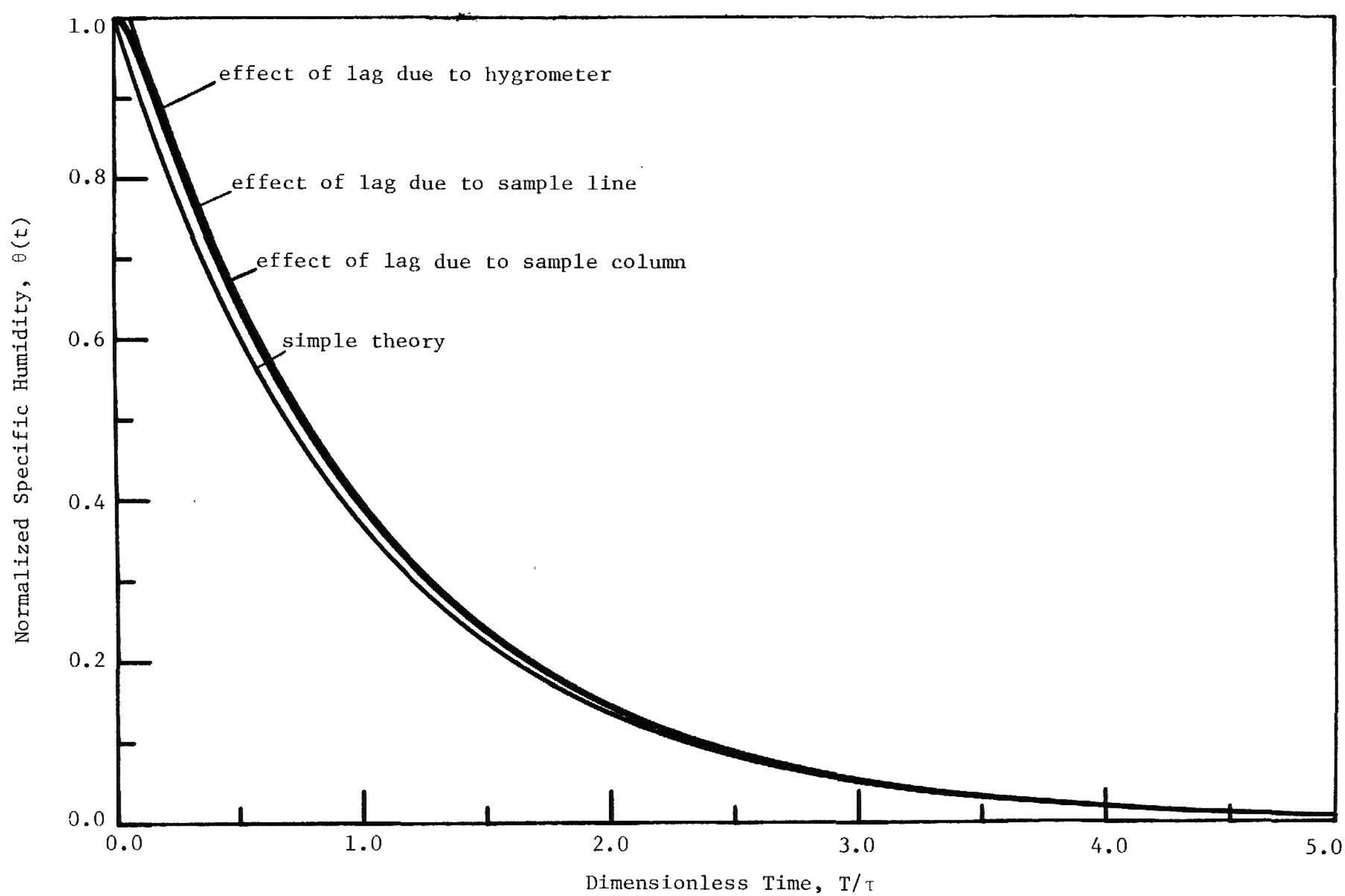

Figure A.4 Effect of lags due to hygrometer, sample columns, and sample lines on the response of sampling system

$$\psi(t = \Delta t) = 1 \tag{A.30}$$

where Δt is the total time lag which is the sum of Δt_s (time lag due to the sample columns alone), Δt_1 (time lag due to the sample lines alone) and Δt_h (time lag due to the dewpoint hygrometer alone); thus

$$\Delta t = \Delta t_s + \Delta t_1 + \Delta t_h \tag{A.31}$$

Applying the condition (A.30) to equation (A.25) gives

$$1 \cong \frac{\omega_n^2 \tau^3}{(\tau - \tau_s)(\omega_n^2 \tau^2 - 2z\omega_n \tau + 1)} \left(1 - \frac{\Delta t_s + \Delta t_h}{\tau}\right)$$

since $\frac{\Delta t_s + \Delta t_h}{\tau} << 1$. Therefore solving for Δt_h, and noting that $\Delta t_s = \tau_s$, yields

$$\Delta t_h = (\tau - \tau_s) \frac{2z\omega_n \tau - 1}{\omega_n^2 \tau^2} \cong \frac{2z}{\omega_n} \tag{A.32}$$

since $\tau_s << \tau$ and $2z\omega_n \tau >> 1$. Thus, the total time lag for the experimental setup is

$$\Delta t = \tau_s + t_1 + t_2 + t_3 + \frac{2z}{\omega_n} \tag{A.33}$$

For step increase

$$\Delta t = 27.6 + 3.56 + 1.68 + 0.86 + 5.0 = 38.7 \text{ sec}$$

For step decrease

$$\Delta t = 27.6 + 3.56 + 1.68 + 0.86 + 9.2 = 42.9 \text{ sec}$$

APPENDIX B

Data Reduction

A detailed explanation of the experimental procedure for the present study was provided in Chapter III. The procedure used to reduce the experimental data is the subject of this appendix. A data reduction was done on a typical experimental test (B-22, see Appendix H). Note that the parameters of interest in this data reduction process are normalized specific humidity ratio $\theta(t)$, mass of dry air M_a, the average air density $\bar{\rho}$, the common normalized factor $\dot{m}'$, the normalized bulk flow $\dot{m}_b/\dot{m}'$, the mass flow rate of dry air $\dot{m}_c$, the time constant τ and finally the dimensionless time t/τ. The raw data taken for the above mentioned test is presented below:

$P_{bar} = 29.0$ in Hg	$T_{ref.} = 21.6°C\ (70.88°F)$	$V_C = 1.715$ mV
$\Delta V_{H-C} = 5.515$ mV	$\dot{m}_{H_2O} = \dfrac{250\ \text{mL}}{1.16\ \text{hr}}$	$T_{c,i} = 6.2°C\ (43.16°F)$
$\Delta P_{dynamic} = 0.584$ in. H_2O	$\Delta P_{static} = 0.80$ in. H_2O	$T_{c,f} = 5.6°C\ (42.08°F)$
$T_{meter} = 30.8°C\ (87.44°F)$	$V = 6 \times 6 \times 6 = 216\ ft^3$	

As described in Chapter III, a storage scope was used to record the dewpoint temperatures with respect to time during a moisture decay (or addition) test. All of these data are tabulated in Appendix H. For simplicity, a typical value of dewpoint temperature $T_{dp}(800\ \text{sec}) = 8.6°C$ is chosen to be reduced.

B.1 <u>Normalized Specific Humidity Ratio</u>

The first step in reducing the data was to use the steam tables to determine the water vapor pressures from the dewpoint temperature data. The specific humidities then could be calculated from the atmospheric pressure and water vapor pressures. A sample calculation is presented in the following for T_{dp}(800 sec) = 8.6°C. The storage scope was connected to the dewpoint hygrometer in a way that the readout of the scope for each 1 mV was equivalent to 1 x 10 = 10°C. Thus, the value of 0.86 mV is equivalent to 8.6°C. From the steam tables the corresponding partial pressure is 0.1621 psi. The specific humidity is calculated by

$$\omega_H(t) = 0.622 \frac{P_v(t)}{P_{atm} - P_v(t)}.$$

The atmospheric pressure is converted from inches of Mercury to lbf/ft^2 by the following

$$P_{atm} = (29 \text{ in. Hg}) \left(\frac{845.5 \text{ lbm/ft}^3}{12 \frac{\text{in}}{\text{ft}}}\right) = 2043.3 \frac{\text{lbf}}{\text{ft}^2}$$

$$\omega_H(800 \text{ sec}) = 0.622 \frac{(0.2386)(144)}{2043.3 - (0.162)(144)} = 0.00719$$

The specific humidity of the cold chamber ω_C was determined by averaging the specific humidity prior to and after the test, so as to give a better representative value of ω_C during the transient. Thus,

$$\bar{T}_{dc} = \frac{6.2 + 5.6}{2} = 5.9°C$$

The specific humidity $\bar{\omega}_c$ was determined by

$$\bar{\omega}_c = 0.622 \frac{(0.1347)(144)}{2043.3 - (0.1347)(144)} = 0.00596$$

The specific humidity $\omega_f = \omega_H(0)$ was determined by

$$\omega_H(0) = \omega_f = 0.622 \frac{(0.2386)(144)}{2043.3 - (0.2386)(144)} = 0.01064$$

The normalized specific humidity ratio is given by

$$\theta(800\ \text{sec}) = \frac{\omega_H(800\ \text{sec}) - \omega_c}{\omega_f - \omega_c} = \frac{0.00719 - 0.00596}{0.01064 - 0.00596} = 0.263$$

B.2 Mass of Dry Air

Mass of dry air in the hot chamber was calculated using the ideal gas equation:

$$M_a = \frac{P_{atm}\ V}{R_a\ T_H}$$

In order to find T_H, the reference temperature was converted to millivolts using standard thermocouple tables for copper-constantan. The reference temperature of 21.6°C is equivalent to 0.8516 mV. From V_c, which is the total voltage of 9 thermocouples in series, the average $\bar{V}$ for the cold chamber is

$$\bar{V}_c = \frac{1.715}{9} = 0.1906\ \text{mV}$$

The voltage corresponding to the average temperature in cold chamber can be determined as follows:

$$V_{ref} + \bar{V}_c = 0.8516 + 0.1906 = 1.042\ \text{mV}$$

By referring to standard thermocouple tables, the average temperature in cold chamber is found to be 26.30°C (79.34°F). Since the thermopile voltage difference between the hot and cold chamber is also known, V_H can be obtained by

$$V_H = \Delta V_{H-C} + V_c$$

thus,

$$V_H = 5.515 + 1.715 = 7.230\ \text{mV}$$

The average temperature in the hot chamber, corresponding to this voltage, is thus $T_H = 41.07°C$ (105.9°F). The mass of dry air in the hot chamber can now be calculated, yielding

$$M_a = \frac{(29)(70.46)(216)}{(53.34)(105.9+459.7)} = 14.62 \text{ lbm } (6.660 \text{ Kg})$$

B.3 The Average Air Density

The air densities, ρ_c and ρ_H, on both sides of the opening can be calculated from the temperatures and gas constant for dry air as well as the atmospheric pressure. Thus,

$$\rho_c = \frac{P_{atm}}{R_a\ T_c} = \frac{(29)(70.46)}{(53.34)(79.34+459.7)} = 0.07103 \text{ lbm/ft}^3$$

$$\rho_H = \frac{P_{atm}}{R_a\ T_H} = \frac{(29)(70.46)}{(53.34)(105.9+459.7)} = 0.06769 \text{ lbm/ft}^3$$

The average density is therefore

$$\bar{\rho} = \frac{\rho_c + \rho_H}{2} = \frac{0.07103 + 0.06769}{2} = 0.06936 \frac{\text{lbm}}{\text{ft}^3} \ (1.115 \text{ Kg/m}^3)$$

B.4 The Common Normalization Factor

The average chamber temperature is given by

$$\bar{T} = \frac{T_H + T_c}{2} = \frac{539.04 + 565.60}{2} = 552.32°R$$

The common normalization factor $\dot{m}'$ is the mass flow rate of air through the opening of 1 ft by 1 ft, when the N.P.L. is shifted all the way up to the top of the opening. This mass flow can be calculated from the following expression:

$$\dot{m}' = \frac{2}{3} W\bar{\rho} \sqrt{2g\bar{T}H^3(\frac{1}{T_c} - \frac{1}{T_H})}$$

Thus,

$$\dot{m}' = \frac{2}{3} (1)(0.06936) \sqrt{2(32.2)(522.32)(1)^3 (\frac{1}{539.04} - \frac{1}{565.6})}$$

$$= 0.08140 \text{ lbm/sec } (0.03692 \text{ Kg/sec})$$

B.5 Mass Flow Rate of Dry Air through the Meter

The density and specific humidity of air exiting the exhaust port and moving through the flowmeter are calculated from the pressure, temperature and water vapor of air passing through the meter. The pressure at the meter is calculated in the following expression:

$$P_{meter} = (P_{atm} - 0.0737 (\Delta P_{static}))(70.46)$$

Thus,

$$P_{meter} = (29 - 0.0737 (0.80))(70.46) = 2039.2 \frac{lbf}{ft^2}$$

The density of moist air also can now be determined by

$$\rho_{meter} = (\frac{P_{meter} - P_v}{R_a} + \frac{P_v}{R_v}) \frac{1}{T_{meter}}$$

where P_v is the time dependent partial pressure of the air in the hot chamber. It is assumed that the humidity inside the hot chamber and that of the meter are the same. Also, only a small error results from using the initial value for P_v in the above relationship. Thus,

$$\rho_{meter} = (\frac{2039.2 - 34.36}{53.35} + \frac{34.36}{85.76}) \frac{1}{(87.44+459.7)} = 0.06941 \text{ lbm/ft}^3$$

The mass flow rate of dry air entering the hot chamber through the opening, which is equivalent to the mass flow rate of dry air exiting the exhaust port and passing through the flowmeter, can be determined from the following relationship:

$$\dot{m}_{da} = \frac{C_m \rho_m}{(1+\omega_m)\sqrt{\frac{\rho_m}{\Delta P_m}}}$$

Here C_m is the flowmeter coefficient, a function of the pressure difference across the flowmeter, ΔP_m. This coefficient can be determined from the calibration curve shown in Figure C.1 in Appendix C. The term ω_m is the time dependent specific humidity of the air in the hot chamber. The time dependence of ω_m is also neglected here; thus

$$\dot{m}_a = \frac{(4.08)(0.06941)}{(1+0.01064)\sqrt{\frac{0.06941}{0.584}}} = 0.8128 \text{ lbm/min } (0.368 \text{ Kg/min})$$

B.6 The Normalized Bulk Flow

The net bulk flow through the opening, $\dot{m}_b$, can be calculated from

$$\dot{m}_b = \dot{m}_a \, (1+\omega_c)$$

where ω_c is the constant specific humidity in cold chamber. Thus,

$$\dot{m}_b = 0.8128 \; (1+0.00596) = 0.8176 \text{ lbm/min}$$

The normalized bulk flow is expressed as

$$\frac{\dot{m}_b}{\dot{m}'} = \frac{0.8176}{(0.08140)(60)} = 0.1674$$

B.7 Flow Rate of Dry Air, $\dot{m}_c$

From equation 2.13, which was developed in Chapter II, the forward mass flowrate, $\dot{m}_c$, can be determined. Thus,

$$\frac{\dot{m}_b}{\dot{m}'} = 0.1674 = \frac{\dot{m}_c}{\dot{m}'} - \left[1 - \left(\frac{\dot{m}_c}{\dot{m}'}\right)^{2/3}\right]^{3/2}$$

This equation is solved for $\dot{m}_c/\dot{m}'$ using a simple trial and error method so that $\frac{\dot{m}_c}{\dot{m}'} = 0.4400$.

The forward mass flowrate can now be calculated

$$\dot{m}_c = (0.44)\ \dot{m}' = (0.44)(0.08140) = 0.03582\ \frac{\text{lbm}}{\text{sec}}\ (0.01625\ \text{Kg/sec})$$

B.8 The Time Constant

The time constant, τ, is calculated using its definition from Chapter II; thus,

$$\tau = \frac{M_a}{\dot{m}_c} = \frac{14.52\ \text{lbm}}{0.03582\ \frac{\text{lbm}}{\text{sec}}} = 408.1\ \text{sec}$$

B.9 The Dimensionless Time

After the recorded time is corrected for the corresponding time lags due to the sample columns, sample lines and hygrometer (see Appendix A), it is scaled by the time constant τ. At t = 800 sec, the dimensionless time is thus

$$\frac{t^* - \Delta t}{\tau} = \frac{t}{\tau} = \frac{800-39}{408.1} = 1.865$$

APPENDIX C

Flowmeter Calibration

As was discussed in Chapter II, in all of the bulk flow tests, an Annubar flowmeter and two micromanometers were used to determine the mass flow rate of dry air through the exhaust port. It is the subject of this appendix to present the results of calibration tests on the flowmeter, in terms of the flow coefficient, C_m, as a function of the pressure difference across the flowmeter. The flow coefficient is defined as

$$C_m = \dot{Q}_m \sqrt{\frac{\rho_m}{\Delta P_m}} \tag{C.1}$$

where $\dot{Q}_m$, is the volumetric flow rate and ρ_m is the density of air passing through the meter.

The experimental setup consisted basically of a bell prover connected to the flowmeter by way of a flexible duct (see Figure C.1). Several tests were conducted for different volumetric flow rates of air through the flowmeter. A known volume of air (2.5 ft^3) was passed through the meter during each calibration test, while a Beckman frequency counter model 6146 was used to measure the corresponding time for that process. The dynamic pressure and static pressure for the meter were measured by the micromanometers. Figure C.2 graphically summarizes the flowmeter calibration data. Once the flow coefficient for a specific pressure difference is known, the mass flow rate of dry air through the meter can easily be determined. Table C.1 summarizes the values of the important parameters $\dot{Q}_m$, C_m, ρ_m, ΔP_m used in calibrating the flowmeter.

The uncertainties in the air density ρ_m, the flow coefficient C_m, and mass flow rate of air in the meter are given below.

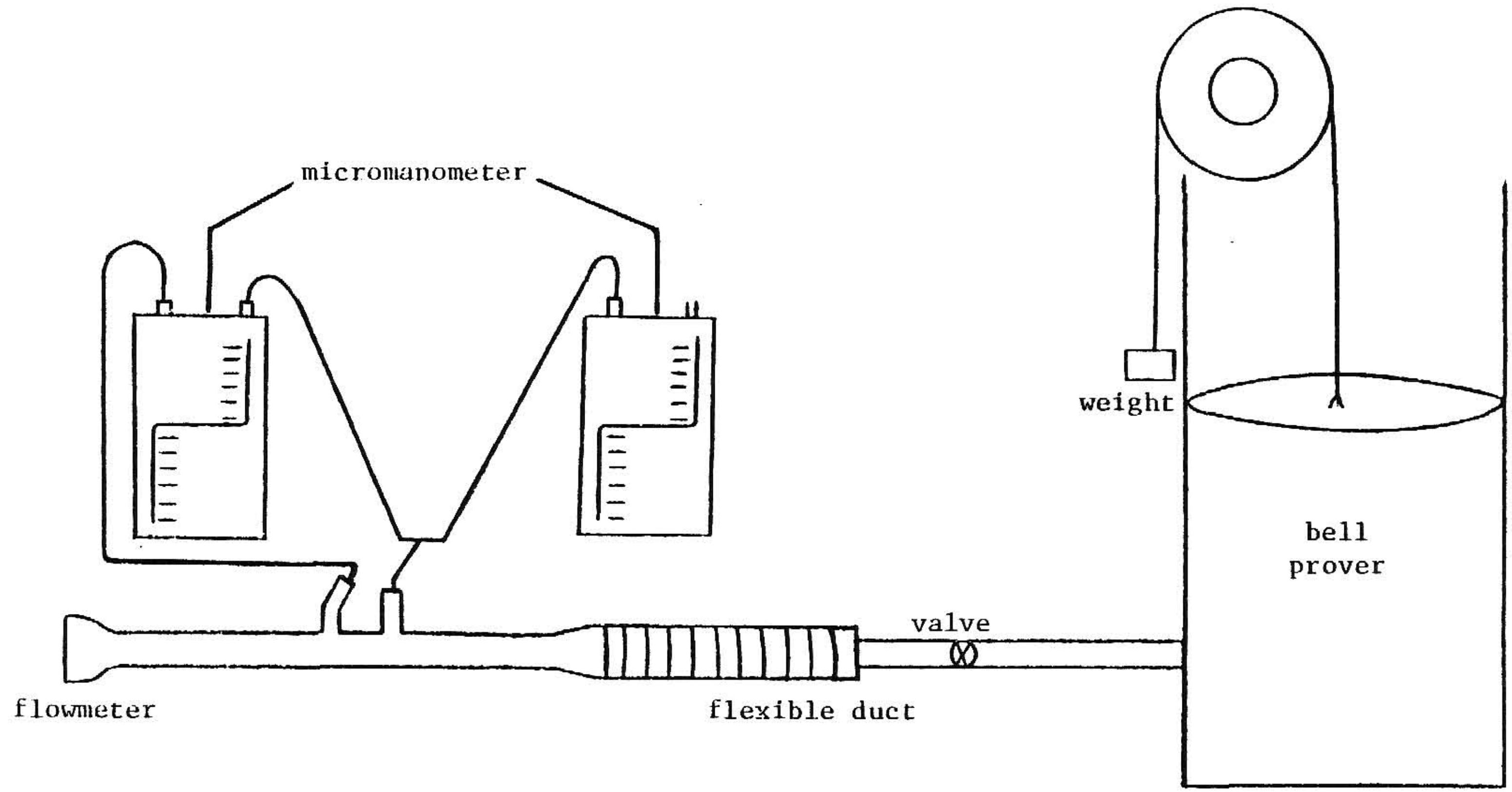

Figure C.1 Flowmeter calibration test set up

C.1 Air Density

The uncertainty in air density ρ_m can be estimated from the equation

$$\rho_m = \frac{\frac{P_{atm}}{R_a} - \frac{P_V}{R_a} + \frac{P_V}{R_V}}{T_m} \cong \frac{P_{atm}}{R_a T_m} \qquad (C.2)$$

Thus,

$$U_{\rho_m} = \left[\left(\frac{\partial P_m}{\partial P_{atm}} \cdot U_{P_{atm}}\right)^2 + \left(\frac{\partial P_m}{\partial T_m} \cdot U_{T_m}\right)^2 \right]^{\frac{1}{2}} \qquad (C.3)$$

where

$$\frac{\partial \rho_m}{\partial P_{atm}} = \frac{1}{R_a T_m} = \frac{1}{(53.34)(547.14)} = 0.000034 \frac{\text{lbm}}{\text{ft. lbf}}$$

$$\frac{\partial \rho_m}{\partial T_m} = - \frac{P_{atm}}{R_a\ T_m^2} = - \frac{2039.2}{(53.34)(547.14)^2} = - 0.000128 \frac{\text{lbm}}{\text{ft}^3\ {}^\circ\text{R}}$$

The uncertainties in P_{atm} and T_m from Appendix E are

$$U_{P_{atm}} = \pm 0.71 \frac{\text{lbf}}{\text{ft}^2},\ U_{T_m} = \pm\ 0.9^\circ\text{R}$$

The uncertainty in ρ_m is thus given by

$$U_{\rho_m} = [(0.000034 \times 0.71)^2 + (0.000128 \times 0.9)^2]^{\frac{1}{2}} = \pm\ 0.000118\ \text{lbm/ft}^3$$

Therefore $\rho_m = 0.06941 \frac{\text{lbm}}{\text{ft}^3} \pm 0.000118 \frac{\text{lbm}}{\text{ft}^3}$ (0.17%)

C.2 The Flow Coefficient

The estimation of the uncertainty in the flow coefficient can be found using equation C.1, thus

$$U_{C_m} = \left[\left(\frac{\partial C_m}{\partial \dot{Q}_m} \cdot U_{\dot{Q}_m}\right)^2 + \left(\frac{\partial C_m}{\partial \rho_m} \cdot U_{\rho_m}\right)^2 + \left(\frac{\partial C_m}{\partial \Delta_{P^m}} \cdot U_{\Delta P_m}\right)^2 \right]^{\frac{1}{2}}$$

where

$$\frac{\partial C_m}{\partial \dot{Q}_m} = \left(\frac{m}{\Delta P_m}\right)^{\frac{1}{2}} = \left(\frac{0.06941}{0.584}\right)^{\frac{1}{2}} = 0.3447 \left(\frac{\text{lbm}}{\text{ft}^3\ \text{in. H}_2\text{O}}\right)^{\frac{1}{2}}$$

$$\frac{\partial C_m}{\partial \rho_m} = \frac{\dot{Q}_m}{2\sqrt{\rho_m \cdot \Delta P_m}} = \frac{11.71}{2(0.06941 \times 0.584)^{\frac{1}{2}}} = 29.08 \frac{\text{ft}^3/\text{min}}{\left(\frac{\text{lbm}\cdot\text{in. H}_2\text{O}}{\text{ft}^3}\right)^{\frac{1}{2}}}$$

$$\frac{\partial C_m}{\partial \Delta P_m} = -\frac{1}{2}\dot{Q}_m \rho_m^{\frac{1}{2}}/\Delta P_m^{3/2} = -\frac{(11.71)(0.06941)^{\frac{1}{2}}}{2(0.584)^{3/2}} = -3.456 \frac{\text{ft}^3 \left(\frac{\text{lbm}}{\text{ft}^3}\right)^{\frac{1}{2}}}{\text{min.}(\text{in.H}_2\text{O})^{3/2}}$$

The uncertainty associated with the volume flowrate $\dot{Q}_m$ using the following equation

$$\dot{Q}_m = \frac{\Delta v}{\Delta t} \tag{C.5}$$

is given by

$$U_{\dot{Q}_m} = \left[\left(\frac{\partial \dot{Q}_m}{\partial \Delta v} \cdot U_{\Delta v}\right)^2 + \left(\frac{\partial \dot{Q}_m}{\partial \Delta t} \cdot U_{\Delta t}\right)^2\right]^{\frac{1}{2}} \tag{C.6}$$

where

$$\frac{\partial \dot{Q}_m}{\partial \Delta v} = \frac{1}{\Delta t} = \frac{1}{0.2135} = 4.684\ \text{min}^{-1}$$

$$\frac{d\dot{Q}_m}{d\Delta t} = -\frac{1}{\Delta t^2} = -\frac{1}{(0.2135)^2} = -54.85\ \frac{\text{ft}^3}{\text{min}^2}$$

The uncertainty in Δv and Δt is given by

$$U_{\Delta v} = \pm\ 0.02\ \text{ft}^3,\ U_{\Delta t} = \pm\ 0.0000167\ \text{min}$$

Thus, the uncertainty in volume flowrate is estimated as

$$U_{\dot{Q}_m} = [(4.684 \times 0.02)^2 + (54.85 \times 0.0000167)^2]^{\frac{1}{2}} = \pm\ 0.0937\ \text{ft}^3/\text{min}$$

The uncertainty in measurement of ΔP_m from the flow calibration data is assumed to be

$$U_{\Delta Pm} = \pm\ 0.03 \text{ in. } H_2O$$

Now, the uncertainty in the flow coefficient C_m can be estimated as

$$U_{C_m} = [(0.3447 \times 0.0937)^2 + (29.08 \times 0.000118)^2 + (-3.456 \times 0.03)^2]^{\frac{1}{2}}$$

$$= \pm\ 0.11\ \frac{ft^3}{min} \left(\frac{lbm}{ft^3 \cdot in.\ H_2O}\right)^{\frac{1}{2}}$$

therefore,

$$C_m = 4.08\ \frac{ft^{3/2}}{min} \left(\frac{lbm}{in.\ H_2O}\right)^{\frac{1}{2}} \pm 0.11\ \frac{ft^{3/2}}{min} \left(\frac{lbm}{in.\ H_2O}\right)^{\frac{1}{2}} \quad (2.7\%)$$

C.3 Mass Flowrate of Dry Air

The uncertainty in mass flowrate of dry air passing through the opening and out through the meter is determined by

$$\dot{m}_a = \frac{C_m\ \rho_m}{(1+\omega_m)\sqrt{\frac{\rho_m}{\Delta P_m}}} \tag{C.5}$$

As it was discussed in Chapter II the value ω_m is negligible with respect to 1 so that equation (5) can be approximated, for uncertainty estimates, as

$$\dot{m}_a = C_m\ \rho_m^{\frac{1}{2}}\ \Delta P_m^{\frac{1}{2}} \tag{C.6}$$

The uncertainty in $\dot{m}_a$ is given by

$$U_{\dot{m}_a} = \left[\left(\frac{\partial \dot{m}_a}{\partial C_m} \cdot U_{C_m}\right)^2 + \left(\frac{\partial \dot{m}_a}{\partial \rho_m} \cdot U_{\rho_m}\right)^2 + \left(\frac{\partial \dot{m}_a}{\Delta P_m} \cdot U_{\Delta P_m}\right)^2 \right]^{\frac{1}{2}}$$

where

$$\frac{\partial \dot{m}_a}{\partial C_m} = \rho_m^{\frac{1}{2}}\ \Delta P_m^{\frac{1}{2}} = 0.2013\ \frac{lbm/ft^3}{\left(\frac{lbm/ft^3}{in.\ H_2O}\right)^{\frac{1}{2}}}$$

$$\frac{\partial \dot{m}_a}{\partial \rho_m} = \frac{1}{2} C_m \Delta P_m^{\frac{1}{2}} \rho_m^{-\frac{1}{2}} = 5.917 \quad \frac{ft^3}{min}$$

$$\frac{\partial \dot{m}_a}{\partial \Delta P_m} = \frac{1}{2} C_m \rho_m^{\frac{1}{2}} \Delta P_m^{-\frac{1}{2}} = 0.1853 \quad \frac{lbm}{min\ in.\ H_2O}$$

The uncertainty in mass flow rate of dry air is now

$$U_{\dot{m}_a} = [(0.2013 \times 0.11)^2 + (5.917 \times 0.000118)^2 + (0.1853 \times 0.03)^2]^{\frac{1}{2}}$$

$$U_{\dot{m}_a} = \pm 0.023 \text{ lbm/min}$$

Thus, $\dot{m}_a = 0.8128 \frac{lbm}{min} \pm 0.023 \frac{lbm}{min}$ (2.8%).

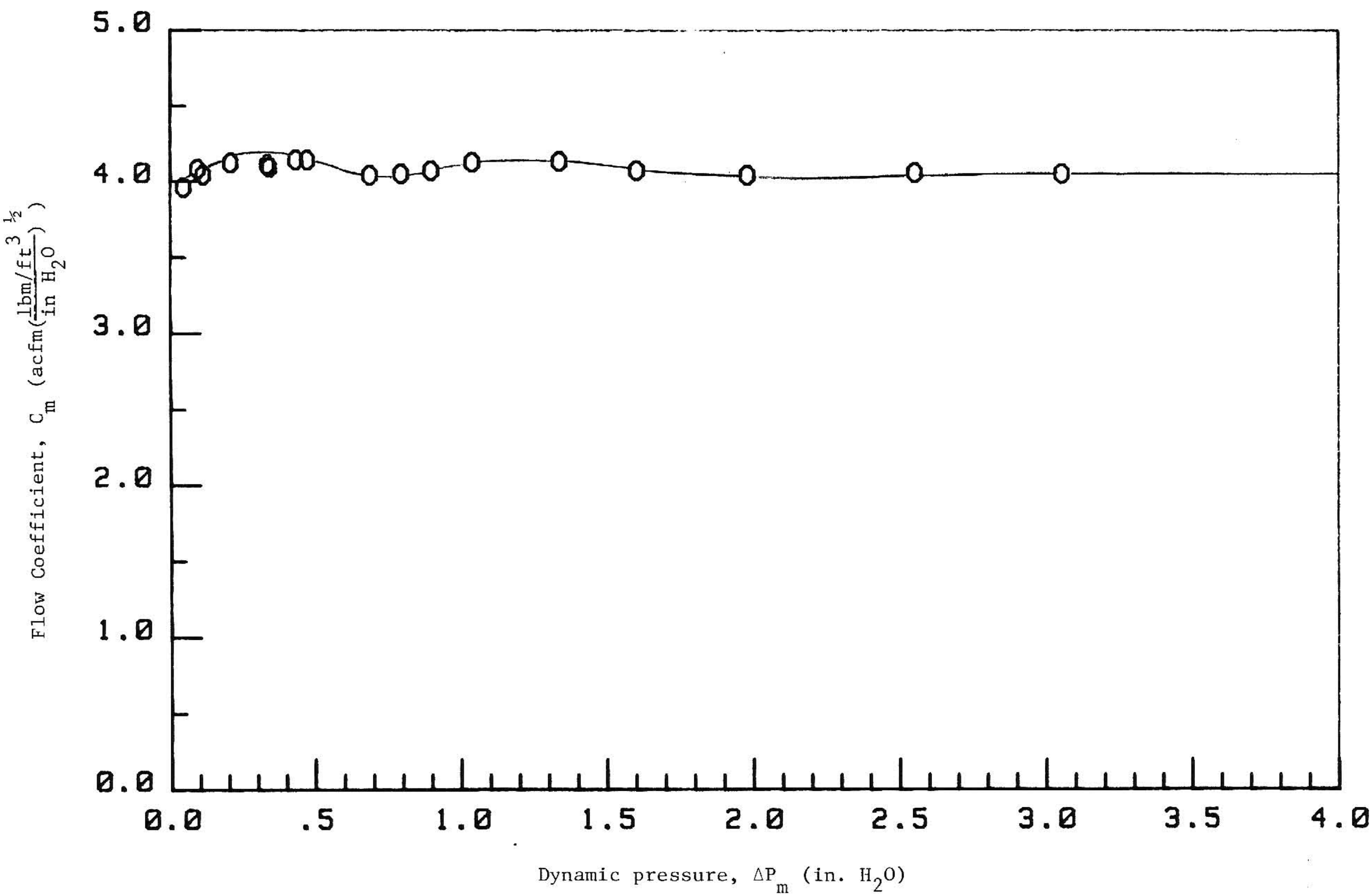

Figure C.2 Flow calibration data

Table C.1

Annubar Flowmeter Calibration

Average Dynamic Pressure ΔP_m (in. H_2O)	Air Density ρ_m (lbm/ft^3)	Volumetric Flowrate $\dot{Q}_m$ (acfm)	Flow Coefficients C_m (acfm) $\left(\frac{lbm/ft^3}{in.\ H_2O}\right)^{1/2}$
0.0447	0.07172	3.124	3.958
0.0940	0.07170	4.666	4.075
0.1132	0.07240	5.049	4.038
0.2083	0.07199	7.007	4.119
0.3350	0.07277	8.818	4.110
0.3417	0.07172	8.928	4.090
0.4383	0.07244	10.18	4.138
0.4743	0.07169	10.64	4.139
0.6887	0.07163	12.53	4.043
0.7960	0.07168	13.50	4.050
0.8987	0.07161	14.43	4.074
1.040	0.07207	15.67	4.125
1.338	0.07156	17.87	4.132
1.603	0.07166	19.27	4.073
1.981	0.07156	21.26	4.040
2.552	0.07151	24.27	4.063
3.054	0.07152	26.44	4.046

APPENDIX D

Effect of Moisture on Driving Force

As was discussed in Chapter II, the model that was developed was based on the density difference (driving force) due to the temperature difference alone. The objective of this appendix is to express the density difference in terms of both temperature and humidity differences. It will then be shown that, for the range of temperature differences investigated in this study, the influence of humidity upon the driving force is negligible.

The air density difference between the hot and cold chambers can be expressed, using the ideal gas law, as

$$\rho_c - \rho_H = \left(\frac{P_{atm}}{R_a} - \frac{P_{VC}}{R_a} + \frac{P_{VC}}{R_v}\right)\frac{1}{T_c} - \left(\frac{P_{atm}}{R_a} - \frac{P_{VH}}{R_a} + \frac{P_{VH}}{R_v}\right)\frac{1}{T_H} \qquad \text{(D.1)}$$

Introducing the definition of specific humidity and the definition of $\Delta\omega = \omega_H - \omega_C$ in equation (D.1), the following is obtained:

$$\rho_C - \rho_H = \frac{P_{atm}}{R_a}\left(\frac{1}{T_C} - \frac{1}{T_H}\right) - P_{atm}\left(\frac{1}{R_a} - \frac{1}{R_v}\right)\left[\frac{\left(\frac{1}{T_c} - \frac{1}{T_H}\right)\left(\omega_C\omega_H + \frac{R_a}{R_V}\omega_C\right) - \frac{R_a}{R_V}\frac{\Delta\omega}{T_H}}{\left(\omega_C + \frac{R_a}{R_V}\right)\left(\omega_H + \frac{R_a}{R_V}\right)}\right]$$

The term $\left(\frac{1}{T_C} - \frac{1}{T_H}\right)\left(\omega_c\omega_H + \frac{R_a}{R_V}\omega_C\right)$ is small (about 2.5%) compared with $\frac{R_a}{R_V}\frac{\Delta\omega}{T_H}$, so that it can be neglected. Since $\omega_C, \omega_H << \frac{R_a}{R_V}$ only a small error results when the ratio $\dfrac{R_a/R_V}{\omega_C + \frac{R_a}{R_V}}$ is assumed to be equal to 1. The final expression for the air density difference across opening can thus be written as:

$$\rho_C - \rho_H = \frac{P_{atm}}{R_a} \left(\frac{\Delta T}{T_H T_C}\right) + \left(\frac{R_V}{R_a} - 1\right) \frac{P_{atm}}{T_H} \frac{\Delta\omega}{R_a} \tag{D.4}$$

Therefore the driving force $\rho_C - \rho_H$ can be expressed in terms of temperature difference and humidity difference. The humidity difference has a positive effect on increasing the driving force. For a typical moisture decay test ($\Delta\omega = 0.007$), an error of about 8% in the density difference is present at the beginning of the experiment. During the course of the experiment the magnitude of error declines as the specific humidity difference decreases. Thus, for the range of air properties in this study, the effect of humidity difference has been neglected. This also suggests that the density of moist air can be assumed to be nearly the same as the density of dry air at the same total pressure.

APPENDIX E

Uncertainty Analysis of Experimental Measurements

The method outlined by Kline and Mclintock [12] was used to determine the uncertainty of the parameters of interest in the experimental measurements. These parameters were the normalized specific humidity ratio $\theta(t)$, the mass of dry air M_a, the average air density $\bar{\rho}$, the common normalization factor $\dot{m}'$, the normalized bulk flow $\dot{m}_b/\dot{m}'$, the forward mass flow rate $\dot{m}_c$, the time constant τ and finally the dimensionless time t/τ. The uncertainty calculations are shown below for a typical experimental test (B-22, shown in Appendix H).

E.1 Normalized Specific Humidity Ratio

The specific humidity is calculated by

$$\omega = \frac{P_v}{P_{atm} - P_v} (0.622)$$

The experimental uncertainty for the specific humidity is expressed as

$$U_w = \left[\left(\frac{\partial\omega}{\partial P_v} \cdot U_{P_v}\right)^2 + \left(\frac{\partial\omega}{\partial P_{atm}} \cdot U_{P_{atm}}\right)^2 \right]^{1/2}$$

where

$$\frac{\partial\omega}{\partial P_V} = \frac{P_{atm}}{(P_{atm} - P_v)^2} = \frac{1039.2}{(2039.2 - 34.36)^2} = 0.00051 \frac{ft^2}{lbf}$$

$$\frac{\partial\omega}{\partial P_{atm}} = \frac{P_{atm}}{(P_{atm} - P_v)^2} = - \frac{34.36}{(2039.2 - 34.36)^2} = 0.0000085 \frac{ft^2}{lbf}$$

With uncertainty in the barometer reading of ±.0.01 Hg, the uncertainty associated with the atmospheric pressure is determined by

$$U_{P_{atm}} = \rho \frac{g}{g_c} U_h = \left(847 \frac{\text{lbm}}{\text{ft}^3}\right)\left(\frac{32.2 \text{ ft/sec}^2}{32.2 \frac{\text{ft.lbm}}{\text{lbf}\cdot\text{sec}^2}}\right)\left(\frac{0.01}{12} \text{ ft}\right) = \pm 0.71 \frac{\text{lbf}}{\text{ft}^2}$$

The uncertainty of partial pressure P_v is dependent on the uncertainty of the dewpoint temperature, as measured by the dewpoint hygrometer. The uncertainty in dewpoint temperature is ±0.3°C (±0.54°F), so that the uncertainty in P_v, using the steam tables, becomes

$$U_{P_v} = \pm 0.0045 \frac{\text{lbf}}{\text{in}^2} \left(\pm 0.65 \frac{\text{lbf}}{\text{ft}^2}\right)$$

The estimation of the uncertainty in specific humidity is thus given by:

$$U_\omega = [(0.00051 \times 0.65)^2 + (0.0000085 \times 0.71)^2]^{\frac{1}{2}} = \pm 0.000331$$

The normalized specific humidity is defined by:

$$\theta(t) = \frac{\omega_H(t) - \omega_c}{\omega_f - \omega_c}$$

The uncertainty associated with $\theta(t)$ is thus

$$U_\theta = \left[\left(\frac{\partial\theta}{\partial\omega_H(t)} \cdot U_{\omega H}\right)^2 + \left(\frac{\partial\theta}{\partial\omega_c} \cdot U_{\omega c}\right)^2 + \left(\frac{\partial\theta}{\partial\omega_f} \cdot U_{\omega f}\right)^2\right]^{\frac{1}{2}}$$

$$\frac{\partial\theta}{\partial\omega_H(t)} = \frac{1}{\omega_f - \omega_c} = \frac{1}{0.00468} = 213.7$$

A typical value of $\omega_H(t)$ for t = 800 sec, which was also used as a data reduction example (see Appendix B), is introduced below, yielding

$$\frac{\partial\theta}{\partial\omega_c} = \frac{\omega_H(t) - \omega_c}{(\omega_f - \omega_c)^2} = \frac{0.00719 - 0.00596}{(0.00468)^2} = 56.16$$

$$\frac{\partial\theta}{\partial\omega_f} = \frac{\omega_c - \omega_H(t)}{(\omega_f - \omega_c)^2} = \frac{0.00596 - 0.00719}{(0.00468)^2} = -56.16$$

The uncertainty of $\theta(t)$ is now given by

$$U_\theta = [(213.7 \times 0.000331)^2 + (56.16 \times 0.000331)^2 + (-56.16 \times 0.000331)^2]^{\frac{1}{2}}$$

$$U_\theta = \pm 0.075$$

Thus, $\theta = 0.263 \pm 0.075$ (28.5%)

E.2 Mass of Dry Air

The mass of dry air, using the ideal gas law, is given by:

$$M_a = \frac{P_{atm}\ V}{R_a\ T_H}$$

The uncertainty in M_a is expressed as

$$U_{M_a} = \left[\left(\frac{\partial M_a}{\partial P_{atm}} U_{P_{atm}}\right)^2 + \left(\frac{\partial M_a}{\partial V} U_V\right)^2 + \left(\frac{\partial M_a}{\partial T} U_T\right)^2\right]^{\frac{1}{2}}$$

where

$$\frac{\partial M_a}{\partial P_{atm}} = \frac{V}{R_a T_H} = \frac{216}{(53.34)(12)^3(565.9)} = 0.0000041\ \frac{\text{lbm} \cdot \text{ft}^2}{\text{lbf}}$$

$$\frac{\partial M_a}{\partial V} = \frac{P_{atm}}{R_a T_H} = \frac{2039.2}{(53.34)(565.9)} = 0.06705\ \frac{\text{lbm}}{\text{ft}^3}$$

$$\frac{\partial M_a}{\partial T_H} = \frac{P_{atm} V}{R_a T_H^2} = -\frac{(2039.2)(216)}{(53.34)(565.9)^2} = -\ 0.02540\ \frac{\text{lbm}}{°\text{R}}$$

For a single copper constantan thermocouple junction, the limit of uncertainty is generally accepted as ±0.9°F. Assuming that thermocouple errors are completely dependent yields,

$$U_{T_H} = U_{T_c} = [(9 \times \frac{0.9}{9})^2]^{\frac{1}{2}} = \pm\ 0.9°R$$

The estimation of the uncertainty for volume, $V = L^3$, is given by:

$$U_V = \left[\left(\frac{\partial V}{\partial L} U_L\right)^2\right]^{\frac{1}{2}}$$

where

$$\frac{\partial V}{\partial L} = 3L^2 = 3(6\ ft)^2 = 108\ ft^2$$

The uncertainty in length is assumed to be ±0.5 inches, thus

$$U_V = (108)\left(\frac{0.5}{12}\right) = \pm 4.50\ ft^3$$

Therefore the uncertainty in M_a can be determined as follows:

$$U_{M_a} = [(0.06705 \times 4.5)^2 + (-0.02540 \times 0.9)^2 (0.0000041 \times 0.71)^2]^{\frac{1}{2}}$$

$$U_{M_a} = \pm 0.30\ lbm$$

thus, $M_a = 14.68\ lbm \pm 0.30\ lbm$ (±2.0%)

E.3 The Average Air Density

For the average air density defined by

$$\bar{\rho} = \frac{\rho_C + \rho_H}{2} = \frac{P_{atm}}{2R_a T_C} + \frac{P_{atm}}{2R_a T_H}$$

the uncertainty is given by

$$U_{\bar{\rho}} = \left[\left(\frac{\partial \bar{\rho}}{\partial T_c} \cdot U_{T_c}\right)^2 + \left(\frac{\partial \bar{\rho}}{\partial P_{atm}} \cdot U_{P_{atm}}\right)^2 + \left(\frac{\partial \bar{\rho}}{\partial T_H} \cdot U_{T_H}\right)^2\right]^{\frac{1}{2}}$$

where

$$\frac{\partial\bar{\rho}}{\partial T_c} = -\frac{P_{atm}}{2R_aT_c^2} = -\frac{2039.2}{2(53.34)(539.3)^2} = -0.000066\ \frac{lbm}{ft.^3\,°R}$$

$$\frac{\partial\bar{\rho}}{\partial T_H} = -\frac{P_{atm}}{2R_aT_H^2} = -\frac{2041.93}{2(53.34)(565.9)^2} = -0.000060\ \frac{lbm}{ft^3\,°R}$$

$$\frac{\partial\bar{\rho}}{\partial P_{atm}} = \frac{T_H + T_c}{2R_aT_cT_H} = \frac{(565.9) + (539.3)}{2(53.34)(539.3)(565.9)} = -0.000034\ \frac{lbm}{ft.lbf}$$

Thus,

$$U_{\bar{\rho}} = [(0.000066 \times 0.9)^2 + (0.000034 \times 0.71)^2 + (0.00006 \times 0.9)^2]^{\frac{1}{2}}$$

$$U_{\bar{\rho}} = \pm\ 0.000059\ \frac{lbm}{ft^3}$$

Therefore

$$\bar{\rho} = 0.06936\ \frac{lbm}{ft^3} \pm 0.000059\ \frac{lbm}{ft^3} \qquad (\pm 0.05\%)$$

E.4 The Common Normalization Factor

The common normalization factor is defined by

$$\dot{m}' = \frac{2}{3} W\bar{\rho}\ \sqrt{2gH^3\bar{T}\left(\frac{1}{T_c} - \frac{1}{T_H}\right)}$$

For the purposes of the uncertainty analysis, the following is obtained by introducing the temperature difference, ΔT:

$$\dot{m}' = \frac{2}{3} W\bar{\rho}\ \sqrt{2gH^3\ \frac{\Delta T + 2T_c}{2T_c(\Delta T + T_c)}} \cong \frac{2}{3} W\bar{\rho}\ \sqrt{2gH^3\ \frac{\Delta T}{T_c}}$$

since $\Delta T << T_c, T_H$. The uncertainty in $\dot{m}'$ is given by

$$U_{\dot{m}'} = \left[\left(\frac{\partial \dot{m}'}{\partial \Delta T} \cdot U_{\Delta T}\right)^2 + \left(\frac{\partial \dot{m}'}{\partial T_c} \cdot U_{T_c}\right)^2 + \left(\frac{\partial \dot{m}'}{\partial H} \cdot U_H\right)^2 + \left(\frac{\partial \dot{m}'}{\partial \bar{\rho}} \cdot U_{\bar{\rho}}\right)^2 + \left(\frac{\partial m'}{\partial W} \cdot U_W\right)^2\right]^{\frac{1}{2}}$$

where

$$\frac{\partial \dot{m}'}{\partial \Delta T} = \frac{1}{3}\,\omega\bar{\rho}\left(\frac{gH^3}{Tc}\right)^{\frac{1}{2}} (\Delta T)^{-\frac{1}{2}} = 0.00148\ \frac{\text{lbm}}{\text{sec.}^\circ\text{R}}$$

$$\frac{\partial \dot{m}'}{\partial T_c} = -\frac{1}{3}\,\omega\bar{\rho}(gH^3\Delta T)^{\frac{1}{2}}\,(T_c)^{-3/2} = -\ 0.000074\ \frac{\text{lbm}}{\text{sec.}^2\,{}^\circ\text{R}}$$

$$\frac{\partial \dot{m}'}{\partial H} = W\bar{\rho}\left(\frac{2g\Delta T}{T_c}\right)^{\frac{1}{2}} \cdot H^{\frac{1}{2}} = 0.1231\ \frac{\text{lbm}}{\text{ft. sec}^2}$$

$$\frac{\partial \dot{m}'}{\partial \bar{\rho}} = \frac{2}{3}\,W\left[2gH^3\,\frac{\Delta T}{T_c}\right]^{\frac{1}{2}} = 1.183\ \frac{\text{ft}^3}{\text{sec}}$$

$$\frac{\partial \dot{m}'}{\partial W} = \frac{2}{3}\,\bar{\rho}\left[2gH^3\,\frac{\Delta T}{T_c}\right]^{\frac{1}{2}} = 0.08204\ \frac{\text{lbm}}{\text{sec. ft}}$$

The uncertainty for ΔT can be determined by

$$U_{\Delta T} = \sqrt{(0.9)^2 + (0.9)^2} = 1.273^\circ\text{R}$$

The uncertainties in measurement of both H and W are assumed to be ± 1/8" $= \pm\,\frac{1}{96}$ ft. The uncertainty in the normalization factor can now be calculated as follows:

$$U_{\dot{m}'} = [(0.001484 \times 0.1273)^2 + (0.000074 \times 0.9)^2 + (0.1231 \times \frac{1}{96})^2$$

$$+ (1.183 \times 0.000059)^2 + (0.08204 \times \frac{1}{96})^2]^{\frac{1}{2}} = \pm\ 0.00244\ \frac{\text{lbm}}{\text{sec}}$$

Thus, $\dot{m}' = 0.08179\ \frac{\text{lbm}}{\text{sec}} \pm 0.00244\ \frac{\text{lbm}}{\text{sec}}$ (±1.8%)

E.5 <u>The Normalized Bulk Flow</u>

The normalized bulk flow is defined as

$$\alpha = \frac{\dot{m}_b}{\dot{m}'}$$

Thus, $$U_\alpha = \left[\left(\frac{\partial\alpha}{\partial\dot{m}_b} U_{\dot{m}_b}\right)^2 + \left(\frac{\partial\alpha}{\partial\dot{m}'} \cdot U_{\dot{m}'}\right)^2\right]^{\frac{1}{2}}$$

where,

$$\frac{\partial\alpha}{\partial\dot{m}_b} = \frac{1}{\dot{m}'} = \frac{1}{0.08179} = 12.23\ \frac{\text{sec}}{\text{lbm}}$$

$$\frac{\partial\alpha}{\partial\dot{m}'} = -\frac{\dot{m}_b}{\dot{m}'^2} = -\frac{0.01363}{(0.08179)^2} = -\ 2.037\ \frac{\text{sec}}{\text{lbm}}$$

For uncertainty analysis purposes, the bulk flow through the opening is approximated by

$$\dot{m}_b = \dot{m}_a\ (1+\omega_c) \cong \dot{m}_a$$

so that the following can be written

$$U_{\dot{m}_b} = U_{\dot{m}_a}$$

The uncertainty in mass flow rate of dry air, passing in through the opening and out through the meter, is given in detail in Appendix C; so that

$$U_{\dot{m}_b} = \pm\ 0.00038\ \frac{\text{lbm}}{\text{sec}}$$

The uncertainty in normalized bulk can now be calculed as follows:

$$U_{\alpha} = [(12.23 \times 0.00038)^2 + (2.037 \times 0.00244)^2]^{\frac{1}{2}}$$

$$U_{\alpha} = \pm\ 0.0068$$

$$\frac{\dot{m}_b}{\dot{m}'} = \alpha = 0.1668 \pm 0.0068 \qquad (4.1\%)$$

E.6 <u>The Forward Mass Flow Rate</u>

The forward mass flow rate at the opening is calculated by the following equation:

$$\frac{\dot{m}_b}{\dot{m}'} = \frac{\dot{m}_c}{\dot{m}'} - \left[1 - \left(\frac{\dot{m}_c}{\dot{m}'}\right)^{2/3}\right]^{3/2}$$

Let $\frac{\dot{m}_c}{\dot{m}'} = \beta$

Thus $\alpha = \beta - [1-\beta^{2/3}]^{3/2}$

The uncertainty in $\beta = \frac{\dot{m}_c}{\dot{m}'}$ is given by:

$$U_{\beta} = \frac{\partial\beta}{\partial\alpha} \cdot U_{\alpha}$$

where

$$\frac{\partial\beta}{\partial\alpha} = \frac{1}{1 + [(1-\beta^{2/3})^{\frac{1}{2}} \cdot \beta^{-1/3}]} = 0.5396$$

The uncertainty of $\frac{\dot{m}_c}{\dot{m}'}$ is calculated as the following:

$$U_\beta = (0.5396)(0.0068) = \pm\ 0.00367$$

Thus,

$$\frac{\dot{m}_c}{\dot{m}'} = \beta = 0.4402 \pm 0.00367 \ (0.8\%)$$

The uncertainty in $\dot{m}_c = \beta\dot{m}'$ is given by:

$$U_{\dot{m}_c} = \left[\left(\frac{\partial\dot{m}_c}{\partial\beta} \cdot U_\beta\right)^2 + \left(\frac{\partial\dot{m}_c}{\partial\dot{m}'} \quad U_{\dot{m}'}\right)^2\right]^{\frac{1}{2}}$$

where

$$\frac{\partial\dot{m}_c}{\partial\beta} = \dot{m}' = 0.08179 \text{ lbm/sec}$$

$$\frac{\partial\dot{m}_c}{\partial\dot{m}'} = \beta = 0.4402$$

Therefore, the uncertainty in $\dot{m}_c$ can now be determined:

$$U_{\dot{m}_c} = [0.08179 \times 0.00367)^2 + (0.4402 \times 0.00244)^2]^{\frac{1}{2}}$$

$$U_{\dot{m}_c} = \pm\ 0.00111 \ \frac{\text{lbm}}{\text{sec}}$$

Thus, $\dot{m}_c = 0.03600 \ \frac{\text{lbm}}{\text{sec}} \pm 0.00111 \ \frac{\text{lbm}}{\text{sec}} \qquad (3.1\%)$

E.7 The Time Constant

The time constant τ, is defined by:

$$\tau = \frac{M_a}{\dot{m}_c}$$

The experimental uncertainty for the time constant is expressed as

$$U_\tau = \left[\left(\frac{\partial \tau}{\partial M_a} U_{M_a} \right)^2 + \left(\frac{\partial \tau}{\partial \dot{m}_c} U_{\dot{m}_c} \right)^2 \right]^{1/2}$$

where

$$\frac{\partial \tau}{\partial M_a} = \frac{1}{\dot{m}_c} = \frac{1}{0.036000} = 27.78 \ \frac{\text{sec}}{\text{lbm}}$$

$$\frac{\partial \tau}{\partial \dot{m}_c} = - \frac{M_a}{\dot{m}_c^2} = - \frac{14.67}{(0.03600)^2} = - 11319.4 \ \frac{\text{sec}^2}{\text{lbm}}$$

The uncertainty of time constant τ therefore becomes

$$U_\tau = [(27.78 \times 0.30)^2 + (11319.4 \times 0.00111)^2]^{1/2}$$

$$U_\tau = \pm 15 \text{ sec}$$

Thus, $\tau = 407.8$ sec $\pm$ 15 sec (3.7%)

E.8 The Dimensionless Time

The dimensionless time is given by

$$\phi = \frac{t}{\tau}$$

the uncertainty in ϕ is calculated by

$$U_\phi = \left[\left(\frac{\partial \phi}{\partial t} \cdot U_t \right)^2 + \left(\frac{\partial \phi}{\partial \tau} \cdot U_\tau \right)^2 \right]^{1/2}$$

where

$$\frac{\partial \phi}{\partial t} = \frac{1}{\tau} = \frac{1}{407.8} = 0.00245 \text{ sec}^{-1}$$

Since time t can have values from zero to about 2000 sec. the uncertainty in t/τ is bounded by determing the uncertainty with respect to three different values of low (10 sec), medium (800 sec), high (2000 sec) t in the following expression, thus:

(a) $\frac{\partial \phi}{\partial \tau} = - \frac{t}{\tau^2} = - \frac{100}{(407.8)^2} = - 0.00060 \text{ sec}^{-1}$

(b) $\frac{\partial \phi}{\partial \tau} = - \frac{800}{(407.8)^2} = - 0.00481 \text{ sec}^{-1}$

(c) $\frac{\partial \phi}{\partial \tau} = - \frac{2000}{(407.8)^2} = - 0.01203 \text{ sec}^{-1}$

The uncertainty in t is assumed to be ± 1 sec. Therefore the uncertainty of dimensionless time at each value of t can now be determined. Thus,

(a) $U_\phi = [(0.00245 \times 1)^2 + (-0.00060 \times 15)^2]^{\frac{1}{2}} = \pm 0.0094$

Thus, $\phi = 0.2452 \pm 0.0094$ (3.8%)

(b) $U_\phi = [(0.00245 \times 1)^2 + (-0.00481 \times 15)^2]^{\frac{1}{2}} = \pm 0.073$

Thus, $\phi = 1.962 \pm 0.073$ (3.7%)

(c) $U_\phi = [(0.00245 \times 1)^2 + (-0.01203 \times 15)^2]^{\frac{1}{2}} = \pm 0.182$

Thus, $\phi = 4.904 \pm 0.182$ (3.7%)

The uncertainties of parameters of interest for this experimental data are approximately valid for all experimental tests.

APPENDIX F

Test Chamber Leakage

The purpose of this appendix is to investigate the leak integrity of the hot chamber. Several leak tests were run to determine the extent of the possible leak as a function of the chamber-to-ambient pressure difference. The experimental setup consisted basically of a bell prover connected to the exhaust port in the hot chamber by way of a flexible duct. After the opening was sealed using a 24" gauge galvanized steel sheet, several tests were conducted for different pressure differences between the hot chamber and surroundings. During each leak test the hot chamber was pressurized (or evacuated) to a known value. The mass flow rate of leakage was determined by measuring the volumetric flowrate of leakage from the bell prover reservoir and the corresponding time for that process. The mass flowrate of water vapor was then calculated for a typical value of ω_c = 0.005 and ω_H = 0.015. Figure F-1 graphically summarizes the mass flow rate of moisture leakage under different pressure differences. From Figure F-1 the leak rate under the ΔP of 0.3" H_2O is expected to be about 6 g/hr which would have only a small effect on the transient moisture transfer through the opening. However, to minimize the effect of moisture leakage upon the measurement of transient moisture transfer the pressure difference for all the conducted transient moisture transfer tests was kept well within ±0.1" H_2O. This pressure difference would cause a leak rate of only about 3.5 g/hr.

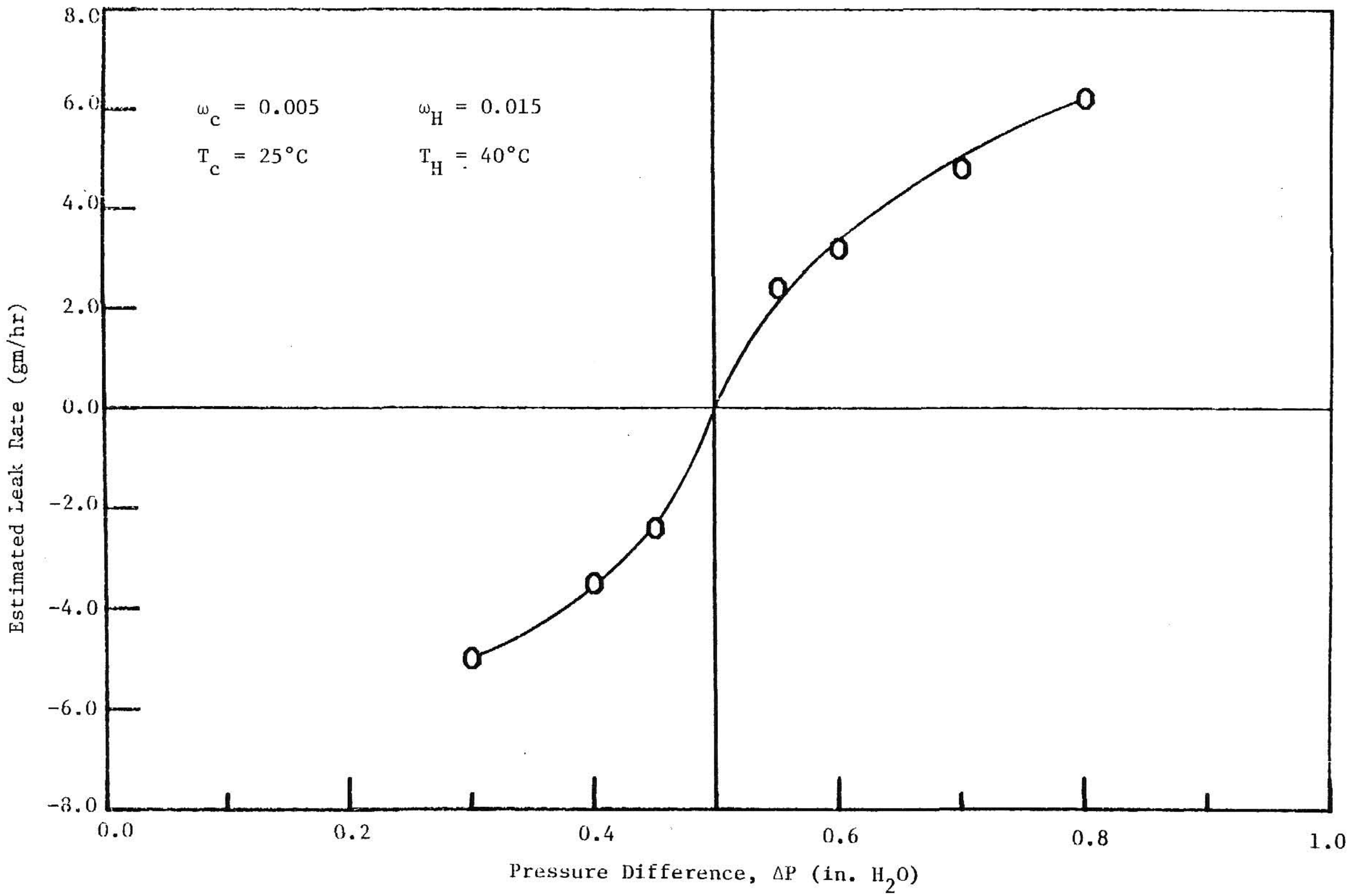

Figure F.1 Test chamber leakage

APPENDIX C

Corrected Theory

As was mentioned in section 4.2, in order to estimate bounds on the transient moisture transfer data, a flow coefficient was introduced into the simple theory. It is the subject of this appendix to express the detailed theory in bracketing the transient data. A modified form of the flow coefficient of Shaw [8] is introduced in the right hand side of equations 2.15a and 2.15b resulting in the following modified form of equation 2.16:

$$\frac{\dot{m}_b}{C\dot{m}'} = \frac{\dot{m}_c^*}{C\dot{m}'} - \left[1 - \left(\frac{\dot{m}_c^*}{C\dot{m}'}\right)^{2/3}\right]^{3/2} \tag{G.1}$$

where $\dot{m}_c^*$ is the corrected mass flow rate of dry air from the cold chamber to the hot chamber and C is the flow coefficient. Note that the mass flow rate, $\dot{m}_c$, in equation 2.16 is equal to $\dot{m}_c^*$ if C is equal to 1. From equation G.1, the corrected time constant τ^* can be written as:

$$\tau^* = \frac{M_a}{\dot{m}_c^*} \tag{G.2}$$

Thus,

$$\frac{\tau^*}{\tau} = \frac{\dfrac{M_a}{\dot{m}_c^*}}{\dfrac{M_a}{\dot{m}_c}} = \frac{\dot{m}_c/\dot{m}'}{\dot{m}_c^*/\dot{m}'} \tag{G.3}$$

The corrected theory can now be expressed as:

$$e^{-\frac{t}{\tau^*}} = e^{-\left(\frac{\tau}{\tau^*}\right)\frac{t}{\tau}} \tag{G.4}$$

In order to bracket the transient data, the lower and upper bound values for the flow coefficient are determined from steady-state data [1]. From Figure G.1 these flow coefficient bounds are found to be 0.65 and 0.85. These coefficients encompass virtually all the steady-state data. From equation G.1, for a known value of $\frac{\dot{m}_b}{C\dot{m}'}$ which ranges from zero to 1, the normalized mass flow rate parameter $\frac{\dot{m}^*_c}{C\dot{m}'}$ can be determined. Thus for each value of flow coefficient the ratio $\frac{\dot{m}^*_c}{\dot{m}'}$ can also be obtained. This suggests that the extreme values of the ratio τ^*/τ can now be calculated and that the corrected theory can be used to put a bracket on the predicted transient response. For $C = 0.85$ the lowest value for $\frac{\tau^*}{\tau}$ is 1.03 corresponding to lower bound on θ. For $C = 0.65$ the highest value for $\frac{\tau^*}{\tau}$ is 1.54 representing the upper bound on θ. The bracket produced by the corrected theory and the above two bounds is shown in Figure 4.8.

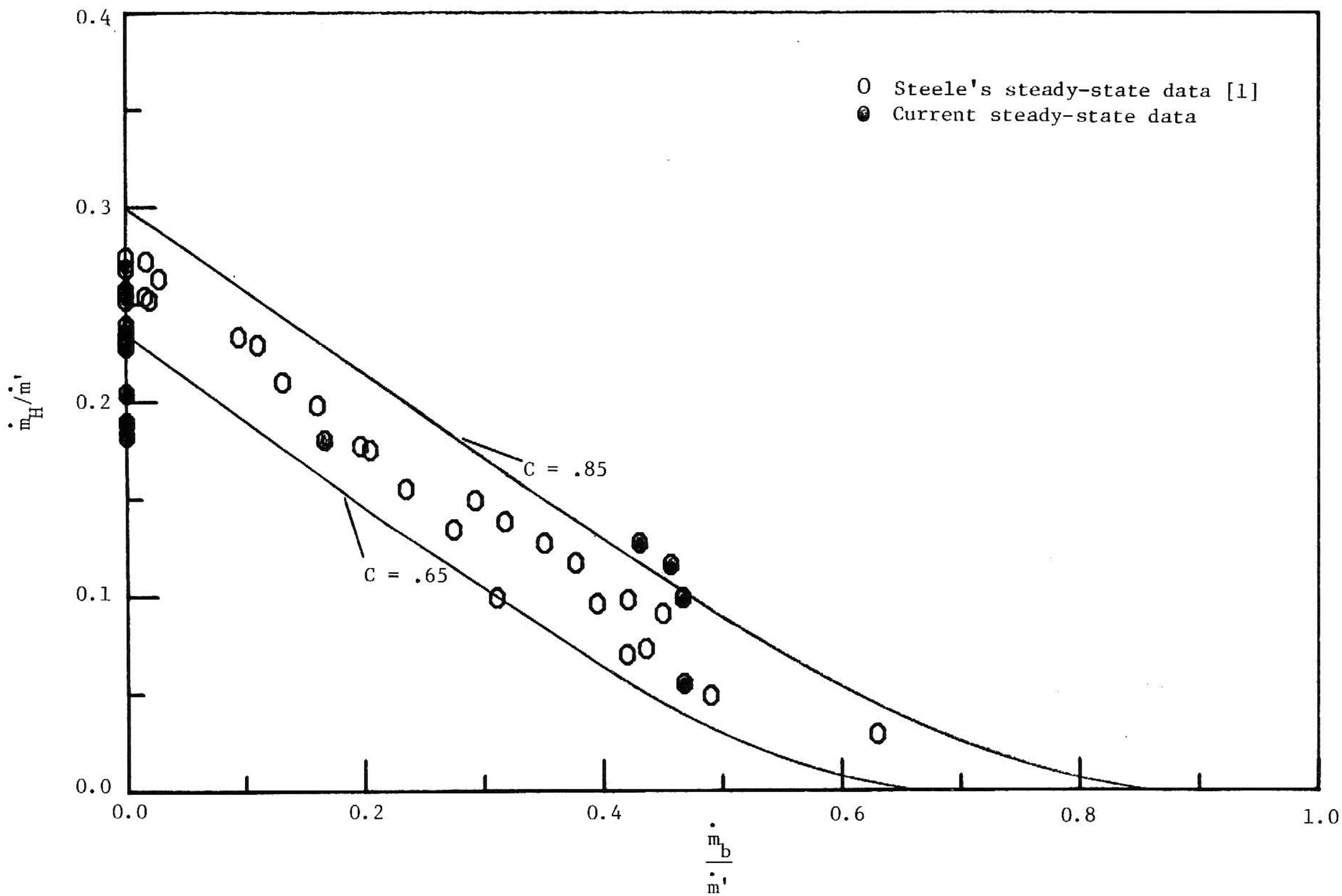

Figure G.1 Steady-state moisture transfer data

APPENDIX H

Tabulation of Experimental Results

Test Identification

Test number:	Nb-21
Opening geometry:	12" x 12" (30 cm by 30 cm), 45° taper
Flow conditions:	No bulk flow
Test type:	Moisture decay

Test Conditions

T_{ref}	= 21.6°C	P_{bar}	= 29.00 in Hg
$T_{dc,i}$	= 6.8°C	F.A.T.	= 2-15/6 ft/min
$T_{dc,f}$	= 5.9°C	$\bar{\omega}_c$	= 0.00615
$\bar{T}_{dc}$	= 6.35°C	$\Delta\omega$	= 0.00687
T_H	= 40.28°C	$\dot{m}_{H_2O}$	= 215.5 ml/hr
ΔT	= 14.77°C		

Reduced Parameters

$\dot{m}' = 0.03719$ kg/s $\qquad \tau = 8.458$ min

$\dfrac{\dot{m}_r}{\dot{m}'} = 0.2343$ $\qquad \Delta t = 39$ sec

Transient Data

Time (min)	T_{dh}(°C)	$\omega_H(t)$	$\theta(t)$	t/τ
0.00	17.55	0.01302	1.000	0.000
0.85	16.95	0.01253	0.929	0.100
1.35	16.70	0.01232	0.898	1.160
3.35	15.65	0.01151	0.780	0.396
5.35	14.70	0.01082	0.680	0.633
7.35	13.75	0.01016	0.584	0.869
9.35	12.95	0.00964	0.508	1.105
14.35	11.15	0.00855	0.349	1.696
19.52	9.65	0.00772	0.228	2.307
24.45	8.75	0.00726	0.161	2.891
29.35	8.00	0.00690	0.109	3.470
34.25	7.50	0.00666	0.074	4.049
41.15	6.90	0.00639	0.035	4.865
50.02	6.50	0.00621	0.009	5.913

Test Identification

Test number:	Nb-34
Opening geometry:	12" x 12" (30 cm by 30 cm), 45° taper
Flow conditions:	No bulk flow
Test type:	Moisture decay

Test Conditions

T_{ref} = 23.9°C	P_{bar} = 28.91 in. Hg
$T_{dc,i}$ = 15.2°C	F.A.T. = 0-5/3 ft/min
$T_{dc,f}$ = 15.0°C	$\bar{\omega}_C$ = 0.01114
$\bar{T}_{dc}$ = 15.1°C	$\Delta\omega$ = 0.00222
T_H = 41.97°C	$\dot{m}_{H_2O}$ = 75.79 ml/hr
ΔT = 15.32°C	

Reduced Parameters

$\dot{m}'$ = 0.03762 kg/s	τ = 8.292 min
$\frac{\dot{m}_r}{\dot{m}'}$ = 0.2521	Δt = 39 sec

Transient Data

Time (min)	T_{dh}(°C)	$\omega_H(t)$	$\theta(t)$	t/τ
0.00	17.90	0.01336	1.000	0.000
1.35	17.50	0.01302	0.847	0.163
3.35	17.20	0.01277	0.735	0.404
5.35	16.95	0.01257	0.643	0.645
7.35	16.70	0.01236	0.550	0.886
9.35	16.40	0.01212	0.444	1.128
11.35	16.20	0.01197	0.373	1.369
14.35	16.00	0.01181	0.303	1.731
16.35	15.80	0.01166	0.235	1.972
19.35	15.65	0.01155	0.185	2.334
22.68	15.50	0.01144	0.135	2.736
34.35	15.25	0.01125	0.049	4.143
42.68	15.15	0.01118	0.017	5.148

Test Identification

Test number:	Nb-35
Opening geometry:	12" x 12" (30 cm by 30 cm), 45° taper
Flow conditions:	No bulk flow
Test type:	Moisture decay

Test Conditions

T_{ref} = 21.7°C	P_{bar} = 28.91 in. Hg
$T_{dc,i}$ = 9.3°C	F.A.T. = 1-4/2 ft/min
$T_{dc,f}$ = 9.1°C	$\bar{\omega}_C$ = 0.00751
$\bar{T}_{dc}$ = 9.2°C	$\Delta\omega$ = 0.01187
T_H = 39.92°C	$\dot{m}_{H_2O}$ = 376.5 ml/hr
ΔT = 15.31°C	

Reduced Parameters

$\dot{m}'$ = 0.03790	τ = 8.284 min
$\frac{\dot{m}_r}{\dot{m}'}$ = 0.2325	Δt = 39 sec

Transient Data

Time (min)	T_{dh} (°C)	$\omega_H(t)$	$\theta(t)$	t/τ
0.00	23.80	0.01938	1.000	0.000
2.68	22.00	0.01733	0.827	0.323
6.02	19.90	0.01518	0.646	0.726
9.35	18.05	0.01349	0.504	1.129
14.35	15.90	0.01174	0.356	1.732
19.35	14.15	0.01047	0.249	2.336
26.02	12.65	0.00948	0.166	3.141
32.68	11.50	0.00878	0.107	3.945
41.02	10.60	0.00826	0.063	4.951
49.86	10.00	0.00793	0.036	6.019
59.36	9.65	0.00775	0.020	7.164

Test Identification

Test number:	Nb-37
Opening geometry:	12" x 12" (30 cm by 30 cm), 45° taper
Flow conditions:	No bulk flow
Test type:	Moisture decay

Test Conditions

$T_{ref} = 23.2°C$	$P_{bar} = 28.94$ in. Hg
$T_{dc,i} = 11.8°C$	F.A.T. = 0-6/3 ft/min
$T_{dc,f} = 11.6°C$	$\bar{\omega}_C = 0.00889$
$\bar{T}_{dc} = 11.7°C$	$\Delta\omega = 0.00809$
$T_H = 35.65°C$	$\dot{m}_{H_2O} = 206.5$ ml/hr
$\Delta T = 9.5°C$	

Reduced Parameters

$\dot{m}' = 0.02970$ Kg/s	$\tau = 10.76$ min
$\dfrac{\dot{m}_r}{\dot{m}'} = 0.2387$	$\Delta t = 39$ sec

Transient Data

Time (min)	T_{dh}(°C)	$\omega_H(t)$	$\theta(t)$	t/τ
0.00	21.70	0.01698	1.000	0.000
1.35	21.40	0.01667	0.962	0.125
3.35	20.50	0.01575	0.848	0.311
5.35	19.90	0.01516	0.775	0.497
7.35	19.25	0.01455	0.700	0.683
9.35	18.65	0.01400	0.632	0.869
14.35	17.25	0.01280	0.483	1.334
19.35	16.10	0.01188	0.370	1.798
24.35	15.20	0.01120	0.286	2.263
32.68	14.00	0.01035	0.181	3.037
41.02	13.25	0.00985	0.119	3.812

Test Identification

Test number:	Nb-33
Opening geometry:	12" x 12" (30 cm by 30 cm), 45° taper
Flow conditions:	No bulk flow
Test type:	Moisture decay

Test Conditions

T_{ref}	= 24.5°C	P_{bar}	= 28.79 in. Hg
$T_{dc,i}$	= 16.6°C	F.A.T.	= 1-5/2 ft/min
$T_{dc,f}$	= 16.6°C	$\bar{\omega}_C$	= 0.01233
$\bar{T}_{dc}$	= 16.6°C	$\Delta\omega$	= 0.00518
T_H	= 51.77°C	$\dot{m}_{H_2O}$	= 218.1 ml/hr
ΔT	= 24.0°C		

Reduced Parameters

$\dot{m}' = 0.04554$ Kg/s $\tau = 6.616$ min

$\frac{\dot{m}_r}{\dot{m}'} = 0.2568$ $\Delta t = 39$ sec

Transient Data

Time (min)	T_{dh}(°C)	$\omega_H(t)$	$\theta(t)$	t/τ
0.00	22.10	0.01751	1.000	0.000
1.35	21.50	0.01686	0.874	0.204
3.35	20.70	0.01604	0.716	0.506
5.35	19.95	0.01529	0.571	0.506
7.35	19.40	0.01477	0.471	1.111
9.35	18.85	0.01426	0.372	1.413
11.68	18.45	0.01390	0.302	1.766
14.35	18.00	0.01350	0.226	2.169
19.35	17.45	0.01303	0.136	2.925
24.35	17.10	0.01274	0.080	3.680
28.72	16.90	0.01260	0.048	4.340

Test Identification

Test number: Nb-27
Opening geometry: 6" x 12" (15 cm by 30 cm), 45° taper
Flow conditions: No bulk flow
Test type: Moisture decay

Test Conditions

T_{ref}	= 21.5°C	P_{bar}	= 28.68 in. Hg
$T_{dc,i}$	= 7.9°C	F.A.T.	= 0-4/2 ft/min
$T_{dc,f}$	= 7.5°C	$\bar{\omega}_C$	= 0.006830
$\bar{T}_{dc}$	= 7.7°C	$\Delta\omega$	= 0.01177
T_H	= 40.38°C	$\dot{m}_{H_2O}$	= 149.5 ml/hr
ΔT	= 15.82°C		

Reduced Parameters

$\dot{m}' = 0.01317$ kg/s $\tau = 23.62$ min

$\frac{\dot{m}_r}{\dot{m}'} = 0.2680$ $\Delta t = 39$ sec

Transient Data

Time (min)	T_{dh}(°C)	$\omega_H(t)$	$\theta(t)$	t/τ
0.00	23.00	0.01860	1.000	0.000
0.85	22.95	0.01854	0.995	0.036
2.35	22.25	0.01772	0.925	0.099
4.35	21.90	0.01736	0.895	0.184
7.35	21.15	0.01656	0.827	0.311
9.35	20.55	0.01595	0.775	0.396
14.35	19.65	0.01506	0.699	0.607
24.35	17.50	0.01313	0.535	1.031
34.35	15.75	0.01172	0.415	1.454
44.35	14.45	0.01076	0.334	1.878
54.35	13.15	0.00988	0.259	2.301
69.35	11.75	0.00900	0.184	2.936
84.35	10.65	0.00836	0.130	3.571
99.35	9.90	0.00794	0.094	4.206
116.02	9.20	0.00757	0.063	4.918
140.58	8.60	0.00727	0.037	5.952

Test Identification

Test number:	Nb-32
Opening geometry:	18" x 12" (45 cm by 30 cm), 45° taper
Flow conditions:	No bulk flow
Test type:	Moisture decay

Test Conditions

T_{ref} = 20.5°C	P_{bar} = 28.82 in. Hg
$T_{dc,i}$ = 3.4°C	F.A.T. = 0-4/2 ft/min
$T_{dc,f}$ = 3.0°C	$\bar{\omega}_C$ = 0.00496
$\bar{T}_{dc}$ = 3.2°C	$\Delta\omega$ = 0.00933
T_H = 38.62°C	$\dot{m}_{H_2O}$ = 522.2 ml/hr
ΔT = 15.03°C	

Reduced Parameters

$\dot{m}'$ = 0.06752 kg/s τ = 4.654 min

$\frac{\dot{m}_r}{\dot{m}'}$ = 0.2303 Δt = 39 sec

Transient Data

Time (min)	T_{dh}(°C)	$\omega_H(t)$	$\theta(t)$	t/τ
0.00	18.90	0.01429	1.000	0.000
1.35	17.80	0.01331	0.895	0.290
3.35	15.45	0.01144	0.694	0.720
5.35	13.50	0.01061	0.547	1.149
7.35	11.85	0.00901	0.434	1.579
9.35	10.30	0.00812	0.339	2.009
14.35	7.65	0.00677	0.194	3.083
19.35	6.10	0.00609	0.121	4.157
24.35	5.10	0.00567	0.076	5.232
29.75	4.15	0.00530	0.037	6.392
36.02	4.00	0.00525	0.031	7.738
44.35	3.70	0.00514	0.019	9.529
54.35	3.35	0.00500	0.005	11.677

Test Identification

Test number:	B-22
Opening geometry:	12" x 12" (30 cm by 30 cm), 45° taper
Flow conditions:	With bulk flow
Test type:	Moisture decay

Test Conditions

T_{ref} = 21.6°C	P_{bar} = 29.0 in. Hg
$T_{dc,i}$ = 6.2°C	F.A.T. = 0-8/2 ft/min
$T_{dc,f}$ = 5.6°C	$\bar{\omega}_C$ = 0.00596
$\bar{T}_{dc}$ = 5.9°C	$\Delta\omega$ = 0.00468
T_H = 41.07°C	$\dot{m}_{H_2O}$ = 215.86 ml/hr
ΔT = 14.77°C	ΔP_{dy} = 0.584 in. H_2O
T_m = 30.8°C	ΔP_s = 0.80 in. H_2O

Reduced Parameters

$\dot{m}'$ = 0.03705 Kg/s $\qquad \tau$ = 6.797 min

$\frac{\dot{m}_r}{\dot{m}'}$ = 0.1797 $\qquad \Delta t$ = 39 sec

$\frac{\dot{m}_b}{\dot{m}'}$ = 0.1668

Transient Data

Time (min)	T_{dh}(°C)	$\omega_H(t)$	$\theta(t)$	t/τ
0.00	14.45	0.01064	1.000	0.000
0.85	14.05	0.01037	0.942	0.125
1.35	13.75	0.01016	0.897	0.199
3.35	12.40	0.00929	0.716	0.493
5.35	11.40	0.00869	0.583	0.787
7.35	10.45	0.00815	0.468	1.081
9.35	9.65	0.00772	0.376	1.376
12.68	8.60	0.00719	0.263	1.866
16.53	7.80	0.00680	0.179	2.432
22.08	6.90	0.00639	0.092	3.249
30.28	6.20	0.00609	0.028	4.456

Test Identification

Test number: B-23
Opening geometry: 12" x 12" (30 cm by 30 cm), 45° taper
Flow conditions: With bulk flow
Test type: Moisture decay

Test Conditions

T_{ref}	= 21.6°C	P_{bar}	= 29.11 in. Hg
$T_{dc,i}$	= 6.1°C	F.A.T.	= 0-8/4 ft/min
$T_{dc,f}$	= 6.1°C	$\bar{\omega}_C$	= 0.00603
$\bar{T}_{dc}$	= 6.1°C	$\Delta\omega$	= 0.00283
T_H	= 41.85°C	$\dot{m}_{H_2O}$	= 216.11 ml/hr
ΔT	= 15.59°C	ΔP_{dy}	= 4.220 in. H_2O
T_m	= 34.6°C	ΔP_s	= 5.40 in. H_2O

Reduced Parameters

$\dot{m}' = 0.03815$ Kg/s $\qquad \tau = 4.923$ min

$\frac{\dot{m}_r}{\dot{m}'} = 0.1266$ $\qquad \Delta t = 39$ sec

$\frac{\dot{m}_b}{\dot{m}'} = 0.4311$

Transient Data

Time (min)	T_{dh}(°C)	$\omega_H(t)$	$\theta(t)$	t/τ
0.00	11.75	0.00886	1.000	0.000
0.68	11.10	0.00849	0.870	0.139
1.27	10.75	0.00829	0.799	0.257
1.82	10.25	0.00802	0.704	0.369
4.23	9.10	0.00741	0.488	0.860
6.17	8.35	0.00703	0.354	1.253
9.58	7.50	0.00664	0.216	1.947
12.65	7.00	0.00641	0.136	2.570
15.42	6.70	0.00628	0.090	3.131
21.08	6.35	0.00615	0.043	4.282
28.37	6.25	0.00608	0.021	5.762

Test Identification

Test number: B-26
Opening geometry: 12" x 12" (30 cm by 30 cm), 45° taper
Flow conditions: With bulk flow
Test type: Moisture addition

Test Conditions

T_{ref} = 21.0°C	P_{bar} = 28.77 in. Hg
$T_{dc,i}$ = 3.6°C	F.A.T. = 0-4/1 ft/min
$T_{dc,f}$ = 3.6°C	$\bar{\omega}_C$ = 0.00511
$\bar{T}_{dc}$ = 3.6°C	$\Delta\omega$ = 0.00281
T_H = 39.77°C	$\dot{m}_{H_2O}$ = 215.1 ml/hr
ΔT = 14.95°C	ΔP_{dy} = 4.595 in. H_2O
T_m = 35.4°C	ΔP_s = 5.8 in. H_2O

Reduced Parameters

$\dot{m}'$ = 0.03727 Kg/s τ = 4.897 min

$\frac{\dot{m}_r}{\dot{m}'}$ = 0.1157 Δt = 39 sec

$\frac{\dot{m}_b}{\dot{m}'}$ = 0.4571

Transient Data

Time (min)	T_{dh}(°C)	$\omega_H(t)$	$\theta(t)$	t/τ
0.00	3.60	0.00511	0.000	0.000
0.85	4.40	0.00541	0.107	0.173
2.35	5.95	0.00603	0.327	0.480
3.35	6.40	0.00622	0.395	0.684
4.35	6.95	0.00646	0.480	0.888
6.02	7.65	0.00679	0.598	1.229
7.68	8.20	0.00705	0.690	1.568
9.35	8.55	0.00722	0.751	1.909
12.68	9.15	0.00752	0.858	2.589
21.02	9.65	0.00778	0.950	4.292
29.35	9.90	0.00792	1.000	5.993

Test Identification

Test number: Nb-24
Opening geometry: 12" x 12" (30 cm by 30 cm), 45° taper
Flow conditions: No bulk flow
Test type: Moisture addition

Test Conditions

T_{ref}	= 22.7°C	P_{bar}	= 28.38 in. Hg
$T_{dc,i}$	= 20.0°C	F.A.T.	= 0-5/2 ft/min
$T_{dc,f}$	= 10.6°C	$\bar{\omega}_C$	= 0.00825
$\bar{T}_{dc}$	= 10.3°C	$\Delta\omega$	= 0.00693
T_H	= 40.64°C	$\dot{m}_{H_2O}$	= 215.04 ml/hr
ΔT	= 15.21°C		

Reduced Parameters

$\dot{m}' = 0.03694$ Kg/s $\qquad \tau = 8.537$ min

$\frac{\dot{m}_r}{\dot{m}'} = 0.2278$ $\qquad \Delta t = 39$ sec

Transient Data

Time (min)	T_{dh}(°C)	$\omega_H(t)$	$\theta(t)$	t/τ
0.00	10.00	0.00808	0.000	0.000
0.85	10.75	0.00850	0.059	0.099
2.35	11.70	0.00906	0.138	0.275
4.35	13.00	0.00989	0.255	0.509
7.35	14.35	0.01081	0.384	0.861
9.35	15.10	0.01135	0.461	1.095
14.35	16.80	0.01268	0.648	1.681
19.35	17.70	0.01344	0.755	2.267
24.35	18.40	0.01406	0.842	2.852
29.35	18.75	0.01438	0.887	3.438
36.02	19.20	0.01480	0.946	4.295
52.68	19.55	0.01504	0.981	6.247
62.68	19.60	0.01518	1.000	7.342

Test Identification

Test number: B-19
Opening geometry: 12" x 12" (30 cm by 30 cm)
Flow conditions: With bulk flow
Test type: Moisture decay

Test Conditions

T_{ref}	= 20.8°C	P_{bar}	= 28.92 in. Hg
$T_{dc,i}$	= 2.0°C	F.A.T.	= 2-15/5 ft/min
$T_{dc,f}$	= 1.4°C	$\bar{\omega}_C$	= 0.00444
$\bar{T}_{dc}$	= 1.7°C	$\Delta\omega$	= 0.00312
T_H	= 39.53°C	$\dot{m}_{H_2O}$	= 215.8 ml/hr
ΔT	= 14.53°C	ΔP_{dy}	= 4.680
T_m	= 34.0°C	ΔP_s	= 6.15

Reduced Parameters

$\dot{m}' = 0.0369$ Kg/s $\qquad \tau = 4.905$ min

$\dfrac{\dot{m}_r}{\dot{m}'} = 0.0549$ $\qquad \Delta t = 39$ sec

$\dfrac{\dot{m}_b}{\dot{m}'} = 0.4678$

Transient Data

Time (min)	T_{dh}(°C)	$\omega_H(t)$	$\theta(t)$	t/τ
0.00	9.30	0.00756	1.000	0.000
0.78	8.70	0.00726	0.902	0.160
1.98	7.35	0.00661	0.695	0.404
3.35	6.00	0.00602	0.506	0.683
5.68	4.70	0.00549	0.336	1.159
7.98	4.05	0.00525	0.260	1.627
10.47	3.20	0.00494	0.160	2.134
13.40	2.55	0.00472	0.090	2.732
15.82	2.35	0.00465	0.067	3.225
18.35	2.00	0.00453	0.029	3.741
22.73	1.90	0.00450	0.019	4.635

Test Identification

Test number:	B-20
Opening geometry:	12" x 12" (30 cm by 30 cm), 45° taper
Flow conditions:	With bulk flow
Test type:	Moisture decay

Test Conditions

T_{ref} = 20.9°C	P_{bar} = 28.95 in. Hg
$T_{dc,i}$ = 1.8°C	F.A.T. = 1-15/5 ft/min
$T_{dc,f}$ = 1.2°C	$\bar{\omega}_C$ = 0.00437
$\bar{T}_{dc}$ = 1.5°C	$\Delta\omega$ = 0.00288
T_H = 39.63°C	$\dot{m}_{H_2O}$ = 216.0 ml/hr
ΔT = 14.54°C	ΔP_{dy} = 4.674 in. H_2O
T_m = 34.4°C	ΔP_s = 6.15 in. H_2O

Reduced Parameters

$\dot{m}'$ = 0.0370 Kg/s τ = 4.908 min

$\frac{\dot{m}_r}{\dot{m}'}$ = 0.0987 Δt = 39 sec

$\frac{\dot{m}_b}{\dot{m}'}$ = 0.4664

Transient Data

Time (min)	T_{dh}(°C)	$\omega_H(t)$	$\theta(t)$	t/τ
0.00	8.70	0.00725	1.000	0.000
0.85	8.20	0.00700	0.913	0.173
1.35	7.70	0.00677	0.833	0.275
2.35	7.00	0.00645	0.722	0.479
3.35	6.25	0.00612	0.608	0.682
5.35	5.15	0.00567	0.451	1.090
7.35	4.10	0.00525	0.305	1.497
9.23	3.30	0.00497	0.208	1.881
12.78	2.55	0.00471	0.118	2.604
18.02	2.05	0.00454	0.059	3.671
22.50	1.75	0.00445	0.028	4.584
27.35	1.60	0.00439	0.006	5.572

Test Identification

Test number:	Nb-12
Opening geometry:	12" x 12" (30 cm by 30 cm), 45° taper
Flow conditions:	No bulk flow
Test type:	Moisture decay

Test Conditions

T_{ref} = 22.4°C	P_{bar} = 28.52 in. Hg
$T_{dc,i}$ = 8.0°C	F.A.T. = 5-35/15 ft/min
$T_{dc,f}$ = 8.0°C	$\bar{\omega}_C$ = 0.00701
$\bar{T}_{dc}$ = 8.0°C	$\Delta\omega$ = 0.00862
T_H = 43.21°C	$\dot{m}_{H_2O}$ = 211.6 ml/hr
ΔT = 14.82°C	

Reduced Parameters

$\dot{m}' = 0.03620$ $\tau = 8.478$ min

$\frac{\dot{m}_r}{\dot{m}'} = 0.1888$ $\Delta t = 39$ sec

Transient Data

Time (min)	T_{dh}(°C)	$\omega_H(t)$	$\theta(t)$	t/τ
0.00	20.15	0.01563	1.000	0.000
1.35	19.40	0.01491	0.916	0.159
3.35	18.35	0.01394	0.804	0.395
5.35	17.45	0.01316	0.713	0.631
7.35	16.75	0.01257	0.645	0.867
9.35	15.95	0.01194	0.571	1.103
14.35	14.35	0.01075	0.433	1.693
19.35	13.00	0.00983	0.327	2.282
24.35	11.85	0.00911	0.243	2.872
29.35	11.00	0.00860	0.184	3.462
34.35	10.35	0.00823	0.142	4.052
39.35	9.90	0.00800	0.113	4.641
44.35	9.45	0.00774	0.085	5.231
59.35	8.75	0.00738	0.043	7.000

Test Identification

Test number:	Nb-36
Opening geometry:	12" x 12" (30 cm by 30 cm), 45° taper
Flow conditions:	No bulk flow
Test type:	Moisture decay

Test Conditions

T_{ref} = 21.7°C	P_{bar} = 28.86 in. Hg
$T_{dc,i}$ = 10.0°C	F.A.T. = 15-80/35 ft/min
$T_{dc,f}$ = 9.8°C	$\bar{\omega}_C$ = 0.00789
$\bar{T}_{dc}$ = 9.9°C	$\Delta\omega$ = 0.00836
T_H = 41.29°C	$\dot{m}_{H_2O}$ = 208.3 ml/hr
ΔT = 15.68°C	

Reduced Parameters

$\dot{m}'$ = 0.03807	τ = 8.178 min
$\dfrac{\dot{m}_r}{\dot{m}'}$ = 0.1817	Δt = 39 sec

Transient Data

Time (min)	T_{dh}(°C)	$\omega_H(t)$	$\theta(t)$	t/τ
0.00	20.95	0.01625	1.000	0.000
0.85	20.40	0.01570	0.933	0.104
2.68	19.85	0.01516	0.869	0.328
6.02	18.70	0.01409	0.741	0.736
9.35	17.30	0.01288	0.596	1.143
14.35	15.90	0.01176	0.463	1.755
19.35	14.55	0.01077	0.344	2.366
24.35	13.55	0.01008	0.262	2.977
29.35	12.70	0.00953	0.196	3.589
36.02	11.90	0.00903	0.137	4.404
42.68	11.30	0.00870	0.094	5.219
54.35	10.55	0.00825	0.043	6.646

Test Identification

Test number:	Nb-25
Opening geometry:	12" x 12" (30 cm by 30 cm), 45° taper
Flow conditions:	No bulk flow
Test type:	Moisture decay

Test Conditions

T_{ref} = 22.7°C	P_{bar} = 28.34 in. Hg
$T_{dc,i}$ = 10.6°C	F.A.T. = 0-5/2 ft/min
$T_{dc,f}$ = 10.4°C	$\bar{\omega}_C$ = 0.00837
$\bar{T}_{dc}$ = 10.5°C	$\Delta\omega$ = 0.00904
T_H = 40.64°C	$\dot{m}_{H_2O}$ = 245.0 ml/hr
ΔT = 15.21°C	

Reduced Parameters

$\dot{m}'$ = 0.0369 Kg/s	τ = 8.568 min
$\frac{\dot{m}_r}{\dot{m}'}$ = 0.204	Δt = 39 sec

Transient Data

Time (min)	T_{dh}(°C)	$\omega_H(t)$	$\theta(t)$	t/τ
0.00	21.75	0.01741	1.000	0.000
1.02	21.25	0.01687	0.940	0.119
2.35	20.45	0.01604	0.848	0.274
3.52	19.70	0.01530	0.767	0.410
5.18	19.10	0.01472	0.702	0.605
6.85	18.15	0.01385	0.606	0.799
9.35	17.05	0.01291	0.502	1.091
14.35	15.40	0.01160	0.357	1.675
19.35	14.05	0.01061	0.248	2.258
24.35	13.10	0.01000	0.180	2.842
29.35	12.45	0.00954	0.129	3.426
39.35	11.70	0.00896	0.065	4.668

APPENDIX I

Nomenclature

C - flow coefficient for an opening

C_m - flowmeter coefficient (acfm) $\left(\frac{Kg/m^3}{cm.H_2O}\right)$

D_L - inside diameter of a sample line, m

D_s - diameter of sample column, m

g - acceleration due to gravity, m/s^2

H - height of the opening, m

h_c - distance from N.P.L. to bottom of opening, m

h_H - distance from N.P.L. to top of opening, m

h_s - height of sample column, m

L_1 - length of the sample line in the first part, m

L_2 - length of the sample line in the second part, m

L_3 - length of the sample line in the third part, m

M_a - mass of dry air in the hot chamber, Kg

M_{as} - mass of dry air in the sample column, Kg

M_s - mass of water vapor in the sample column, Kg

M_v - mass of water vapor in the hot chamber, Kg

$\dot{m}_a$ - mass flow rate of dry air, Kg/s

$\dot{m}_b$ - bulk mass flow rate of moist air, Kg/s

$\dot{m}_c$ - mass flow rate of moist air from cold to hot chamber, Kg/s

$\dot{m}_{da}$ - mass flow rate of dry air exiting the exhaust port, Kg/s

$\dot{m}_H$ - mass flow rate of moist air from hot to cold chamber, Kg/s

$\dot{m}_{H_2O,net}$ - net water vapor mass flow rate through an opening, Kg/s

$\dot{m}_s$ - net rate at which water vapor enters the sample column, Kg/s

$\dot{m}_v$ - net rate at which water vapor enters the chamber, Kg/s

τ_s - time constant for moisture transfer through the sample column, sec

$\dot{m}_w$ - mass flow rate of liquid water into humidity generator, Kg/s

$\dot{m}'$ - normalizing parameter, Kg/s

N.P.L. - the neutral pressure line

n - number of sample columns in the hot chamber

P_{atm} - atmospheric pressure, N/m^2

P_c - the local pressure in cold air space, N/m^2

P_H - the local pressure in hot air space, N/m^2

R - gas constant $\frac{N \cdot m}{Kg.K}$

T_c - temperature of air in the cold chamber, K

T_H - temperature of air in the hot chamber, K

t - time, sec

t_1 - time lag for first part, sec

t_2 - time lag for second part, sec

t_3 - time lag for third part, sec

U - uncertainty in the measurements of parameters

V - Volume of hot subchamber, m^3

$\bar{V}$ - volume of the sample column, m^3

$\dot{V}_s$ - total volume flow rate through sample line, m^3/hr

W - width of the opening, m

z - damping ratio

ΔP - pressure difference across the opening, N/m^2

Δt - total time lag, sec

Δt_h - time lag due to hygrometer, sec

Δt_l - time lag due to sample line, sec

Δt_s - time lag due to sample column, sec

θ - normalized specific humidity ratio

ρ_c, ρ_H - air density in cold (hot) chamber, Kg/m^3

τ - time constant, sec

ω_c - specific humidity in the cold chamber

ω_H - specific humidity in the hot chamber

ω_n - natural frequency

ω_s - specific humidity in the sample column

ACKNOWLEDGEMENTS

The author wishes to express his sincere appreciation to Dr. B. Terry Beck, major advisor, who accepted the author as a graduate student and for his unselfish assistance and patience in planning and conducting the experiments. Secondly, I wish to express my appreciation to the members of my committee, Dr. Byron W. Jones and Dr. Subhash C. Sinha, for their on going support and advice in this research. I am also grateful to Connie Schmidt for her careful and efficient typing. Finally I would like to express thanks to Olga L. Vindiola for her love, care and encouragement throughout this research project.

This thesis is dedicated to my father, Mohammad Hossein Fartaj, and to my mother, Agdas Fartaj. They gave me life, love, and the freedom to learn. I couldn't begin to repay them.

TRANSIENT MOISTURE TRANSFER THROUGH AN OPENING IN A VERTICAL PARTITION

by

SAYED AMIR FARTAJ

B.S., Kansas State University, 1980

AN ABSTRACT OF A THESIS

Submitted in partial fulfillment of the requirements for the degree

MASTER OF SCIENCE

Department of Mechanical Engineering

KANSAS STATE UNIVERSITY
Manhattan, Kansas

1983

ABSTRACT

This research project specifically addressed the problem of transient moisture infiltration through openings in environmentally controlled air spaces where the magnitude of the latent load was significant. The objective of the present study was to determine experimentally the effect of various physical and geometrical parameters upon the transient rate of moisture transfer through openings in a vertical partition. This was accomplished indirectly, by measuring the transient humidity in the chamber. The parameters investigated were temperature, humidity difference, dimensions of the opening and bulk flow of air through the opening. Tests were carried out for single rectangular openings in a partition which subdivided a chamber of 6 ft. by 12 ft. into two cubical subchambers. These experiments were conducted on openings ranging from 6" x 12" (15 cm by 30 cm) to 18" x 12" (45 cm by 30 cm), with temperature differences ranging from 16°F to 43°F (9°C to 24°C), humidity ratio ranging from 2.2×10^{-3} to 11.9×10^{-3} and bulk mass flow rates ranging from zero to 59 Kg/hr (0 to 130 lbm/hr).

A simple transient theory was presented to correlate the experimental data. Data taken for both free as well as combined forced and free convection through the opening are presented graphically on a normalized set of coordinates.